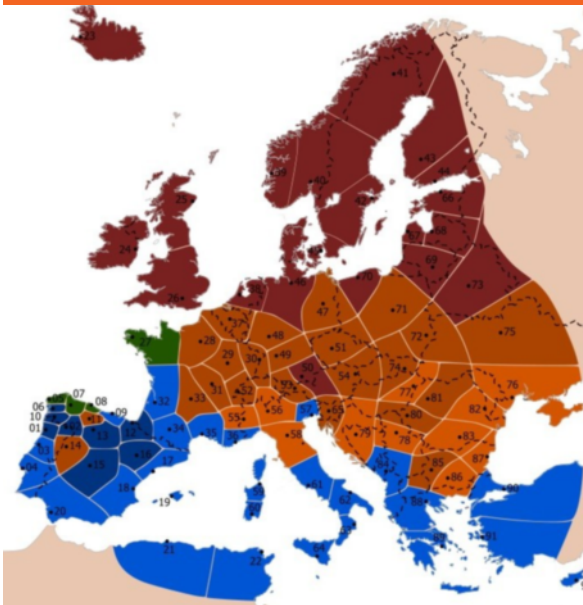


Possibilities and Limitations of Thermally Activated Building Systems



Benjamin Behrendt

PhD Thesis

Department of Civil Engineering
2016

DTU Civil Engineering Report R-361

Possibilities and Limitations of Thermally Activated Building Systems

- Simply TABS and a Climate Classification for TABS

Benjamin Behrendt

Ph.D. Thesis

Department of Civil Engineering
Technical University of Denmark

2016

Supervisors:

Ass. Professor Jørgen Erik Christensen, DTU Civil Engineering, Denmark
Professor Bjarne W. Olesen, DTU Civil Engineering, Denmark

Assesment Committee:

Ass. Professor Jianhua Fan, DTU Civil Engineering, Denmark
Professor Jan Hensen, Technical University of Eindhoven, Netherland
Ass. Professor Kjell Kolsaker, NTNU, Norway

Possibilities and Limitations of Thermally Activated Building Systems

-Simply TABS and a Climate Classification for TABS

Copyright © 2016 by Benjamin Behrendt

Printed by DTU-Tryk

Department of Civil Engineering

Technical University of Denmark

ISBN: 9788778774545

ISSN: R-361

Abstract

The strong political market drive towards energy savings in the building sector calls for efficient solutions. Using so called low temperature heating and high temperature cooling systems such as for instance thermally activated building systems (TABS) has a significant impact on the required energy source. With TABS it is possible to utilize otherwise insufficient energy sources such as waste heat or ground coupled heat exchangers.

Today simulation of TABS is possible with most building simulation tools. However such simulations are rather time consuming and cost intensive. It would be beneficial to have a tool that can be used to assess the general usability of TABS considering only rough boundary conditions. The Simple Simulation Tool in combination with the Climate Classification for TABS introduced in this thesis offer this solution.

The Simple Simulation Tool has proven to be a valid tool for the early assessment for the use of TABS in modern Buildings. Not only is it possible to run simulations in accordance to ISO 11855-4 but also to determine the minimal required plant sizes for cooling, the duration until overheating, the maximum internal temperatures for insufficient plant sizes (using a simplified heat loss approach) and the maximum allowed cooling power to prevent undercooling.

The climate Classification can be used to predict the building behaviour throughout Europe. Based on a very select number of building characteristics it can be seen if heating, cooling or both will be mostly needed to operate the building within acceptable boundaries. It will also allow the user to see if dehumidification will be needed for undisturbed operation of TABS.

With the combination of both tools it is possible to provide a holistic evaluation of a building proposal at a very early design stage.

Resumé

Stærke politiske kræfter arbejder for energibesparelser i byggesektoren, hvilket kræver effektive løsninger. Anvendelse af termisk aktive byggesystemer (TABS) med lav-temperatur opvarmning og høj-temperatur køling, har en stor indflydelse på den valgte energikilde. Med TABS er det muligt at udnytte ellers utilstrækkelige energikilder som spildvarme eller jordkoblede varmevekslere.

Simulering af TABS er i dag muligt med de fleste bygningssimuleringsværktøjer. Sådanne simuleringer er dog temmelig tidskrævende og omkostningstunge. Det ville derfor være gavnligt at have et mere enkelt simuleringsværktøj, der med simplificerede randbetingelser, kan anvendes til en overordnet vurdering af anvendeligheden af TABS. For at håndtere denne udfordring er der i denne afhandling introduceret et forenklet simuleringsværktøj i kombination med klima klassificering for TABS.

Det forenklete simuleringsprogram har vist sig at være et effektivt værktøj til indledende vurderinger for anvendelse af TABS i nyere bygninger. Med programmet er det muligt at simulere i overensstemmelse med ISO 11.855-4, bestemme den mindste anlægsstørrelse til køling, risikoen for overophedning, den maksimale indetemperatur for en utilstrækkelige anlægsstørrelse (ved hjælp af en forenklet varmetabsberegning) og maksimal tilladt køleeffekt for at undgå underafkøling.

Klima klassificeringen kan anvendes til at forudsige bygningens respons i hele Europa. Baseret på et udvalg af nøgleparametre for bygningsmæssige forhold kan det beregnes, hvorvidt opvarmning, køling eller begge dele er nødvendige for under bygningsdriften at opnå et acceptabelt indeklima. Klassificeringen vil også gøre det muligt for brugeren at se, om der vil være behov affugtning for at almindelig drift af TABS kan finde sted.

Med kombination af de to værktøjer er det muligt at give en helhedsvurdering af et bygningsprojekt på et tidligt tidspunkt af projekteringsfasen.

Contents

1	Introduction	1
2	General information about radiant systems	5
2.1	What is a radiant system?	5
2.2	TABS in detail	6
2.2.1	Building design and TABS	8
2.2.2	Ventilation and TABS	9
2.2.3	Humidity and TABS	9
2.2.4	Energy - and exergy - efficiency	9
2.2.5	Heat sinks for TABS	10
3	Simply TABS	11
3.1	Methods	12
3.1.1	Heat Balance	13
3.1.2	Thermal Nodes	14
3.1.3	Resistance Network of the Active Layer	26
3.1.4	Simulation Progress	29
3.1.5	Simulation Duration	30
3.1.6	Requirements for a Stationary Simulation	30
3.1.7	Follow-up Simulations	31
3.1.8	Heat load reduction	33
3.1.9	Undercooling prevention	34
3.2	System Validation	37
3.2.1	Validation against ISO 11855	38
3.2.2	Validation against IDA ICE 4.5	38
4	Climate Classification for TABS	43
4.1	Existing climate classifications	43
4.2	Methods	44
4.2.1	Base Temperature	45
4.2.2	Degree Day Calculation	46

4.2.3	Dew point hours	51
4.3	Criteria for the climate classification	52
4.3.1	Thermal Classification	52
4.3.2	Humidity Classification	52
4.3.3	The combined classification	53
4.4	Locations included in the climate classification database	53
4.5	New and pre-defined Climate Classifications	57
4.6	System Validation	62
5	Conclusion	71
6	Further studies	73
	References	79
	List of Symbols	81
	Appendices	89
A	<i>Simply TABS Project Setup</i>	89
A.1	Configuration File	89
A.2	Start File	89
A.3	Project File	90
A.4	Boundary File	90
A.5	Room File	92
A.6	Slab File	93
A.7	Circuit File	95
A.8	Pipe File	95
A.9	Start conditions	96
B	List of all cases used in this paper	99
C	Data for Validation with ISO 11855 - 4	103
D	<i>Climate Classification for TABS Data</i>	105
E	Appended Papers	113

Paper I

"Climate Classification for the Simulation of Thermally Activated Building Systems (TABS)",

B. Behrendt & J. E. Christensen.

Published in: *Proceedings of Building Simulation, 2013* 115

Paper II

"A system for the comparison of tools for the simulation of water-based radiant heating and cooling systems",

B. Behrendt, D. Raimondo, Y. Zhang, S. Schwarz, J. E. Christensen & B. W. Olesen.

Published in: *Proceedings of Building Simulation, 2011* 125

Paper III

"Thermische Behaglichkeit und Energieaufwand bei Flaechenheizungen in Buero- gebaeuden",

B. M. Behrendt & B. W. Olesen.

Published in: *Proceedings of BauSim, 2013* 135

List of Figures

3.1	Simply TABS Heat Balance	14
3.2	Node network definition	15
3.3	Heat balance for floor surface node	16
3.4	Heat balance for internal nodes	17
3.5	Heat balance for active layer node	20
3.6	Heat balance for ceiling surface node	21
3.7	Heat balance for internal wall surface node	22
3.8	Heat balance for internal wall node	24
3.9	Heat balance for air node	25
3.10	Resistance network of the active layer	26
3.11	Temperature development in the Simply TABS	29
3.12	Temperature development deviation in Simply TABS.	32
3.13	Temperature development using simulated environmental heat loss in Simply TABS.	35
3.14	Temperature development in the Simply TABS	37
3.15	Comparison of calculated and given temperatures	39
3.16	Comparison of calculated and given heat flux	40
3.17	Comparison of temperatures for Simply TABS and IDA ICE 4.5 . . .	41
3.18	Comparison of heat flux from Simply TABS and IDA ICE 4.5 . . .	42
4.1	Heat balance scenarios	45
4.2	Different scenarios for the attribution to HDD and CDD	47
4.3	Comparison of degree day calculation methods.	49
4.4	ECC Locations and Zones Only	54
4.5	Map of Europe based on the new climate classification system. . . .	57
4.6	Influence of CDD_L on the climate classification	58
4.7	Influence of HDD_L on the climate classification	59
4.8	Influence of $DPH_{L,U}$ and $DPH_{L,L}$ on the climate classification . . .	59
4.9	Influence of changing base temperatures for heating and cooling degree days	61
4.10	Building Data - Measurements	62
4.11	Thermal comfort categories for select locations for summer and winter	64

A.1	Possible slab constructions	95
D.1	Climate map for case 1414AaBb-1day	109

List of Tables

3.1	Comparison of the capabilities of the standard tool (ISO 11855-4) and <i>Simply TABS</i>	12
3.5	Assignment of node indices including one example.	15
4.6	Building Data - Ventilation, TABS and loads	63
4.7	Data for Copenhagen, Denmark (Location 45)	65
4.8	Data for Banja Luka, Bosnia and Herzegovina (Location 79)	66
4.9	Data for Belgrade, Serbia (Location 78)	67
4.10	Data for Porto, Portugal (Location 01)	68
4.11	Data for Madrid, Spain (Location 15)	69
4.12	Data for Larnaca, Cyprus (Location 92)	70
A.1	File: P_Files/Example.proj → This file contains the names of the input files needed for this project.	90
A.2	File: I_Files/Boundary/11855_4.inp → This file contains all relevant boundary informations for the simulation. There can be multiple "TimeStepData" sets.	91
A.3	File: I_Files/Room/11855_4.inp → This file contains all relevant room informations.	93
A.4	File: I_Files/Slab/11855_4.inp → This file contains the name of the project that should be simulated.	94
A.5	File: I_Files/Circuit/11855_4.inp → This file contains the name of the project that should be simulated.	96
A.6	File: I_Files/Pipe/11855_4.inp → This file contains the name of the project that should be simulated.	96
A.7	File: SSTe.start → This file contains the name of the project that should be simulated.	97
B.1	List of all simulations created with <i>Simply TABS</i> included in this thesis	99
B.2	Setting used in cases with cooling limitation [°C]	100
B.3	Setting used in cases simulated environmental heat loss [°C]	100

B.4	List of all simulations created with IDA ICE 4.5 included in this thesis	101
C.1	Expected results as given in ISO 11855-4	103
C.2	SSTe results based on input data from ISO 11855-4	104
D.1	Case: 1414AaBb	105
D.2	Case: 1616AaBb	109

Chapter 1

Introduction

Buildings account for around 40% of the EU's total energy use and are Europe's largest source of emissions, so improving their energy performance would help reach CO₂ emission goals.

European Union (EU) (2010b)

A strong political and market drive towards low energy, passive and even energy positive buildings is currently taking place in Europe. All buildings erected after 2020 have to comply with high energy-saving standards and use renewable energy if possible. Older buildings need to be upgraded during major renovations where possible. Owners will be encouraged to install smart-meters, upgrade heating systems, hot-water plumbing and air-conditioning systems with high-efficiency alternatives such as heat pumps (European Union (EU), 2010a,b). This is not only a European development, but also takes place in other countries around the world (IEA, 2013).

Consequently, there is a strong need to develop sustainable low energy heating and cooling solutions. With changing building codes, changing comfort requirements and possibly more extreme weather conditions, it is becoming increasingly important in indoor climate and energy management of buildings to provide cooling and manage cooling loads. In the process of developing and adapting new renewable and low energy solutions, it is vital that both energy and comfort requirements are addressed in order for the HVAC systems to comply with the new low energy regulations and at the same time to provide an adequate indoor climate for the building occupants (Jäger, 2006).

One of the most promising strategies for sustainable cooling is to apply water-based solutions utilising large radiant surfaces at relatively high temperatures, coupled with free and renewable cooling energy sources. By using large surfaces,

both heating and cooling can be obtained at temperatures close to the desired temperature levels in the building. This has a number of advantages both for the energy efficiency and for the indoor environment. Heating and cooling transmission at temperature levels close to ambient allows for the use of energy with a low exergy content, such as for example waste heat and surplus heat from local electricity production. In addition, these temperature levels allow for an optimal integration of renewable energy sources such as ground heating and cooling, heat pumps or solar heat. (Babiak et al., 2007a,c)

Embedded water based systems activating the thermal mass of the building - or thermally activated building systems (TABS) - come along with an additional advantage for buildings where occupancy patterns produce large cooling loads during day time. They can substantially reduce peak loads due to their high thermal capacities and consequently plant sizes may be reduced (Rijksen et al., 2010). The use of TABS for cooling also has a direct impact on the required ventilation rates of a building. Ventilation requirements may be reduced to the point where it is only needed for hygienic reasons. Reducing the air change rate may have a significant beneficial effect on ventilation costs (Finke et al., 2006; Santos and Leal, 2012).

Although various embedded water based radiant solutions already exist on the market, a number of technical problems and feasibility issues are yet to be analysed and solved. Optimal operation and control strategies under different operation conditions are only partly understood (Lehmann et al., 2011). What is further needed to evaluate cooling or heating strategies, is a proper benchmarking of embedded water based systems against other HVAC systems as well as a benchmarking of design and calculation against real building performance. Optimised design concepts and simplified modelling and calculation methods have been developed to a limited extend only. A simplified approach that delivers the needed results is however preferential (Crawley et al., 2008).

Many users rely on a single, multipurpose tool for building simulations. Using tools that are tailored for the problem at hand will however be beneficial. Especially during early design, a detailed simulation will be too time consuming and costly. This is further emphasised by the inherent added uncertainties found in the results of complex simulation tools, if part of the input data is not yet available and has to be guessed (Behrendt et al., 2011).

Under special circumstances, the utilisation of TABS introduces a challenge to the system operation that is foreign to air-based systems. This potential disadvantage stems from the different methods of cooling the room air. In the case of an air-based cooling system, the lowest air temperatures occur in the central air handling unit (AHU), where it is easy to remove condensed water. In a building cooled with TABS, the lowest air temperatures typically occur in the boundary layer at the

controlled surfaces.

During the design of TABS, it is therefore important to evaluate the risk of condensation within the building. If a complete building simulation is undertaken, most building simulation tools today recognise potential condensation risks and notify the user. Since simulations of the like are however time consuming, it is of considerable value if the usability of TABS could be quickly assessed in a simplified approach. To this end the ISO 11855-4 suggests the use of a simplified simulation method. This type of simulation however does not consider humidity at all, but focuses solely on thermal performance. A possible result of a simulation with such tool could be that the building may be sufficiently cooled by TABS, a full building simulation would however reveal that the system likely causes condensation on the controlled surfaces.

To identify this risk, it would therefore be beneficial if a Climate Classification for TABS existed. Until now, this was however not the case as most available climate classifications consider precipitation, but not humidity. The Köppen-Geiger (Kottek et al., 2006) or the ASHRAE Climate classification (ASHRAE, 2010) are two examples for well established systems. In terms of simulating TABS they are however not quite fitting the needs.

The developed tool Simply TABS is a quick and easy program for the calculation of cooling design days for TABS. In addition, it is possible to do a preliminary sizing of the required cooling capacity and evaluate partial as well as total failure of the cooling system.

The developed Climate Classification for TABS provides a general classification based on a selected number of key building parameters in relation to the local climate. The key output of the tool is to conclude if cooling (or heating) is needed at a given location. Additionally, it provides an estimation if surface condensation has to be considered in case that TABS are used as a cooling system. Especially the information about dehumidification greatly enhances the significance of the results obtained with Simply TABS.

Introduction

Chapter 2

General information about radiant systems

2.1 What is a radiant system?

The term radiant system describes any application that exchanges heat with its surroundings, both through convection and by radiation, if more than 50% of the heat transfer is due to radiant processes. These systems are typically operated with water as heat-carrier (Causone et al., 2010; Babiak et al., 2007b). Of all possible systems, "radiant heating and cooling panels", "pipes isolated from main building structures" and "thermal active building systems" are further introduced in the following.

Radiant Heating and Cooling Panels Radiant heating and cooling panels are mostly prefabricated panels with an integrated pipe system. These panels are suspended from the ceiling of a room and thermal energy is then exchanged between the panels and the room as well as directly with the occupants. (ASHRAE, 2002)

Radiant panels can be installed after construction has been finished and are available in a number of different varieties as units suspended from the ceiling, attached to the ceiling or even fully integrated into the ceiling. (Babiak et al., 2007b)

Pipes isolated from main building structure Pipes isolated from main building structure belong to the group of embedded surface heating and cooling systems. The aim of these systems is to minimise the heat transfer between the building structure and the system itself. To minimise this effect, a separating layer of thermal insulation is commonly installed between the layer in which the pipes are located and the adjacent building structure. (Babiak et al., 2007b)

This type of systems is increasingly used in new buildings, especially in central Europe and Nordic countries. They can also be found in refurbished buildings. This is possible since they are placed right next to (or on top of) the building structure and are not an actual part of it.

Thermally Active Building Systems In contrast to the other systems, TABS are deliberately linked to the building mass, exploiting the thermal storage capacity of the building structure and increasing the heating and cooling energy efficiency in a number of ways. (Causone et al., 2010; Ali, 2007; Babiak et al., 2007b) This type of system is also increasingly used in new buildings, especially in central Europe and Nordic countries. However, they can practically not be used in refurbished buildings as they are usually a part of the building structure itself. Nonetheless is it this connection to the building structure that makes it the most interesting system and puts it in the focus of this study.

2.2 TABS in detail

TABS have many advantages compared to other cooling and heating systems, but also have their very own limitations and requirements. The general operation of TABS with all its benefits and shortcomings is discussed in the following.

Decoupling of thermal loads and peak load reduction with TABS By allowing the room temperature to drift within the comfort range during the day, it is possible to decouple the loads from the plant operation. During day time, a considerable amount of the thermal loads is then stored within the building structure. Due to this heat storage, it is possible to distribute the cooling load throughout the entire (24h) day, reducing peak loads - and plant sizes - by up to 50% while maintaining good thermal comfort. Rijksen et al. (2010); Lehmann et al. (2007); Armstrong et al. (2009)

Installation, maintenance and operation costs of TABS TABS have low installation costs, require a relatively low amount of maintenance as they are a closed system and have lower operation costs than other cooling systems. (Deecke et al., 2003; Lehmann et al., 2011; Babiak et al., 2007b)

High temperature cooling and low temperature heating with TABS Due to their large heat transfer areas and active control of surface temperatures, TABS allow for cooling (and heating) supply temperatures relatively close to the desired room temperature. This makes it possible to combine TABS with environmental friendly energy sources/sinks such as heat pumps, condensation boilers,

solar collectors and ground coupled heat exchangers (Deecke et al., 2003; Koschenz and Lehmann, 2000).

Time constant of TABS TABS typically have a relatively high time constant due to the high thermal storage capacity between the circuit and the room. For any change in the supply temperature to effect the room, it has to first heat (or cool) the entire slab. This is a challenge for the active control of the system, but also an advantage as it is closely connected to the self regulation inherent to TABS. (Rijksen et al., 2010; Lehmann et al., 2007)

Self regulation of TABS As TABS are high temperature cooling and low temperature heating systems, the temperature difference between the controlled surfaces and the room are usually very small. Combined with the high thermal capacity of the system, this creates a self regulating effect. If the loads in the room suddenly increase and thereby start to offset the temperature difference, the heat transfer to or from the controlled surfaces is changed as well. Thanks to the high thermal capacity of the system, it will however only slowly change its own temperature. (Karlson, 2008; Karlsson, 2010; Lehmann et al., 2011, 2007).

Control strategies for TABS In the past, various control strategies for TABS have been implemented. Most of them have however suffered from one or more of the following flaws identified by Gwerder et al. (2009, 2008):

- Different control solutions for cooling and heating
- Frequent switching between heating and cooling mode
- Only manual switching between heating and cooling mode
- High energy consumption for circulation pumps
- Required manual adjustment of parameters

A number of different approaches are introduced in the following.

Base control strategy / Continuous operation The most commonly used control is "outside temperature compensated supply water temperature control". With this control, the system is either operating continuously (pumps) or completely off. In order to improve comfort and energy efficiency, it can be extended with optional control parameters. (Gwerder et al., 2008, 2009; Olesen and Dossi, 2003; Lehmann et al., 2011)

Night time re-cooling This control makes use of the large thermal inertia of TABS. This inertia allows for a time delay between the energy storage in the slab and its discharge. This makes it possible to use e.g. colder night time air for cooling, thus saving energy. In case of a pure night time cooling, the systems

would engage at night time (e.g. 10 pm) and disengage once the desired start-off temperature is reached. In extreme cases with high heat gains, this could mean that cooling is not turned off but continuing to run for 24h. (Lehmann et al., 2011)

2.2.1 Building design and TABS

Just as for any other cooling or heating system, the overall performance of a radiant system such as TABS is greatly influenced by the building itself. The proper design of the building is of very high importance. The most common placement of TABS is inside the floor/ceiling construction making it especially interesting for multistorey buildings.

System heat capacity and space requirements of TABS TABS are commonly operated using water as a heat carrier. This leads to a number of advantages compared to systems that rely on air for the same task. The heat capacity of water is roughly four times that of air ($\approx 4.18kJ/(kg \cdot K)$ vs. $\approx 1kJ/(kg \cdot K)$). In addition, water is roughly 775 times as dense as air ($\approx 998kg/m^3$ vs. $\approx 1.293kg/m^3$). As a result, the same volume of water can transport roughly 3.100 times as much heat as air (with the same temperature lift) reducing the entire infrastructure considerably. Consequently, the entire building height can be reduced substantially. Especially in urban areas this does not only reduce material and equipment costs, but may also increase the usable space in a building substantially (e.g. seven instead of only six floors) while maintaining the same room height.

Thermal mass The thermal mass of a building is crucial for the operation of TABS. If the activated mass is too low, the system is unable to perform as desired and the room temperatures might leave the comfort area. A way to increase the thermal capacity of the concrete slab is to embed phase-change materials into the concrete. A number of studies have been made to this end (Tyagi and Buddhi, 2007), but phase-change materials have not been widely used as not all associated problems have been solved yet.

Acoustic properties of TABS Depending on the cooling load, the often cited acoustic problems of buildings using TABS can be circumvented as acoustic panels may be installed on 85% of the ceiling while only reducing the cooling capacity by 30% (Olesen and Pittarello, 2008).

Solar radiation and TABS The proportion of glazing of the building envelope has increased over the last decades. Modern buildings often come with consider-

able proportions of glazed areas. This means that more light enters the building and with it solar gains are increasing. One advantage of radiant systems is their capability to remove parts of the solar radiation into the building without it taking part in the thermal absorption phenomena. A portion of the solar heat gain - the direct solar load - is directly captured in the slab and then removed by the cooling system. In other words, the radiant heat gains are divided into two parts when a radiant cooling system is used. One part is directly removed by the controlled surface and the remaining part is re-dispersed into the room with a time lag, depending on the thermal mass. Causone et al. (2010); Corgnati (2002); Corgnati et al. (2000)

2.2.2 Ventilation and TABS

Radiant systems can do much to improve indoor environment, however, they will most often require a supplementary air system to achieve best indoor conditions. The air system has to supply the required fresh air and often needs to regulate the dew point temperature to prevent condensation on the controlled surfaces. TABS can be used under various extreme climatic conditions. They often achieve the best results in combination with fresh air ventilation. The ventilation can then optionally cover cooling peak loads and remove the latent heat, where the radiant system covers the base load. Using a ventilation system with heat recovery, good comfort at a minimum energy consumption can be achieved. Compared to an all air system, the total air flow rate in the system may be decreased by up to 75%. (Behrendt and Olesen, 2010; Babiak et al., 2010a,b)

2.2.3 Humidity and TABS

In some cases - mostly in regions with high relative humidity - it is possible that surface temperatures may be lower than the dew point temperature of the air. In those cases water would start to condense on the surface (Behrendt and Olesen, 2010) which would not only be unpleasant, but could also lead to serious problems such as mould growth if happening repeatedly. This can be addressed through dehumidification of the air and proper control of the system (Tian and Love, 2009; Vangtook and Chirarattananon, 2007) or in part through improvements in the building envelope to prevent moisture penetration and reduced infiltration rates (Chungpaibulpatana and Praditsmanont, 2008).

2.2.4 Energy - and exergy - efficiency

In general, TABS can achieve a high energy efficiency for cooling and heating of buildings (El Ahwany, 2014; Kalz, 2009). Energy use was found to be reduced by

25% in coastal subtropical Barcelona (Spain), by over 50% in inland subtropical Seville (Spain) and by up to 60% in UAE (Babiak et al., 2010a).

As the heat transfer from the TABS to the room takes place at near environmental temperature, the exergy consumption is very low. Combined with low exergy heat sinks and sources, a very exergy efficient cooling system can be achieved. (Asada and Boelman, 2004)

2.2.5 Heat sinks for TABS

Radiant cooling systems can be used together with many different heat sinks. Depending on the chosen heat sink, the total energy consumption may vary considerably. Between a (monovalent) cooling tower and a mechanical chiller with and without optional bypass of the chiller (use of free cooling), the cooling tower has the lowest electricity demand ($2.8kWh/m^2a$), followed by both mechanical cooling options with about $4kWh/m^2a$ Lehmann et al. (2011). In the following, a few possible heat sinks are introduced.

Free cooling Any heat sink that can be accessed without any - or very limited - costs is considered to be free cooling. Depending on the climate, TABS can be used in low energy buildings in combination with free cooling sources (e.g. ground coupled heat exchangers, open water tanks or night time ventilation). (Babiak et al., 2010a; Ali, 2007).

Heat pumps Heat pumps are a near perfect match for TABS. With operation temperatures close to the ambient temperatures, only a small temperature lift is needed to remove the heat from the circuit. Heat pumps are often used in combination with ground- or sometimes even air heat exchangers. (Babiak et al., 2007b)

Evaporative cooling tower Wet cooling towers can be used to exploit the lower night time temperatures of the outside air. In return, an essential part of the cooling has to be shifted to night time and the running time of the system is increased (Lehmann et al., 2011).

Mechanical chillers Mechanical chillers can provide higher outputs than e.g. wet cooling towers and thereby have shorter run times (Lehmann et al., 2011).

Chapter 3

Simply TABS



TABS are a contributor towards the goal of a sustainable society. Many modern buildings have been making use of this inexpensive heating and cooling technology in recent years.

At its core, *Simply TABS* is based on the procedures suggested in ISO 11855-4. It is written in C++ and relies solely on text file in- and output for operation. The input consists of a file defining the setup of the program and the remaining files represent the actual input data. These text files can be generated in any way, as long as certain formatting requirements are met. This makes it possible to use the *Simply TABS* as it is or to develop custom graphical user interfaces. In this Thesis only the text based input is described.

Apart from the core purpose set in ISO 11855-4, additional features as listed in table 3.1 have been implemented in the program.

It has been shown that *Simply TABS* works as expected. At an early design stage it can be used to dimension the cooling facilities, to test different control strategies as well as to evaluate cooling failure (partial and complete). Essentially *Simply TABS* can be used as an early design tool for the quick and easy dimensioning of TABS without requiring too detailed input data that would ordinarily not be available at an early design stage in any case.

Table 3.1: Comparison of the capabilities of the standard tool (ISO 11855-4) and Simply TABS.

	ISO 11855-4	Simply TABS	See:
Number of simulations			
Follow-up simulations	–	X	3.1.7
Total resistance of the active layer			
Provided as single input value	X	X	3.1.3
Internal calculation for pipes embedded in massive concrete slab	–	X	3.1.3
Internal calculation for pipes embedded at inside surface	–	X	3.1.3
Simulation length			
24 hour simulation	X	X	3.1.5
unlimited simulation time	–	X	3.1.5
Follow-up simulations			
Follow-up simulations with reduced cooling	–	X	3.1.7
Heat loss model			
Simulated connection to environment	–	X	3.1.8
Control strategy			
Standard control for minimal operative temperature	X	X	3.1.9
Advanced control to eliminate undercooling	–	X	3.1.9

3.1 Methods

Simply TABS is an extension of the model proposed in ISO 11855-4. Apart from the fundamental functions defined in ISO 11855-4, *Simply TABS* offers a number of options to facilitate the design of water based embedded systems.

At its core *Simply TABS* is based on a finite difference method. The room is represented by heat balances for a node network as detailed in sections 3.1.1 and 3.1.2. Rather than using a system of equations an iterative solution is used. The use of an iterative approach require that the difference between iterations is below a certain threshold and that this is reached after a finit number of iterations. The

details of this approach are detailed in section 3.1.6.

It will always simulate a single room with adiabatic internal walls and its own ceiling connected to its floor. External walls are not included in the simulation as further detailed in section 3.1.1.

3.1.1 Heat Balance

The general heat balance for the room is described in equation 3.1 and illustrated in figure 3.1(a).

$$Q_{pa}^h + Q_{Sun}^h + Q_i^h + Q_{Tran}^h + Q_{Inf}^h + Q_{circ}^h = c \frac{d\theta}{dt} \quad (3.1)$$

where

Q_{pa}^h	primary air convective heat gains for each h th hour [W]
Q_{Sun}^h	solar heat gains in the room for each h th hour [W]
Q_i^h	total internal heat gains for each h th hour [W]
Q_{Tran}^h	transmission heat gains for each h th hour [W]
Q_{Inf}^h	infiltration based heat gains and losses for each h th hour [W]
Q_{circ}^h	delivered cooling capacity of the circuit [W]
$c \frac{d\theta}{dt}$	internal energy storage [W]

For *Simply TABS* all external heat sources are however used as if they were internal sources as well. Equations 3.2 and 3.3 describe how these internal heat sources have to be calculated. For this purpose, the internal gains (Q_i^h) are also divided into their radiant ($Q_{rad,i}^h$) and convective ($Q_{con,i}^h$) components. In accordance to ISO 11855-4 15% of the heat gains passing through the external walls (Q_{Tran}^h), are assumed to behave convective, while the remaining 85% are considered as radiant head load.

$$Q_{con}^h = 0.15 \cdot Q_{Tran}^h + Q_{con,i}^h + Q_{pa}^h + Q_{Inf}^h \quad (3.2)$$

$$Q_{rad}^h = 0.85 \cdot Q_{Tran}^h + Q_{rad,i}^h + Q_{Sun}^h \quad (3.3)$$

where

Q_{con}^h	convective heat gains for each h th hour [W]
Q_{Inf}^h	infiltration based heat gains and losses for each h th hour [W]
$Q_{con,i}^h$	internal convective heat gains for each h th hour [W]
$Q_{rad,i}^h$	internal radiant heat gains for each h th hour [W]
Q_{pa}^h	primary air convective heat gains for each h th hour [W]
Q_{rad}^h	total radiant heat gains for each h th hour [W]
Q_{Sun}^h	solar heat gains in the room for each h th hour [W]
Q_{Tran}^h	transmission heat gains for each h th hour [W]

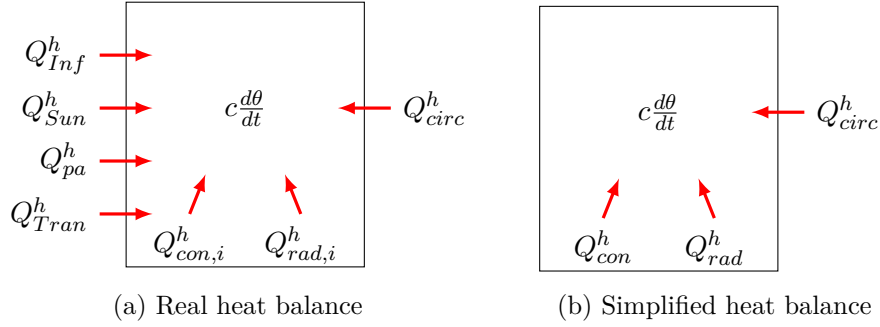


Figure 3.1: Illustration of the heat balance simplifications used for *Simply TABS*.

The simplified simple heat balance as illustrated in figure 3.1(b) is then described by equation 3.4

$$Q_{rad}^h + Q_{con}^h + Q_{circ}^h = c \frac{d\theta}{dt} \quad (3.4)$$

where

Q_{rad}^h	total radiant heat gains for each h th hour [W]
Q_{con}^h	total convective heat gains for each h th hour [W]
Q_{circ}^h	delivered cooling capacity of the circuit [W]
$c \frac{d\theta}{dt}$	internal energy storage [W]

This simplification entails a practical problem. In a real building the heat load will always depend on the environment. With higher differences between internal and external temperatures the load (cooling or heating) on the building will increase. In *Simply TABS* this connection does not exist. Thus, the heat loads connected to transmission (Q_{Tran}^h) and ventilation (Q_{pa}^h) will not change. Therefore care has to be taken when setting the heat load for the tool.

Properly including this connection to the environment would however require a substantial amount of additional data as for instance environmental temperature, descriptions of the building envelope and information about any fenestration. Including the outside wall in the model would also increase the tool's complexity significantly. For the purpose of *Simply TABS* the stated simplifications are therefore considered acceptable.

3.1.2 Thermal Nodes

In *Simply TABS* the room is represented by a thermal node network. Within the slab, each node is connected with the node directly above and below. For better readability each node is given a specific index where possible, in any other case

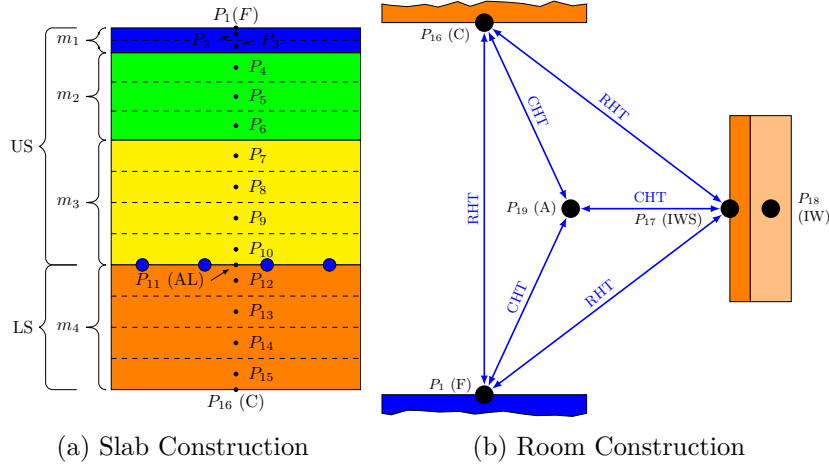


Figure 3.2: Scheme for the node numbering

Table 3.5: Assignment of node indices including one example.

Node	Index	Index P	Example
Floor	F	1	1
Upper Slab	I	2 to $1 + \sum_1^{J_{US}} m_j$	2 to 10
Pipe	P	$2 + \sum_1^{J_{US}} m_j$	11
Lower Slab	I	$3 + \sum_1^{J_{US}} m_j$ to $2 + \sum_1^{J_{US}+J_{LS}} m_j$	12 to 15
Ceiling	C	$3 + \sum_1^{J_{US}+J_{LS}} m_j$	16
Internal wall surface	IWS	$4 + \sum_1^{J_{US}+J_{LS}} m_j$	17
Internal wall	IW	$5 + \sum_1^{J_{US}+J_{LS}} m_j$	18
Air	A	$6 + \sum_1^{J_{US}+J_{LS}} m_j$	19

The example is calculated with $J_{US} = 3$ (Number of material layers in upper part of slab), $J_{LS} = 1$ (Number of material layers in lower part of slab), m_j (Number of nodes in material layer), $m_1 = 2$, $m_2 = 3$, $m_3 = 4$ and $m_4 = 4$. ISO 11855 part 4

”p” is used. The node indices are determined according to the logic in table 3.5 that follows the recommendations given in ISO 11855 part 4. Figure 3.2 illustrates the node network for the example specified in table 3.5.

Heat can only be transferred between connected nodes. All radiant heat is ab-

sorbed by the three surface nodes and the convective heat load is only connected to the air node. Generally the only way for any energy to leave the system is through the active layer node inside of the slab. It is however possible to define negative heat loads and thereby remove heat from the room. This may be of use if outside temperatures are considerably lower during nighttime and the heat losses are higher than the gains. Energy may be stored in any node that has a physical heat capacity.

Floor Surface Node

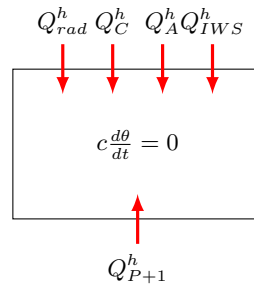


Figure 3.3: Heat balance for floor surface node

The floor surface node is a representation of the surface temperature and connects the upper part of the slab construction with the room. It does not have any mass or dimension of its own and therefore no heat is stored within. The heat balance for the floor node illustrated in figure 3.3 can be written as

$$c \frac{d\theta}{dt} = Q_A^h + Q_C^h + Q_{IWS}^h + Q_{P+1}^h + Q_{rad,F}^h = 0$$

with

$$\begin{aligned} Q_A^h &= A_F \cdot h_{A-F} \cdot (\theta_A^h - \theta_F^h) \\ Q_C^h &= A_F \cdot h_{C-F} \cdot (\theta_C^h - \theta_F^h) \\ Q_{IWS}^h &= A_F \cdot h_{C-W} \cdot (\theta_{IWS}^h - \theta_F^h) \\ Q_{P+1}^h &= \frac{A_F}{R_{add,F} + \frac{\delta_{P+1}}{\lambda_{P+1}}} \cdot (\theta_{P+1}^h - \theta_F^h) \\ Q_{rad,F}^h &= \frac{A_F}{2A_F + A_W} \cdot Q_{rad}^h \end{aligned}$$

can be solved to

$$\theta_F^h = \frac{h_{A-F} \cdot \theta_A^h + h_{F-W} \cdot \theta_{IWS}^h + h_{F-C} \cdot \theta_C^h + \frac{\theta_{F+1}^h}{R_{add,F} + \frac{\delta_{P+1}}{\lambda_{P+1}}} + \frac{Q_{rad}^h}{2A_F + A_W}}{h_{A-F} + h_{F-W} + h_{F-C} + \frac{1}{R_{add,F} + \frac{\delta_P}{\lambda_{P+1}}}} \quad (3.5)$$

where

A_F	floor area [m^2]
A_W	internal wall area [m^2]
$c \frac{d\theta}{dt}$	internal energy storage [W]
δ_{P+1}	half of the thickness of the material represented by the next (p+1)-th node [m]
h_{A-F}	convective heat transfer coefficient between air and floor [$W/(m^2 \cdot K)$]
h_{C-F}	convective heat transfer coefficient between ceiling and floor [$W/(m^2 \cdot K)$]
h_{C-W}	convective heat transfer coefficient between ceiling and internal walls [$W/(m^2 \cdot K)$]
λ_{P+1}	thermal conductivity of the material represented by the p+1-th node [$W/(m \cdot K)$]
Q_A^h	heat flow to from air node [W]
Q_C^h	heat flow to from ceiling node [W]
Q_{IWS}^h	heat flow from wall surface node [W]
Q_{P+1}^h	heat flow from the next node [W]
$Q_{rad,F}^h$	total radiant heat gains at floor node for each h^{th} hour [W]
$R_{add,F}$	additional thermal resistance covering the floor [$(m^2 \cdot K)/W$]
θ_A^h	temperature of the air thermal node in the h^{th} hour [$^{\circ}C$]
θ_C^h	temperature of the ceiling surface thermal node in the h^{th} hour [$^{\circ}C$]
θ_F^h	temperature of the floor surface thermal node in the h^{th} hour [$^{\circ}C$]
θ_{IWS}^h	temperature of the internal wall surface thermal node in the h^{th} hour [$^{\circ}C$]
θ_{P+1}^h	temperature of the next node [$^{\circ}C$]

Internal Nodes

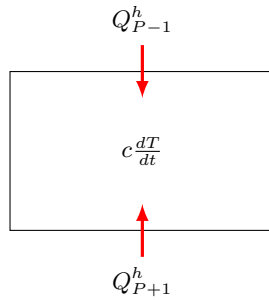


Figure 3.4: Heat balance for internal nodes

The internal nodes are a representation of the slab construction. Each material layer has at least one or more individual nodes. The embedded pipes split the slab into two parts. The part above the pipes is the upper part and the one below is the lower part of the slab.

The number of internal nodes varies from case to case. It is determined by the slab used in the current model. Depending on their position within the slabs internal nodes are slightly different. There are five possible scenarios. The top most internal node is connected to the floor node and the lowest internal node is connected to the ceiling node. The two internal nodes above and below the active layer are connected to it. All remaining internal nodes are connected to the respective internal nodes below and above them.

All internal nodes can be described with the same formula if the indices are adjusted accordingly. The heat balance for any internal node is illustrated in figure 3.4 and can be written as

$$c \frac{d\theta}{dt} = Q_{P-1}^h + Q_{P+1}^h$$

and with

$$\begin{aligned} c \frac{d\theta}{dt} &= \frac{c_P \cdot A_F}{\Delta t} \cdot (\theta_I^h - \theta_I^{h-1}) \\ Q_{P-1}^h &= \frac{A_F}{RD_{P-1} + RU_P} \cdot (\theta_{P-1}^h - \theta_I^h) \\ Q_{P+1}^h &= \frac{A_F}{RD_P + RU_{P+1}} \cdot (\theta_{P+1}^h - \theta_I^h) \end{aligned}$$

solved to

$$\theta_I^h = \frac{\frac{\theta_{I-1}^h}{RD_{P-1} + RU_P} + \frac{\theta_{I+1}^h}{RD_P + RU_{P+1}} + \frac{c_P}{\Delta t} \cdot \theta_I^{h-1}}{\frac{1}{RD_{P-1} + RU_P} + \frac{1}{RD_P + RU_{P+1}} + \frac{c_P}{\Delta t}} \quad (3.6)$$

with

$$RD_{P-1} = \begin{cases} \frac{\delta_{P-1}}{\lambda_{P-1}} & \text{if } P-1 = \text{node } I \\ R_{add,F} & \text{if } P-1 = \text{node } F \\ 0 & \text{if } P-1 = \text{node } AL \end{cases} \quad RD_P = \frac{\delta_P}{\lambda_P}$$

and

$$RU_{P+1} = \begin{cases} \frac{\delta_{P+1}}{\lambda_{P+1}} & \text{if } P+1 = \text{node } I \\ R_{add,C} & \text{if } P+1 = \text{node } C \\ 0 & \text{if } P+1 = \text{node } AL \end{cases} \quad RU_P = \frac{\delta_P}{\lambda_P}$$

and

$$c_P = \rho_j \cdot c_j \cdot \frac{\delta_j}{m_j}$$

where

A_F	floor area [m^2]
$c \frac{d\theta}{dt}$	internal energy storage [W]
c_P	specific heat of the respective layer of the slab [$J/(m^2 \cdot K)$]
c_j	specific heat of the j-th layer of the slab [$J/(kg \cdot K)$]
δ_P	half of the thickness of the material represented by the p-th node $\delta_P = \frac{\delta_j}{2m_j}$ [m]
Δt	calculation time step ($\Delta t = 3600$ for hourly simulations) [s]
λ_P	thermal conductivity of the material represented by the p-th node [$W/(m \cdot K)$]
λ_{P-1}	thermal conductivity of the material represented by the p-1-th node [$W/(m \cdot K)$]
Q_{P+1}^h	heat flow from the next node [W]
Q_{P-1}^h	heat flow from the previous node [W]
RD_P	conduction thermal resistance connecting node (p) with the previous node ($p-1$) [$(m^2 \cdot K)/W$]
RD_{P-1}	conduction thermal resistance connecting the previous node ($p-1$) with the current node (p) [$(m^2 \cdot K)/W$]
RU_P	conduction thermal resistance connecting node (p) with the previous node ($p-1$) [$(m^2 \cdot K)/W$]
RU_{P+1}	conduction thermal resistance connecting the next node ($p+1$) with the current node (p) [$(m^2 \cdot K)/W$]
ρ_j	density of the j-th layer of the slab [kg/m^3]
θ_I^h	temperature of the I th slab thermal node in the h th hour [$^{\circ}C$]
θ_{I+1}^h	temperature of the below the I th slab thermal node in the h th hour [$^{\circ}C$]
θ_{I-1}^h	temperature of the node above the I th slab thermal node in the h th hour [$^{\circ}C$]
θ_{P+1}^h	temperature of the next node [$^{\circ}C$]
θ_{P-1}^h	temperature of the previous node [$^{\circ}C$]
θ_I^{h-1}	temperature of the I th slab thermal node in the previous hour [$^{\circ}C$]
m_j	number of nodes within the respective construction layer [-]

Active Layer Node (Pipe)

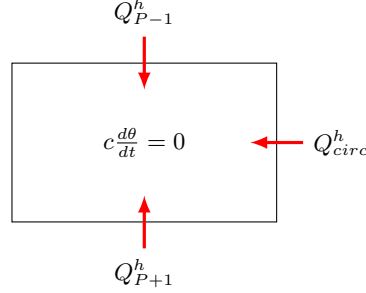


Figure 3.5: Heat balance for active layer node

The active layer node (or pipe layer node) is always located within the slab. Depending on the construction it may be close to the slab surface. In any case at least one internal node has to be located between the active layer and either surface node. The heat balance for the active layer node illustrated in figure 3.5 can be written as

$$c \frac{d\theta}{dt} = Q_{P-1}^h + Q_{P+1}^h + Q_{circ}^h = 0$$

with

$$\begin{aligned} Q_{P-1}^h &= \frac{A_F \cdot \lambda_{P-1}}{\delta_{P-1}} \cdot (\theta_{P-1}^h - \bar{\theta}_{AL}^h) \\ Q_{circ}^h &= \frac{A_F}{R_t} \cdot (\theta_{f,In}^h - \bar{\theta}_{AL}^h) \\ Q_{P+1}^h &= \frac{A_F \cdot \lambda_{P+1}}{\delta_{P+1}} \cdot (\theta_{P+1}^h - \bar{\theta}_{AL}^h) \end{aligned}$$

solved to

$$\bar{\theta}_{AL}^h = \frac{\frac{\theta_{P-1}^h \cdot \lambda_{P-1}}{\delta_{P-1}} + \frac{\theta_{f,In}^h \cdot \lambda_{P+1}}{\delta_{P+1}} + \frac{1}{R_t} \cdot \theta_{f,s}^h \cdot f_{rm}^h}{\frac{\lambda_{P-1}}{\delta_{P-1}} + \frac{\lambda_{P+1}}{\delta_{P+1}} + \frac{1}{R_t}} \quad (3.7)$$

where

A_F	floor area [m^2]
$c \frac{d\theta}{dt}$	internal energy storage [W]
δ_{P+1}	half of the thickness of the material represented by the next (p+1)-th node [m]
δ_{P-1}	half of the thickness of the material represented by the previous (p-1)-th node [m]
λ_{P+1}	thermal conductivity of the material represented by the p+1-th node [$W/(m \cdot K)$]

λ_{P-1}	thermal conductivity of the material represented by the p-1-th node [W/(m · K)]
Q_{circ}^h	delivered cooling capacity of the circuit [W]
Q_{P+1}^h	heat flow from the next node [W]
Q_{P-1}^h	heat flow from the previous node [W]
R_t	total thermal resistance of the active layer [(m ² · K)/W]
$\bar{\theta}_{AL}^h$	average active layer temperature at the h th hour [°C]
$\bar{\theta}_{AL}^h$	average active layer temperature at the h th hour [°C]
θ_{P+1}^h	temperature of the next node [°C]
θ_{P-1}^h	temperature of the previous node [°C]
$\theta_{f,In}^h$	water inlet temperature in the h th hour [°C]

Ceiling Surface Node

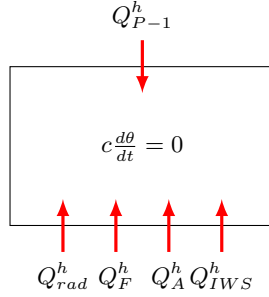


Figure 3.6: Heat balance for ceiling surface node

The ceiling surface node always follows the last of the internal nodes. It connects the lower part of the slab with the rest of the room. As a surface node it does not have any heat capacity of its own. The heat balance for the ceiling node that is illustrated in figure 3.6 can be written as

$$c \frac{d\theta}{dt} = Q_A^h + Q_F^h + Q_{IWS}^h + Q_{P-1}^h + Q_{rad,C}^h = 0$$

with

$$\begin{aligned} Q_A^h &= A_F \cdot h_{A-F} \cdot (\theta_A^h - \theta_C^h) \\ Q_F^h &= A_F \cdot h_{C-F} \cdot (\theta_F^h - \theta_C^h) \\ Q_{IWS}^h &= A_F \cdot h_{C-W} \cdot (\theta_{IWS}^h - \theta_C^h) \\ Q_{P-1}^h &= \frac{A_F}{R_{add,F} + \frac{\delta_{P-1}}{\lambda_{P-1}}} \cdot (\theta_{P-1}^h - \theta_C^h) \\ Q_{rad,C}^h &= \frac{A_F}{2A_F + A_W} \cdot Q_{rad}^h \end{aligned}$$

solved to

$$\theta_C^h = \frac{h_{A-F} \cdot \theta_A^h + h_{F-W} \cdot \theta_{IWS}^h + h_{F-C} \cdot \theta_F^h + \frac{\theta_{C-1}^h}{R_{add,F} + \frac{\delta_{P-1}}{\lambda_{P-1}}} + \frac{Q_{rad}^h}{2A_F + A_W}}{h_{A-F} + h_{F-W} + h_{F-C} + \frac{1}{R_{add,F} + \frac{\delta_{P-1}}{\lambda_{P-1}}}} \quad (3.8)$$

where

A_F	floor area [m^2]
A_W	internal wall area [m^2]
$c \frac{d\theta}{dt}$	internal energy storage [W]
δ_{P-1}	half of the thickness of the material represented by the previous (p-1)-th node [m]
h_{A-F}	convective heat transfer coefficient between air and floor [$W/(m^2 \cdot K)$]
h_{C-F}	convective heat transfer coefficient between ceiling and floor [$W/(m^2 \cdot K)$]
h_{C-W}	convective heat transfer coefficient between ceiling and internal walls [$W/(m^2 \cdot K)$]
λ_{P-1}	thermal conductivity of the material represented by the p-1-th node [$W/(m \cdot K)$]
Q_A^h	heat flow to from air node [W]
Q_F^h	heat flow to from floor node [W]
Q_{IWS}^h	heat flow from wall surface node [W]
Q_{P-1}^h	heat flow from the previous node [W]
$Q_{rad,C}^h$	total radiant heat gains at ceiling node for each h^{th} hour [W]
Q_{rad}^h	total radiant heat gains for each h^{th} hour [W]
$R_{add,F}$	additional thermal resistance covering the floor [$(m^2 \cdot K)/W$]
θ_A^h	temperature of the air thermal node in the h^{th} hour [$^{\circ}C$]
θ_C^h	temperature of the ceiling surface thermal node in the h^{th} hour [$^{\circ}C$]
θ_F^h	temperature of the floor surface thermal node in the h^{th} hour [$^{\circ}C$]
θ_{IWS}^h	temperature of the internal wall surface thermal node in the h^{th} hour [$^{\circ}C$]
θ_{P-1}^h	temperature of the previous node [$^{\circ}C$]

Internal Wall Surface Node

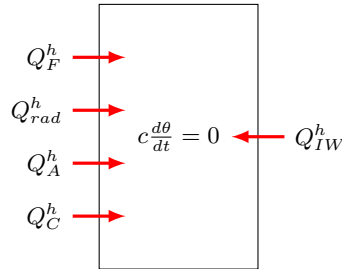


Figure 3.7: Heat balance for internal wall surface node

The internal wall surface node connects the internal wall with the rest of the room. Like the other surface nodes it does not have any heat capacity of its own. The heat balance for the wall surface node illustrated in figure 3.7 can be written as

$$c \frac{d\theta}{dt} = Q_A^h + Q_C^h + Q_F^h + Q_{IW}^h + Q_{rad,IWS}^h = 0$$

and with

$$\begin{aligned} Q_A^h &= A_W \cdot h_{A-F} \cdot (\theta_A^h - \theta_{IWS}^h) \\ Q_C^h &= A_F \cdot h_{C-F} \cdot (\theta_C^h - \theta_{IWS}^h) \\ Q_F^h &= A_F \cdot h_{C-W} \cdot (\theta_F^h - \theta_{IWS}^h) \\ Q_{IW}^h &= \frac{A_W}{2R_{add,W}} \cdot (\theta_{IW}^h - \theta_F^h) \\ Q_{rad,IWS}^h &= \frac{A_W}{2A_F + A_W} \cdot Q_{rad}^h \end{aligned}$$

solved to

$$\theta_{IWS}^h = \frac{A_W \left(h_{A-W} \cdot \theta_A^h + \frac{\theta_{IW}^h}{2R_{add,W}} + \frac{Q_{rad}^h}{2A_F + A_W} \right) + A_F \cdot h_{F-W} (\theta_F^h + \theta_C^h)}{A_W \left(h_{A-W} + \frac{1}{2R_{add,W}} \right) + 2A_F \cdot h_{F-W}} \quad (3.9)$$

where

A_F	floor area [m^2]
A_W	internal wall area [m^2]
$c \frac{d\theta}{dt}$	internal energy storage [W]
h_{A-F}	convective heat transfer coefficient between air and floor [$W/(m^2 \cdot K)$]
h_{C-F}	convective heat transfer coefficient between ceiling and floor [$W/(m^2 \cdot K)$]
h_{C-W}	convective heat transfer coefficient between ceiling and internal walls [$W/(m^2 \cdot K)$]
Q_A^h	heat flow to from air node [W]
Q_C^h	heat flow to from ceiling node [W]
Q_F^h	heat flow to from floor node [W]
Q_{IW}^h	heat flow from internal wall node [W]
$Q_{rad,IWS}^h$	total radiant heat gains at internal wall surface node for each h^{th} hour [W]
Q_{rad}^h	total radiant heat gains for each h^{th} hour [W]
$R_{add,W}$	wall surface thermal resistance [$(m^2 \cdot K)/W$]
θ_A^h	temperature of the air thermal node in the h^{th} hour [$^{\circ}\text{C}$]
θ_C^h	temperature of the ceiling surface thermal node in the h^{th} hour [$^{\circ}\text{C}$]
θ_F^h	temperature of the floor surface thermal node in the h^{th} hour [$^{\circ}\text{C}$]
θ_{IW}^h	temperature of the internal wall thermal node in the h^{th} hour [$^{\circ}\text{C}$]
θ_{IWS}^h	temperature of the internal wall surface thermal node in the h^{th} hour [$^{\circ}\text{C}$]

Internal Wall Node

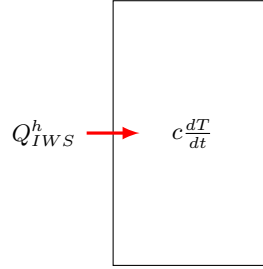


Figure 3.8: Heat balance for internal wall node

The internal wall node is only connected to the internal wall surface node. *Simply TABS* assumes that the simulated zone is connected to (thermally) identical zones through any internal wall, thus internal walls are considered to be adiabatic. Any heat that is stored in this node will eventually have to be removed again through the internal wall surface. The heat capacity of the wall is represented by one average value. The heat balance for the internal wall node illustrated in figure 3.8 and can be written as

$$c \frac{d\theta}{dt} = Q_{IWS}^h$$

and with

$$Q_{IWS}^h = \frac{A_W}{2R_{add,W}} \cdot (\theta_{IWS}^h - \theta_{IW}^h)$$

$$c \frac{d\theta}{dt} = \frac{c_{IW} \cdot A_W}{\Delta t} \cdot (\theta_{IW}^{h-1} - \theta_{IW}^h)$$

solved to

$$\theta_{IW}^h = \frac{\frac{\theta_{IWS}^h}{2R_{add,W}} + \frac{c_{IW}}{\Delta t} \cdot \theta_{IW}^{h-1}}{\frac{1}{2R_{add,W}} + \frac{c_{IW}}{\Delta t}} \quad (3.10)$$

where

A_W	internal wall area [m^2]
$c \frac{d\theta}{dt}$	internal energy storage [W]
c_{IW}	average specific heat of internal walls [$J/(m^2 \cdot K)$]
Δt	calculation time step ($\Delta t = 3600$ for hourly simulations) [s]
Q_{IWS}^h	heat flow from wall surface node [W]
$R_{add,W}$	wall surface thermal resistance [$(m^2 \cdot K)/W$]
θ_{IW}^h	temperature of the internal wall thermal node in the h^{th} hour [$^{\circ}C$]
θ_{IW}^{h-1}	temperature of the internal wall node in the previous time step [$^{\circ}C$]
θ_{IWS}^h	temperature of the internal wall surface thermal node in the h^{th} hour [$^{\circ}C$]

Air Node

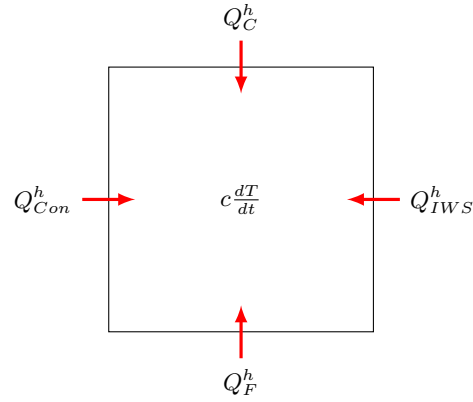


Figure 3.9: Heat balance for air node

The air node receives the entire convective heat load and is connected to the three internal room surfaces. As air has a considerably lower heat capacity than typical construction materials (e.g. concrete), it is neglected within Simply TABS. The resulting heat balance for the air node illustrated in figure 3.9 can be written as

$$c \frac{d\theta}{dt} = Q_C^h + Q_F^h + Q_{IWS}^h + Q_{con}^h$$

and with

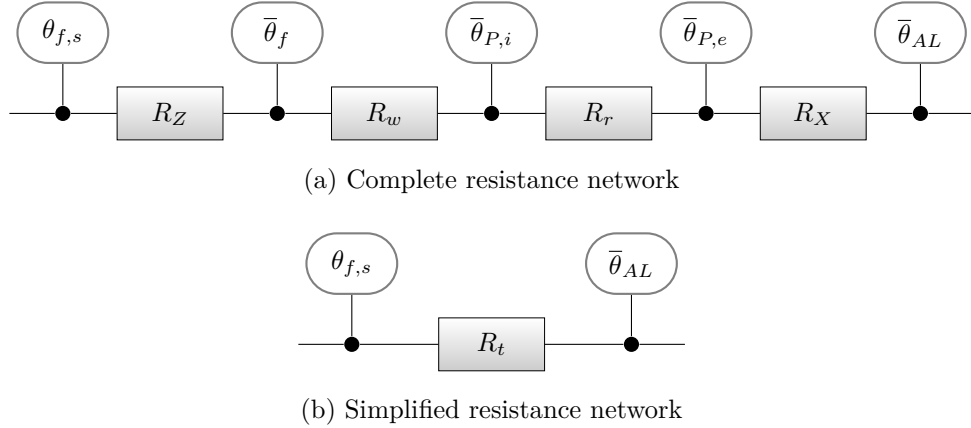
$$\begin{aligned} c \frac{d\theta}{dt} &= 0 \\ Q_C^h &= A_F \cdot h_{A-C} (\theta_C^h - \theta_A^h) \\ Q_F^h &= A_F \cdot h_{A-F} (\theta_F^h - \theta_A^h) \\ Q_{IWS}^h &= A_W \cdot h_{A-W} (\theta_{IWS}^h - \theta_A^h) \\ Q_{con}^h &= Q_{con}^h \end{aligned}$$

solved to

$$\theta_A^h = \frac{h_{A-W} \cdot A_W \cdot \theta_{IWS}^h + h_{A-F} \cdot A_F \cdot \theta_F^h + h_{A-C} \cdot A_F \cdot \theta_C^h + Q_{con}^h}{h_{A-W} \cdot A_W + h_{A-F} \cdot A_F + h_{A-C} \cdot A_F} \quad (3.11)$$

where

A_F	floor area [m^2]
A_W	internal wall area [m^2]
$c \frac{d\theta}{dt}$	internal energy storage [W]

Figure 3.10: *Resistance network of the active layer.*

h_{A-C}	convective heat transfer coefficient between air and ceiling [$W/(m^2 \cdot K)$]
h_{A-F}	convective heat transfer coefficient between air and floor [$W/(m^2 \cdot K)$]
h_{A-W}	convective heat transfer coefficient between air and internal walls [$W/(m^2 \cdot K)$]
Q_C^h	heat flow to from ceiling node [W]
Q_{con}^h	convective heat gains for each h^{th} hour [W]
Q_{con}^h	total convective heat gains for each h^{th} hour [W]
Q_F^h	heat flow to from floor node [W]
Q_{IWS}^h	heat flow from wall surface node [W]
θ_A^h	temperature of the air thermal node in the h^{th} hour [$^{\circ}C$]
θ_C^h	temperature of the ceiling surface thermal node in the h^{th} hour [$^{\circ}C$]
θ_F^h	temperature of the floor surface thermal node in the h^{th} hour [$^{\circ}C$]
θ_{IWS}^h	temperature of the internal wall surface thermal node in the h^{th} hour [$^{\circ}C$]

3.1.3 Resistance Network of the Active Layer

Simply TABS uses a linear thermal resistance model to connect the supply temperature ($\theta_{f,s}$) with the active layer temperature ($\bar{\theta}_{AL}$), turning the original 3D into a 2D problem. The standard version of the program requires the total resistance (R_t) of the active layer as an input value. In addition to this default behaviour, two internal calculations have been implemented that are described below.

Calculation of the Total Resistance for Pipes Embedded in Massive Concrete Slab

For system configurations in which the pipes are embedded towards the center of the slab, the total resistance can be calculated within *Simply TABS*. To do so, the individual resistances illustrated in figure 3.10(a) are calculated by means of equa-

tions 3.12 to 3.17. The total resistance is the sum of the individual resistances as described in equation 3.19. As for the default configuration of the tool, the actual calculations will then again be carried out using the resulting single total resistance (R_t) connecting the supply temperature ($\theta_{f,s}$) with the active layer temperature ($\bar{\theta}_{AL}$) based on the simplified resistance model illustrated in figure 3.10(b).

$$R_Z = \frac{1}{2 \cdot \dot{m}_{H,sp} \cdot c_F} \quad (3.12)$$

$$\text{valid if } \dot{m}_{H,sp} \cdot c_F \cdot (R_w + R_r + R_X) \geq 0.5 \quad (3.13)$$

$$R_w = \frac{T^{0.13}}{8 \cdot \pi} \left(\frac{d_e - 2 \cdot s_r}{\dot{m}_{H,sp} \cdot l} \right)^{0.87} \quad (3.14)$$

$$\text{valid if } Re > 2300 \quad (3.15)$$

$$R_r = \frac{T \cdot \ln \left(\frac{d_e}{d_e - 2 \cdot s_r} \right)}{2 \cdot \pi \cdot \lambda_r} \quad (3.16)$$

$$R_X = \frac{T \cdot \ln \left(\frac{T}{\pi \cdot d_e} \right)}{2 \cdot \pi \cdot \lambda_b} \quad (3.17)$$

$$\text{valid if } \frac{s_{US}}{T} > 0.3 \text{ and } \frac{s_{LS}}{T} > 0.3 \text{ and } \frac{d_e}{T} < 0.2 \quad (3.18)$$

$$R_t = R_Z + R_w + R_r + R_X \quad (3.19)$$

where

c_F	specific heat of the fluid, typically water [$J/(kg \cdot K)$]
d_e	external pipe diameter [m]
$\dot{m}_{H,sp}$	specific fluid mass flow in the circuit [$kg/(m^2 \cdot s)$]
λ_b	thermal conductivity of the material of the layer the pipe is embedded in [$W/(m \cdot K)$]
λ_r	pipe material thermal conductivity [$W/(m \cdot K)$]
l	pipe length [m]
T	pipe spacing [m]
Re	Reinolds number [-]
R_r	thermal resistance through pipe [$(m^2 \cdot K)/W$]
R_w	thermal resistance on the pipe inner side [$(m^2 \cdot K)/W$]
R_X	fictive pipe level thermal resistance [$(m^2 \cdot K)/W$]
R_Z	fictive thermal resistance for water circuit [$(m^2 \cdot K)/W$]
s_{LS}	thickness of the slab construction below the active layer [m]
s_r	pipe wall thickness [m]
s_{US}	thickness of the slab construction above the active layer [m]

Calculation of Total Resistance

As the method to calculate the fictive resistance (R_Z) described in equation 3.12 is limited by the conditions given in 3.13, an additional method to determine the total resistance (R_t) has been implemented. In this case R_Z can be calculated independently of these limitations.

$$R_t = \frac{1}{\dot{m}_{H,sp} \cdot c_F \cdot \left(1 - \exp \left(- \frac{1}{(R_w + R_r + R_X + \frac{1}{U_{US} + U_{LS}}) \cdot \dot{m}_{H,sp} \cdot c} \right) \right)} - \frac{1}{U_{US} + U_{LS}} \quad (3.20)$$

with

$$\frac{1}{U_{US} + U_{LS}} = \frac{1}{h_F} + \sum_{j=1}^{J_{US} + J_{LS}} \left(\frac{\rho_j}{\lambda_j} \right) + \frac{1}{h_C} \quad (3.21)$$

and

$$h_F = h_{F-W} + h_{F-A} + h_{F-C} \quad (3.22)$$

$$h_C = h_{C-W} + h_{C-A} + h_{C-F} \quad (3.23)$$

where

c_F	specific heat of the fluid, typically water [$J/(kg \cdot K)$]
h_C	convective heat transfer coefficient between ceiling and other surfaces [$W/(m^2 \cdot K)$]
h_{C-A}	convective heat transfer coefficient between ceiling and air [$W/(m^2 \cdot K)$]
h_{C-F}	convective heat transfer coefficient between ceiling and floor [$W/(m^2 \cdot K)$]
h_{C-W}	convective heat transfer coefficient between ceiling and internal walls [$W/(m^2 \cdot K)$]
h_F	convective heat transfer coefficient between floor and other surfaces [$W/(m^2 \cdot K)$]
h_{F-A}	convective heat transfer coefficient between floor and air [$W/(m^2 \cdot K)$]
h_{F-C}	convective heat transfer coefficient between floor and ceiling [$W/(m^2 \cdot K)$]
h_{F-W}	convective heat transfer coefficient between floor and internal walls [$W/(m^2 \cdot K)$]
J_{LS}	Number of material layers in lower part of slab [-]
J_{US}	Number of material layers in upper part of slab [-]
λ_j	thermal conductivity of the j-th layer of the slab [$W/(m \cdot K)$]
$\dot{m}_{H,sp}$	specific fluid mass flow in the circuit [$kg/(m^2 \cdot s)$]
ρ_j	density of the j-th layer of the slab [kg/m^3]
R_r	thermal resistance through pipe [$(m^2 \cdot K)/W$]
R_t	total thermal resistance of the active layer [$(m^2 \cdot K)/W$]
R_w	thermal resistance on the pipe inner side [$(m^2 \cdot K)/W$]
R_X	fictive pipe level thermal resistance [$(m^2 \cdot K)/W$]
U_{LS}	heat transfer coefficient of the lower part of the slab [$W/(m^2 \cdot K)$]
U_{US}	heat transfer coefficient of the upper part of the slab [$W/(m^2 \cdot K)$]

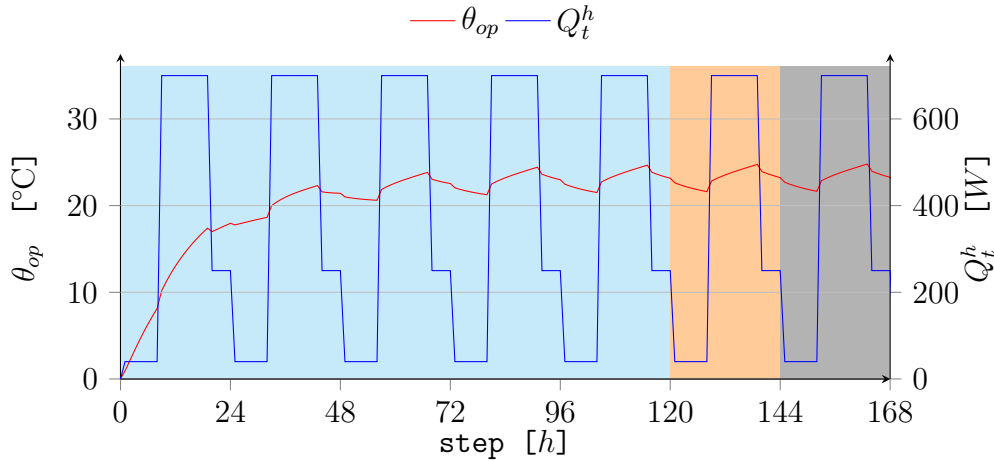


Figure 3.11: *Temperature development from start to end of a simulation. By default, only the final solution (middle box) is reported. The first iterations (first box) are usually discarded. Because the simulation stops as a valid solution is found, the remaining data (last box) would not be calculated. For this example all temperatures and heat fluxes have been initialised with 0 °C and 0 W respectively.*

The resistances R_w , R_r and R_X are unchanged and can be calculated as described in equations 3.14 through 3.18.

3.1.4 Simulation Progress

At the beginning of any simulation executed with *Simply TABS* all node temperatures are initialised with default values.¹ Starting from here, one full cycle is executed and evaluated as described in section 3.1.6. If the results lie within the tolerated accuracy range, the current iteration is saved to the result file. If not, one additional iteration is executed and the new results are again evaluated.

In figure 3.11 the cyan area represents the startup phase. The orange area indicates the data that is stored in the result file and the gray area would usually not be calculated at all as the simulation is terminated after arriving at a valid solution. This procedure is the same for all simulations. Depending on the input data, the startup phase can be substantially longer than in the included example. In some cases a stationary solution might not be possible. In these cases the simulation is aborted after a defined number of iterations.

¹all thermal nodes $\theta_p^{h=0} = 0^\circ\text{C}$ and all heat flows $Q^{h=0} = 0\text{W}$.

3.1.5 Simulation Duration

One purpose behind *Simply TABS* is to have a tool that can determine the minimal needed plant size for series of days with high cooling loads. As is shown in section 3.1.4 the same simulation will be repeated until a solution is found. For such a case, input data has to be provided for only one day. *Simply TABS* is however capable of executing simulations of any given length. With this it is possible to further investigate the capabilities of TABS in question. The following sections partly rely on this capability.

3.1.6 Requirements for a Stationary Simulation

For each individual step of the simulation the stationarity is tested. After all temperatures have been calculated, the results are compared with those of the previous iteration as described in equation 3.24. If the temperature change between the two iterations drops below a specified threshold (as determined by equation 3.25), the current results are accepted as the results for the current time step. If no solution is found within a predetermined number of iterations (see equation 3.26), the simulation fails.

$$\xi^{step} = \sum_{P=1}^{P_{last}} (\theta_P^h - \theta_P^{h'}) \quad (3.24)$$

with

$$\xi^{step} < \xi^{max,step} \quad (3.25)$$

$$n^{actual,step} < n^{max,step} \quad (3.26)$$

where

θ_P^h	temperature of node P at the current step of this iteration [°C]
$\theta_P^{h'}$	temperature of node P at the previous step of this iteration [°C]
ξ^{step}	current deviation between calculation steps [K]
$\xi^{max,step}$	maximum tolerance allowed in calculation step [K]
$n^{actual,step}$	current iteration [-]
$n^{max,step}$	maximum number of allowed iterations [-]

To evaluate if a valid solution for the entire simulation (all time steps) has been found, the same principle is used. However, the results of the current step are compared with those of the same time step within the previous simulation run rather than the previous time step of the same simulation run (see equation 3.27). Again, if the differences are below a predefined threshold (see equation 3.28), the

solution is accepted and the simulation ends. If the differences are too big, an additional loop is executed as long as the maximum number of loops has not been reached (see equation 3.29). If this should be the case, the simulation is terminated without a solution.

$$\xi^{day} = \sum_{P=1}^{P_{last}} \left(\theta_P^h - \theta_P^{h_{prevDay}} \right) \quad (3.27)$$

with

$$\xi^{day} < \xi^{max,day} \quad (3.28)$$

$$n^{actual,day} < n^{max,day} \quad (3.29)$$

where

θ_P^h	temperature of node P at the current step of this iteration [°C]
$\theta_P^{h_{prevDay}}$	temperature of node P at the same step during previous iteration [°C]
ξ^{day}	current deviation between calculation iterations [K]
$\xi^{max,day}$	maximum tolerance allowed in iterative calculation [K]
$n^{actual,day}$	current iteration [-]
$n^{max,day}$	maximum number of allowed iterations [-]

3.1.7 Follow-up Simulations

Simply TABS can be configured to run follow-up simulations. Follow-up simulations can be used to easily determine the minimal plant size needed to still achieve sufficient cooling. Secondly, it can determine how long the simulated room stays within acceptable parameter limits if cooling is further reduced (or even completely shut off).

In order for follow-up simulations to be executed, the original simulation needs to have a stationary solution as explained in section 3.1.6. The starting conditions for each of the follow-up simulations are the temperatures and heat fluxes reached at the end of the original simulation. *Simply TABS* will report their results regardless of stationarity. The maximum available cooling power is reduced for each of the follow-up simulations according to:

$$P_{circ}^{h,max,new} = P_{circ}^{h,max} \cdot \left(1 - \frac{\text{follow up simulation no X of Y}}{Y} \right) \quad (3.30)$$

where

$P_{circ}^{h,max,new}$	maximum cooling capacity of the circuit in the h th hour for follow-up simulations [W]
$P_{circ}^{h,max}$	maximum cooling capacity of the circuit in the h th hour [W]

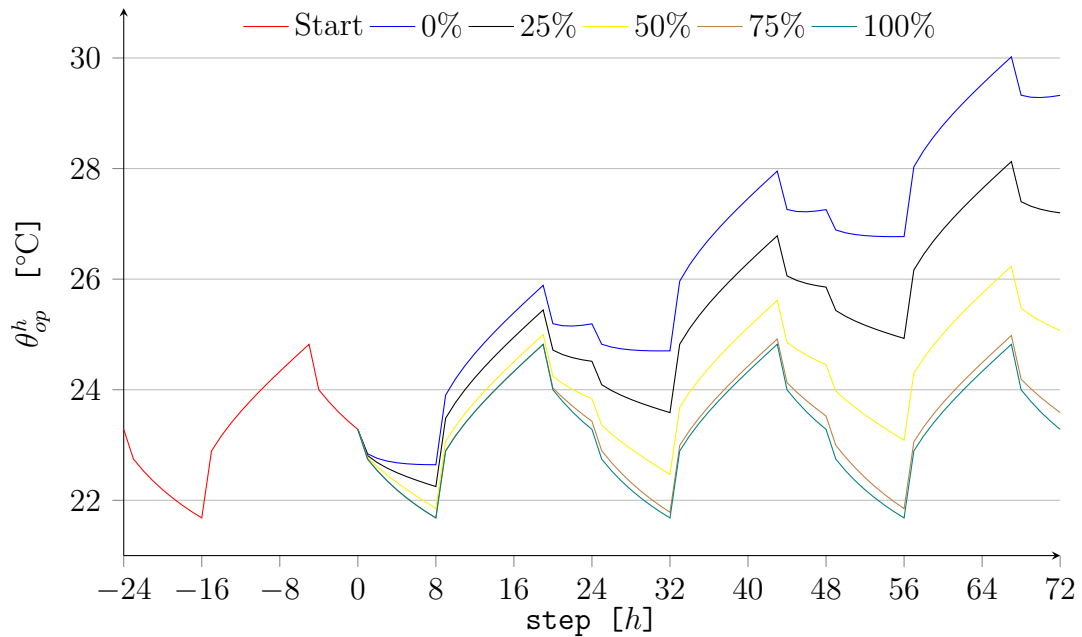


Figure 3.12: *Development of the operative temperature with reduced maximum cooling power during three days time. Case: RT_3days*

As can be seen in figure 3.12, in this example (Case: RT_3days), the operative temperature would still be acceptable after three days with a maximum cooling power reduced to only 50% of the original. If the cooling system however fails completely, the results show that temperatures will exceed comfort levels on the second day.

The apparent drop in operative temperature even for the case with complete cooling failure is a result of the heat distribution throughout the thermal nodes. During hours with high loads, individual nodes store more energy than they lose to connected cooler nodes while they are able to cool down a bit during times when heat sources are not present.

In order to compensate for heat losses to the environment with high internal temperatures, follow-up simulations can be combined with the optional heat load reduction introduced in section 3.1.8. The effects of the reduced maximum cooling power are mostly seen for longer simulation periods.

Follow-up simulations can also be used to evaluate the temperature development in a building if the cooling load exceeds the installed cooling capacity. For this purpose the original simulation has to be set up with an increased maximum cooling capacity and the follow-up simulations have to be set up in a way that the desired maximum cooling load is among the desired output levels. Also this should always be combined with the optional heat load reduction.

3.1.8 Reduction of Heat Loads to Simulate Connection with the Environment

As *Simply TABS* in itself is not aware of the environment, the temperatures in the room would rise indefinitely if the loads exceed the available cooling capacity. With the introduction of a fictional connection to the environment (section 3.1.8) this problem can be overcome. Using careful configuration of the parameters, the heat loss to the environment can be simulated by gradually reducing the loads with rising internal temperatures. The intent of this is to get more realistic results in cases with overheating. The option should always be used in a way that the maximum temperature is above the temperature range of interest. If the function would be used to limit the room temperatures to stay within the comfort area, the conclusions based on the results would likely be faulty. Using this function should therefore be carefully considered. This option is only relevant for cases where the provided cooling cannot keep the internal temperatures at acceptable levels. Without the heat load reduction temperatures would rise indefinitely as the external heat gain is independent of the indoor temperature. To simulate this behaviour the heat load are simply reduced if certain operative temperatures are exceeded. It may be used to emulate the effects of high difference between indoor and outdoor temperatures in a greatly simplified way.

In combination with follow-up simulations (section 3.1.7), this can be used to achieve more realistic results as the temperatures would otherwise rise indefinitely. In some cases it is also possible to use this option to run simulations that originally fail the stability requirements set in section 3.1.6. This is mostly the case if the available cooling power throughout the simulation time is insufficient. The assumed heat loss through the facade can be calculated as the difference between the specified heat loads and the ones reported with the other simulation results.

In order to reduce the heat loads, a heat load fraction (f_Q^h) is introduced. The total heat load (Q_t^h) is then calculated through equation 3.31.

The function 3.32 uses three parameters that can be adjusted on an hourly base. The maximum temperature ($\theta_{op,max}^h$) is setting the base line at which the simulated heat loss should take effect. The temperature range ($\theta_{op,range}^h$) defines the reduction of the heat loads on the room from the original 100% to 0%. The temperature offset ($\theta_{op,os}^h$) can be used to move this range relative to the maximum temperature. Table B.3 presents the parameters used for the simulations displayed in figure 3.13.

$$Q_t^h = (Q_{rad}^h + Q_{con}^h) \cdot f_Q^h \quad (3.31)$$

with

$$f_Q^h = \begin{cases} 1 & \text{if } \theta_{op} \leq \theta_{op,max}^h + \theta_{op,os}^h = A \\ 1 - \frac{\theta_{op}^h - (\theta_{op,max}^h + \theta_{op,os}^h)}{\theta_{op,range}^h} & \text{if } A < \theta_{op}^h < B \\ 0 & \text{if } \theta_{op}^h \geq \theta_{op,max}^h + \theta_{op,os}^h + \theta_{op,range}^h = B \end{cases} \quad (3.32)$$

where

f_Q^h	fraction of the heat load actually impacting the room [%]
Q_{con}^h	convective heat gains for each h th hour [W]
Q_{rad}^h	total radiant heat gains for each h th hour [W]
Q_t^h	total convective heat gains for each h th hour [W]
$\theta_{op,max}^h$	internal temperature at which simulated heat loss starts to take effect [°C]
θ_{op}^h	operative temperature in the h th hour in the room [°C]
$\theta_{op,os}^h$	can be used to offset $\theta_{op,range}^h$ [K]
$\theta_{op,range}^h$	temperature range in which the reduction takes place [K]

Figure 3.13 shows this function in use. The input is the same that has been used in figure 3.12 but extended to 6 days. For better comparison, the results for continuous cooling ($RH_{P_{circ}^{h,max}} = 100\%$) have been included. As can be seen, the temperature of the original case rises unchecked, whereas the temperatures in the three cases with active environmental heat loss all converge on 26°C.

As this approach is greatly simplified, it is important to keep in mind that reported results do not represent reality. However, with careful control of the configuration, the function may be used to avoid unreasonably high operative temperatures. Within the limitations of *Simply TABS* this was however the best possible solution. A more sophisticated model of the environment would have conflicted with its basic design principles.

3.1.9 Reduction of the Applied Cooling to Avoid Undercooling

Originally, *Simply TABS* had been developed solely to evaluate if the installed chiller and the selected operation could provide sufficient cooling during a design day. This would however often lead to undercooling in the room. To prevent this, a simple method was devised to limit cooling (section 3.1.9) based on the operative temperature at the time. The maximum cooling is gradually reduced if the operative temperature falls below a previously defined threshold. Thanks to a flexible implementation of the feature, it is possible to set different thresholds. With this it is possible to slightly undercool the building during night time in order to have an additional cooling reserve during the next day if desired. Using

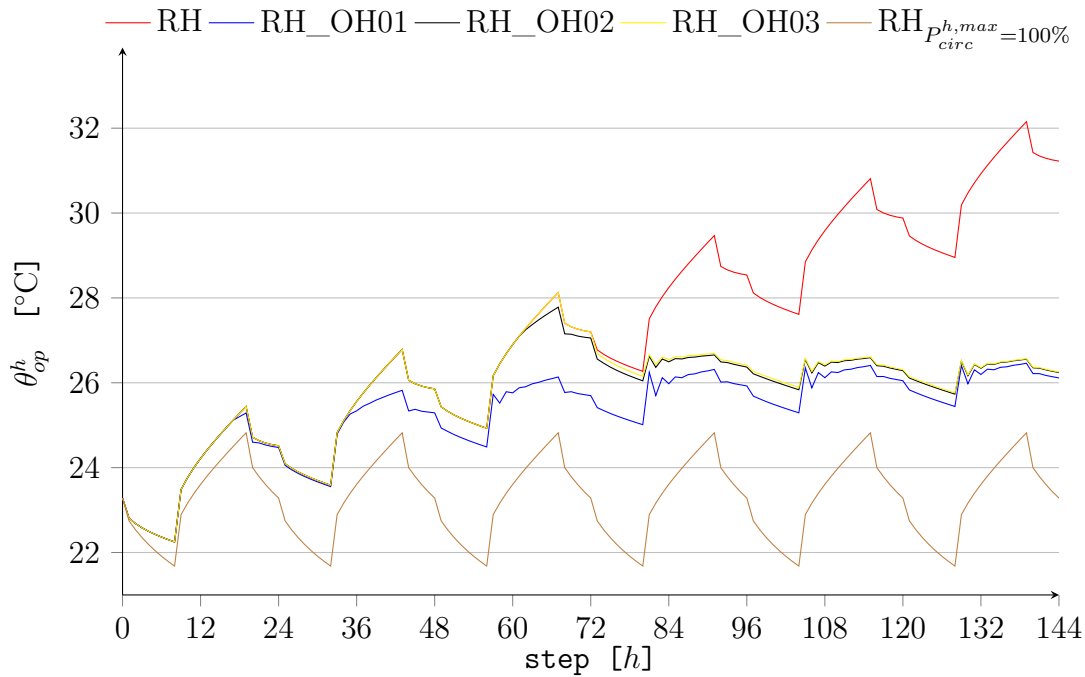


Figure 3.13: *Development of the operative temperature with simulated environmental heat loss (cases RH_OH01-03) and reduced maximal cooling power (25%) during six days. Case: RT_6days_OH, see table B.1 and B.3 for setup*

the function while trying to optimise the installed cooling capacity should be done with care as it may directly influence the usable cooling capacity itself.

In the original concept, the control of the supply water temperature is limited to two parameters and independent of the operative temperature in the room. The extended version offers additional controls connecting the applied cooling capacity to the operative temperature.

Standard Control Function

The control proposed in ISO 11855-4 aims at providing cooling based on a single set point as long as sufficient cooling capacity is available. If the cooling capacity of the chiller is sufficient, the return mass flow is cooled to the desired supply temperature ($\theta_{f,In}^{h,set}$). Otherwise, the lowest achievable supply temperature is used. This approach basically means that there is no control. If possible, the supply temperature will always be the set point temperature, regardless of indoor tem-

peratures.

$$\theta_{f,In}^h = \max \left(\theta_{f,In}^{h,set}, \theta_{f,In}^{h,set} + \frac{Q_{circ}^h - P_{circ}^{h,max}}{\dot{m}_{H,sp} \cdot A_F \cdot c_W} \right) \quad (3.33)$$

where

A_F	floor area [m^2]
c_W	specific heat of the fluid in the circuit [$J/(kg \cdot K)$]
$\dot{m}_{H,sp}$	specific fluid mass flow in the circuit [$kg/(m^2 \cdot s)$]
$P_{circ}^{h,max}$	maximum cooling capacity of the circuit in the h^{th} hour [W]
Q_{circ}^h	delivered cooling capacity of the circuit [W]
$\theta_{f,In}^{h,set}$	water inlet set-point temperature in the h^{th} hour (also minimal supply temperature) [$^{\circ}C$]
$\theta_{f,In}^h$	water inlet temperature in the h^{th} hour [$^{\circ}C$]

Extended Control Function

Using the standard control as described before will in many cases lead to undercooling. To prevent this, equation 3.33 has been extended to include a cooling power fraction (f_P^h), shown in equation 3.34.

$$\theta_{f,In}^h = \max \left(\theta_{f,In}^{h,set}, \theta_{f,In}^h + \frac{Q_{circ}^h - P_{circ}^{h,max} \cdot f_P^h}{\dot{m}_{H,sp} \cdot A_F \cdot c_W} \right) \quad (3.34)$$

with

$$f_P^h = \begin{cases} 1 & \text{if } \theta_{op}^h \geq \theta_{op,min}^h + \theta_{op,os}^h = A \\ 1 - \frac{\theta_{op,min}^h + \theta_{op,os}^h - \theta_{op}^h}{\theta_{op,range}^h} & \text{if } A > \theta_{op}^h > B \\ 0 & \text{if } \theta_{op}^h \leq \theta_{op,min}^h + \theta_{op,os}^h + \theta_{op,range}^h = B \end{cases} \quad (3.35)$$

where

A_F	floor area [m^2]
c_W	specific heat of the fluid in the circuit [$J/(kg \cdot K)$]
f_P^h	fraction of the maximum cooling power that is used [%]
$\dot{m}_{H,sp}$	specific fluid mass flow in the circuit [$kg/(m^2 \cdot s)$]
$P_{circ}^{h,max}$	maximum cooling capacity of the circuit in the h^{th} hour [W]
Q_{circ}^h	delivered cooling capacity of the circuit [W]
θ_{op}^h	operative temperature in the h^{th} hour in the room [$^{\circ}C$]
$\theta_{op,min}^h$	internal temperature at which heat load reduction takes effect [$^{\circ}C$]
$\theta_{op,os}^h$	can be used to offset $\theta_{op,range}^h$ [K]
$\theta_{op,range}^h$	temperature range in which the reduction takes place [K]
$\theta_{f,In}^{h,set}$	water inlet set-point temperature in the h^{th} hour (also minimal supply temperature) [$^{\circ}C$]
$\theta_{f,In}^h$	water inlet temperature in the h^{th} hour [$^{\circ}C$]

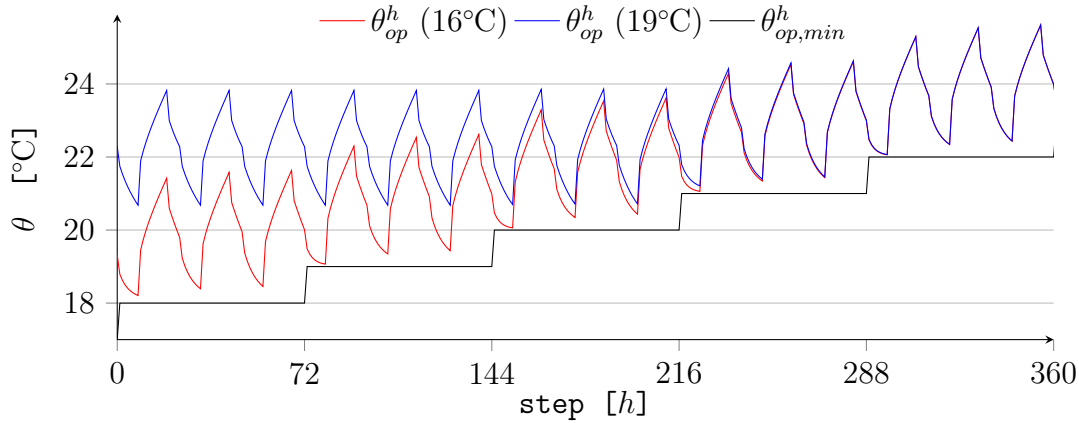


Figure 3.14: *Temperature change due to cooling power limitation to prevent undercooling. The minimal operative temperature ($\theta_{op,min}^h$) is increased by 2°C every 72 hours. Relevant settings can be found in table B.2.*

The cooling power fraction as described in equation 3.35 is depending on three input values. The minimal operative temperature ($\theta_{op,min}^h$) is the value the actual operative temperature (θ_{op}^h) should never fall below. The temperature offset ($\theta_{op,os}^h$) can be used to change the point at which cooling will be reduced away from the minimal operative temperature. Finally the temperature range ($\theta_{op,range}^h$) defines the temperature band in which cooling will be reduced from 100% to 0%.

With a proper setup of these values it is possible to avoid undercooling throughout the simulation. Since the input for this function needs to be provided for every hour, it is also possible to relax or tighten the rules during specific hours. Figure 3.14 illustrates the use of this function. The minimal operative temperature ($\theta_{op,min}^h$) is increased by 2°C every 72 hours. As can be seen, the setup can prevent undercooling efficiently. However, as temperatures never get as low as the allowed minimal temperature, some fine tuning of the parameters (see table B.2) might be useful.

3.2 System Validation

In order to validate the simulation results of *Simply TABS*, two comparisons have been made. First *Simply TABS* has been tested against ISO 11855-4, based on the input data provided in ISO 11855-4 Annex C. Second a slightly modified simulation in *Simply TABS* has been compared with simulation results from IDA ICE 4.5. The input for all simulations can be found in Appendix B.

3.2.1 Validation against ISO 11855

The available results for the ISO 11855 are limited to air-, floor surface- and ceiling surface temperature as well as the heat flows at the floor-, ceiling-, internal wall- and circuit nodes.

Temperature results

Where data for the ISO 11855 is available, the correlation with the results of *Simply TABS* is generally very high. Figures 3.15(a), 3.15(b) and 3.15(c) show that the results from *Simply TABS* and ISO 11855 are nearly identical and well within acceptable limits. It should be noted that the results from ISO 11855 do not look entirely as expected. The temperature should increase linearly between steps 8 and 19 as the input is constant during this time. The small visual deviations are however caused by the results having been provided with one decimal digit only. This is of course correct as additional decimal digits would be well below the accuracy of any simulation tool. It can however raise questions such as this when plotting the data.

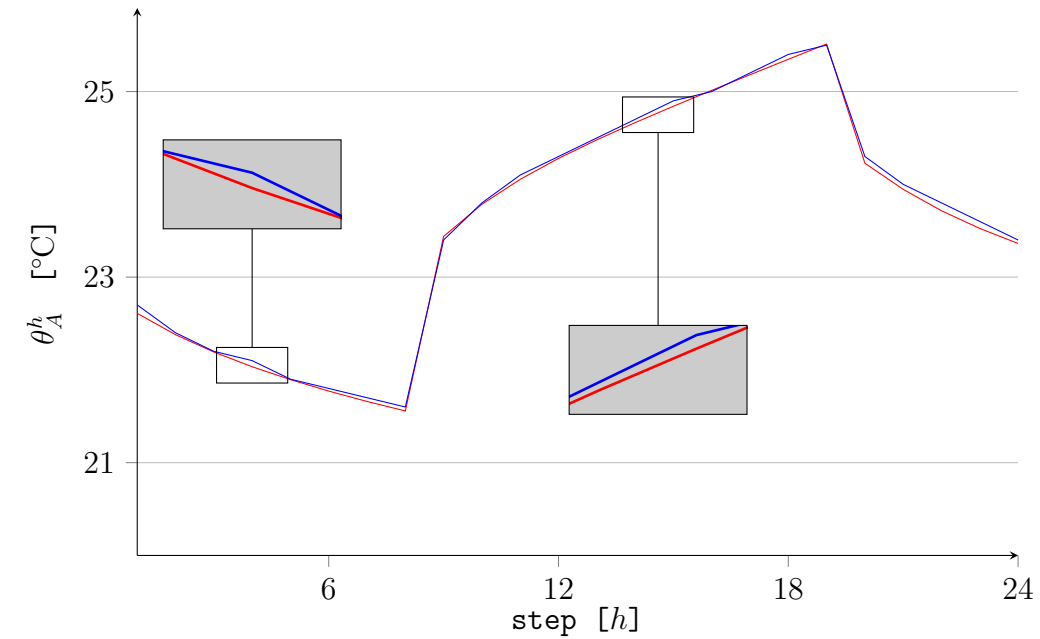
Heat Flow results

Regarding the heat flow through ceiling (figure 3.16(a)) and floor (figure 3.16(b)), *Simply TABS* and ISO 11855 are on par. The heat that is entering the room as radiant and convective loads can temporarily be stored inside the internal walls and the slab construction. This is for instance the case when the TABS are not operational. In figure 3.16(c) it can be seen that the heat flow to and from the internal wall is highest shortly after the system operation is switched off (step 8) or on (step 19).

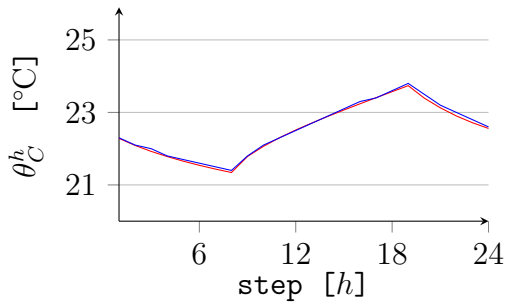
The only significant difference accrues for the heat removed by the circuit displayed in figure 3.16(d). Once the system is turned back on, ISO 11855 only uses 87% of the maximum power ($P_{circ}^{h,max}$) for cooling whereas *Simply TABS* instantly cools at maximum power as was to be expected.

3.2.2 Validation against IDA ICE 4.5

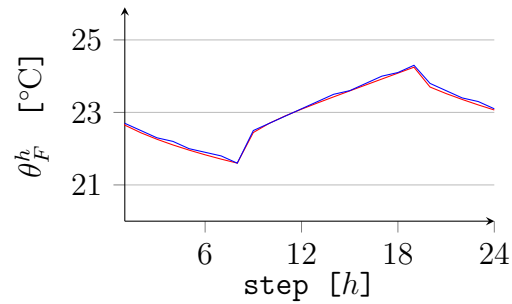
The input data used for the comparison with IDA ICE 4.5 is identical to the data used for the previous comparison, except for the added thermal resistance for the floor surface that has been set to zero ($R_{add,F} = 0 \text{ (m}^2 \cdot \text{K)/W}$).



(a) Air temperature



(b) Ceiling temperature



(c) Floor temperature

— *Simply TABS* — ISO 11855

Figure 3.15: Comparison of calculated and given temperatures for Case RT that can be found in table B.1 and ISO 11855-4

Temperature results

Comparing *Simply TABS* with IDA ICE 4.5 does not result in the same level of correlation as with ISO 11855. Figure 3.17(a) shows that the air temperature reported by IDA ICE 4.5 is about 0.4°C lower during the cooling period but is about 0.3°C higher while the system is off. Throughout the simulation the ceiling- (θ_C^h) and floor (θ_F^h) temperatures reported by IDA are about 0.7°C lower as can be

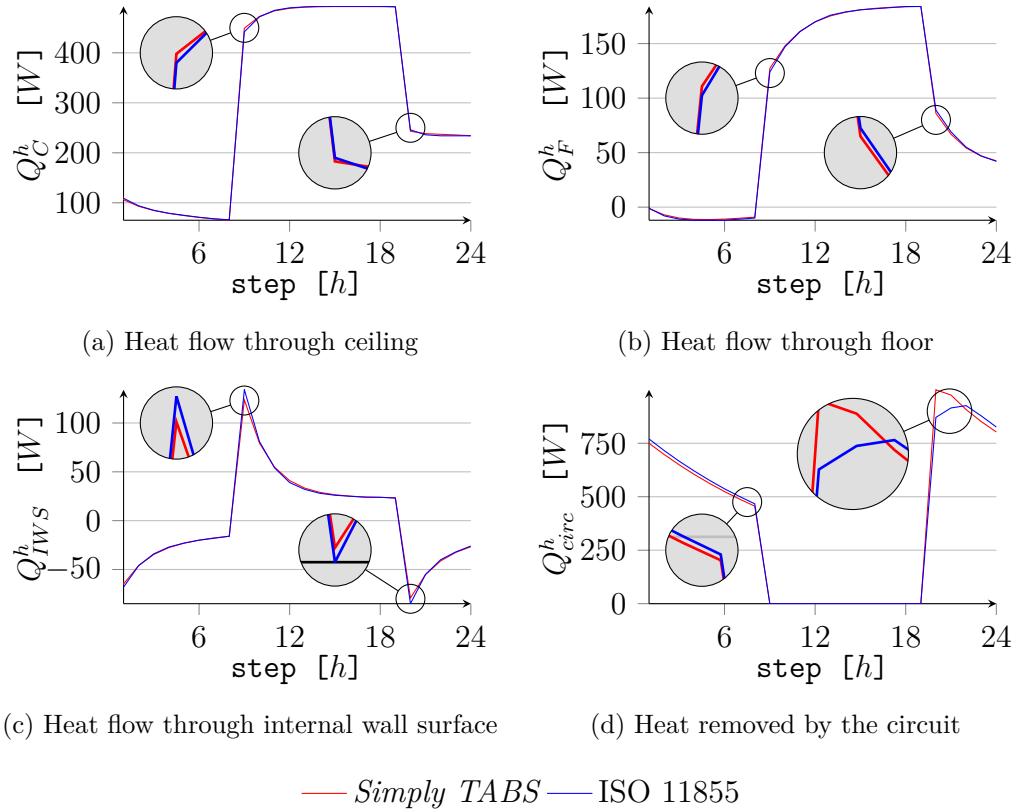


Figure 3.16: Comparison of calculated and given heat flux for Case RT that can be found in table B.1 and ISO 11855-4

seen in figures 3.17(b) and 3.17(c). For the internal wall temperature (θ_{IWS}^h) this difference is back down to about 0.3°C as illustrated in figure 3.17(d).

Since the mean radiant temperature is based on the surface temperatures of the room, it was expected that it is on average lower for IDA ICE 4.5 than for *Simply TABS* as displayed in figure 3.17(e). Due to the higher air temperature during the day time, the reported operative temperature during the day time is nearly identical for both tools (see figure 3.17(f)). In the early morning, after the system has been operational for some hours, the difference increases to a maximum of 0.5°C . Due to the fact that the operative temperature is usually used to evaluate thermal comfort in a space, both IDA ICE 4.5 as well as *Simply TABS* would lead to the same conclusions.

Considering the general differences in building simulation Behrendt et al. (2011), the observed differences are generally within acceptable limits at all times and similar conclusions would be drawn from the presented data.

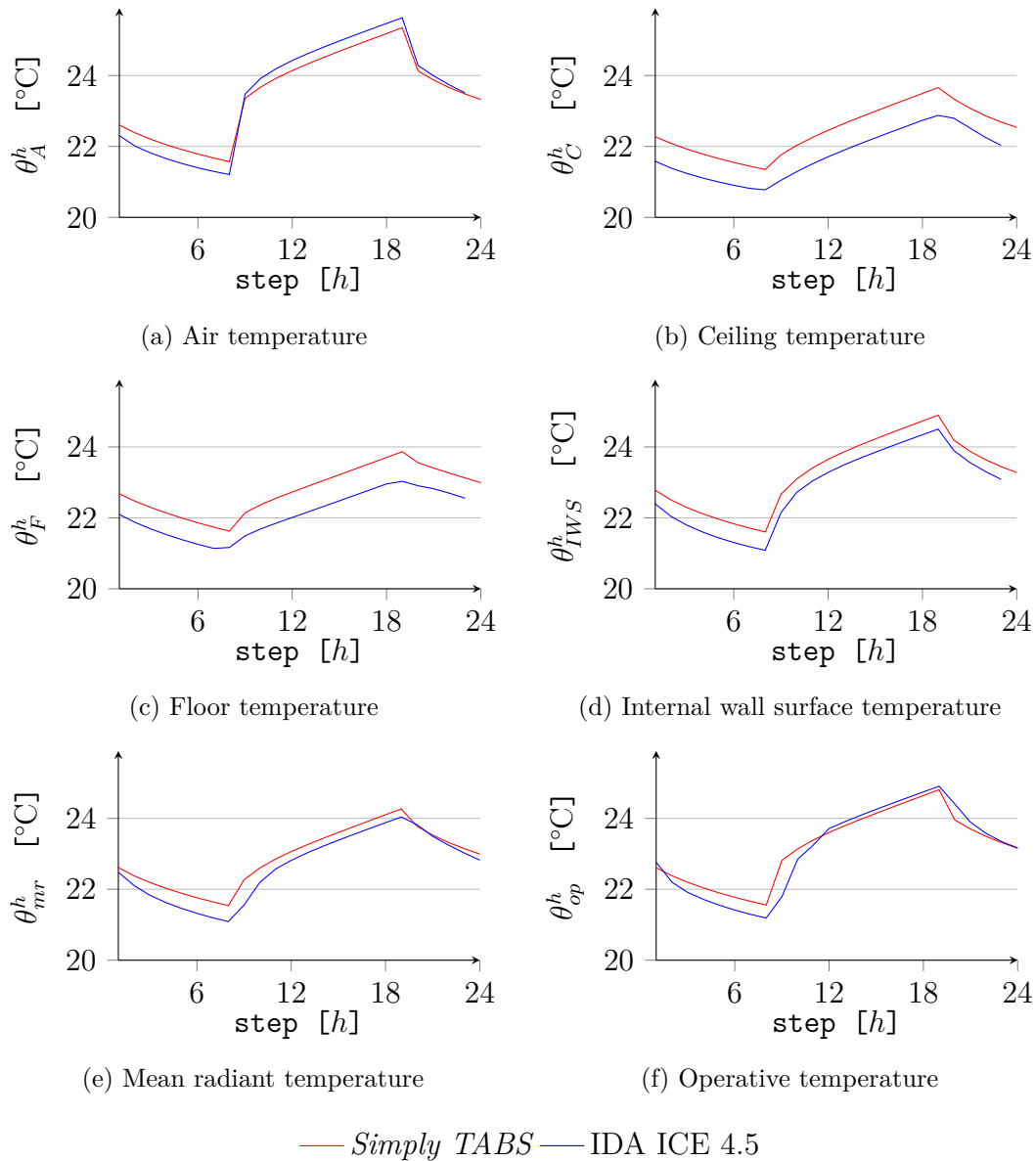


Figure 3.17: Comparison of temperatures for *Simply TABS* and *IDA ICE 4.5* for Case *RT_NoAddRes*

Heat Flow results

The differences between *Simply TABS* and *IDA ICE 4.5* are also relatively low for the observed heat transmissions within the room. For both, the heat transfer through the ceiling as shown in figure 3.18(a) and through floor as shown in figure

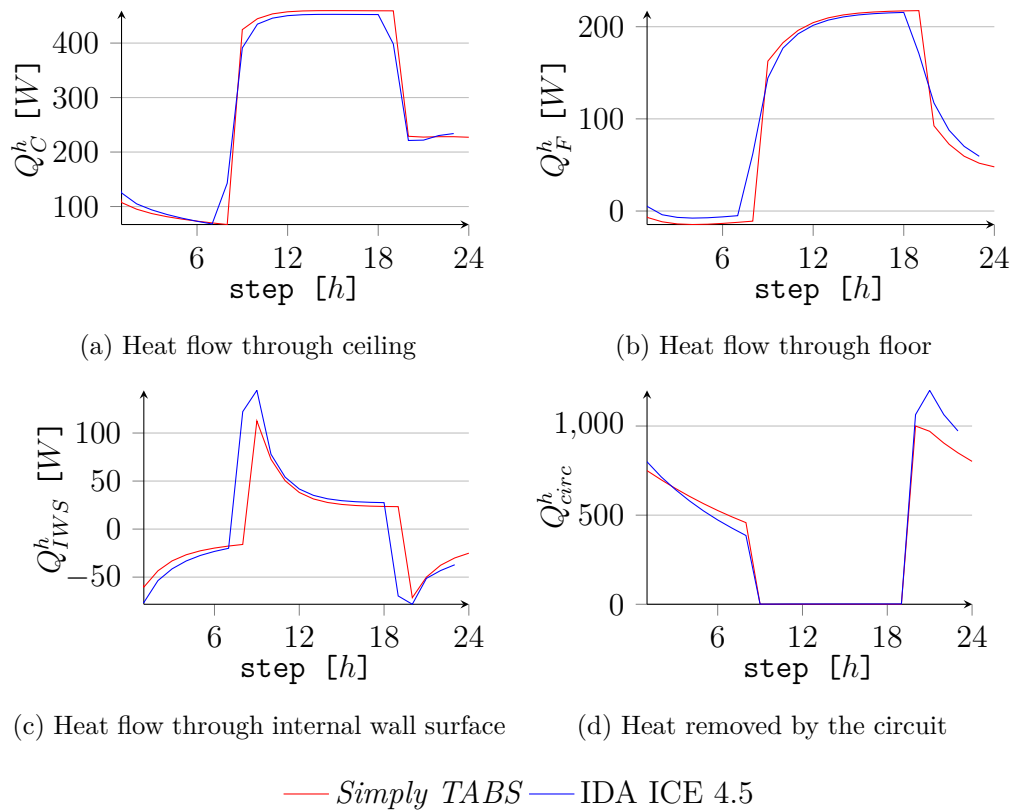


Figure 3.18: Comparison of heat flux from *Simply TABS* and *IDA ICE 4.5* for Case *RT_NoAddRes*

3.18(b), results only differ when operations are switched from ‘on’ to ‘off’ or vice versa. In both cases IDA ICE 4.5 seems to react ahead of time. This time shift is most visible for the heat transmission to the internal wall shown in figure 3.18(c). Only for the heat removed by the circuit this offset is not visible. However as can be seen in figure 3.18(d), IDA ICE 4.5 removes up to 1,200 W from the circuit, exceeding the maximum available cooling power by 20%. The overall heat removed by the circuit is however nearly identical in both cases.

Chapter 4

Climate Classification for TABS

Today TABS are often used for cooling in new buildings. During the design of buildings utilising TABS it is important to consider the possibility of condensation on controlled surfaces.

The intention is to create a simple Climate Classifications to determine the usability of TABS for a modern building throughout Europe. The classification should provide a quick answer to the following questions:

Does the building need ...

- ... a heating system?
- ... a cooling system?
- ... a heating and cooling system?
- ... no dehumidification?
- ... intermittent dehumidification?
- ... continuous dehumidification?

4.1 Existing climate classifications

A number of already existing climate classifications have been considered but due to different shortcomings they could not be used.

The first existing climate classification that has been investigated is the Köppen-Geiger system. It has a history of over 100 years and has been continuously developed and updated ever since. This strong basis made it the perfect candidate for further investigations. For the purpose of the intended climate classification for TABS, it was determined that the provided data on perspiration would not be sufficient, instead some measure of humidity would be needed. As the original intend of the Köppen-Geiger classification was to establish different vegetation zones, this is not surprising. For this purpose, precipitation is more important than humidity levels.

Another system that has been considered are the ASHRAE Climate Zones. However, in this case insufficient data was provided as climate data only includes precipitation for the USA and humidity is completely omitted. Nevertheless the ASHRAE Climate Zones have been used in a previous study (Tian and Love, 2009) comparing the use of TABS to a variable air volume (VAV) and radiator based systems with regard to energy savings. Only US cities have been included in this study.

Since the operation of TABS can be greatly limited by humidity, it is important to have a classification that pays attention to this aspect. The new introduced classification as a combination of heating and cooling degree days as well as humidity can achieve this.

The here presented system is an extension of the climate classification introduced by Behrendt and Christensen (2013).

4.2 Methods

The new Climate Classification for TABS provides information about the thermal and the humidity load at a given location. For each location, the proposed classification is based on input for ...

- ... the ambient air temperature for a reference year.
- ... the ambient dew point temperature for a reference year.
- ... the base temperature of a reference building.

Both, the ambient air- and dew point temperature, are depending on location and time. The base temperature of a building however is a constant for any given building¹ and not usually changing with the location or over time.

The ambient air temperature and the base temperature are used to calculate so-called HDDs and CDDs. The dew point temperature is used for the calculation of dew point hours (DPH).

The climate classification results from comparing these values to user defined upper and lower limits. Thus, the classification can be adopted to fit the user requirements, as for instance how many hours of cooling may be required before the climate is actually considered cooling based.

¹It is possible that some building systems (e.g. external blinds) influence the base temperature to some degree.

4.2.1 Base Temperature

The base temperature (θ_b) - or balance point temperature - is defined as the outside air temperature at which the heating and cooling demand is zero. Including any gains from occupants, solar radiation, lighting, equipment, etc. - i.e. the average gains are equal to the average heat loss of the building in the given period. Or in simpler terms: No system (heating or cooling) is required, if the outside temperature is equal to the base temperature (ASHRAE, 2001).

With this definition, three distinct cases can be defined. The heating case, in which additional heating is needed to achieve the desired operative temperature (θ_{op}). The balance case, in which heat losses and gains are the same and the operative temperature is equal to the current set point temperature (θ_{set}). The cooling case in which the heat loads exceed the heat losses and in turn require active cooling to maintain the desired set point temperatures.

For a practical application one base temperature has to be defined for each set point temperature in a building. Considering only a heating and a cooling season with different desired indoor temperatures, two base temperatures are necessary. Assuming constant net heat gains ($Q_{net,gain}$) for each season, equation 4.1 can be used to calculate the appropriate base temperatures for a given building.

$$Q_{net,gain} = h \cdot (\theta_{set} - \theta_b) \quad (4.1)$$

In a real application however the net heat flow would not be constant for extended periods of time. Instead, with changing internal and external conditions the real base temperature would fluctuate as well. Never-

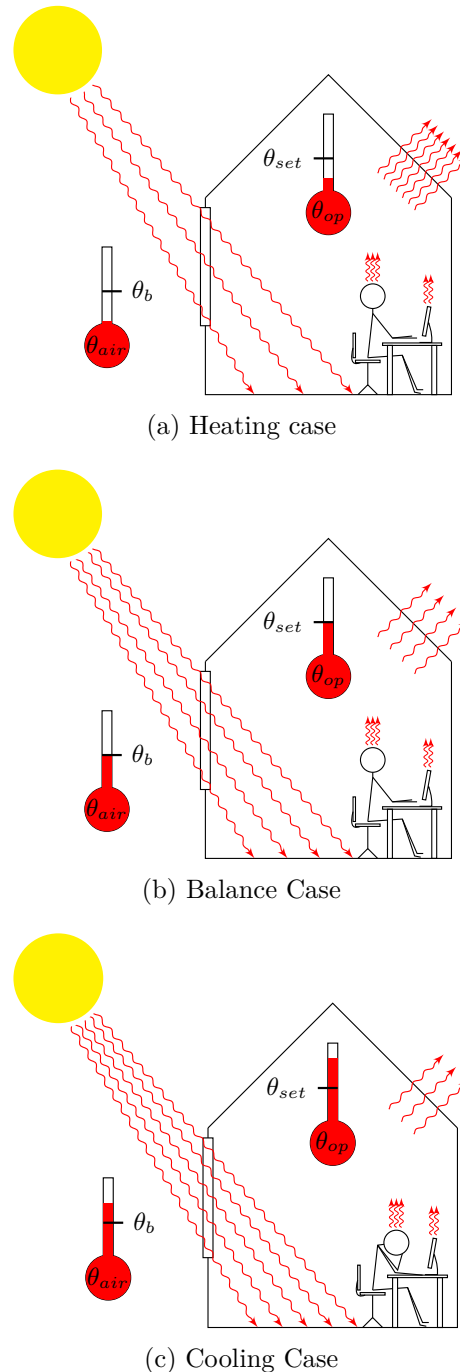


Figure 4.1: *Heat balance scenarios*

theless it is a good approximation to determine the expected heating and cooling requirements of a building. For the heating case illustrated in figure 4.1(a), the loads are too low and the operative temperature will drop well below the set point temperature if no additional heating is provided. During the heating season this is the expected behaviour. As external loads rise, they will reach a point that is illustrated in figure 4.1(b) at which heat losses and gains cancel each other out. In this case the operative temperature is equal to the set point temperature and by definition the current external air temperature must be equal to the base temperature. If the external loads continue to rise, the conditions as illustrated in figure 4.1(c) reflect the cooling case. The high loads would cause the building to overheat unless cooling is applied.

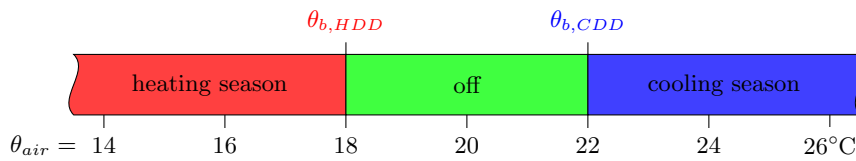
For a widespread application of the degree day method additional attention is to be paid to the building heat loss coefficient (h). Within the existing building stock it varies greatly and thus would have a great influence on the base temperature of different buildings.

All this shows that it is impossible to have one standardized correct base temperature as buildings vary in their construction (heat loss coefficient), location and use (average gains from equipment, occupants, solar radiation, etc.) as well as desired indoor temperature (thermal comfort requirements). This is reflected by the different base temperatures currently used in different countries. In Denmark, based on an daily degree day calculation as explained in section 4.2.2, 17°C are commonly used as base temperature for heating degree days with a minimum indoor temperature of 20°C. The remaining 3°C are assumed to be provided through internal and external heat gains. (ASHRAE, 2001; Cappelen, 2012) The same base temperature is applied in several European countries. In others, like the United Kingdom and Germany, the base temperatures of 15.5°C and 15°C respectively are considerably lower. The USA on the other hand use a higher base temperature of 18.3°C (Energy Lens, 2012). ASHRAE defines a base temperature of only 10°C, assuming that the remaining heat to reach thermal comfort is supplied through a combination of internal and external gains (ASHRAE, 2001). For the calculation of cooling degree days, less countries have set a base temperature.

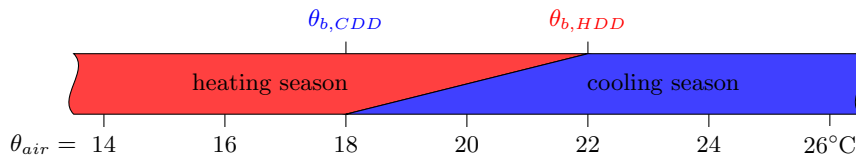
4.2.2 Degree Day Calculation

The underlying idea of degree days is to quantify the amount of heating or cooling needed for a building at a given location based on a simple approach. The problem however is that there is not one single way degree days are calculated but in fact a number of different concepts exist. Figure 4.3(a) and 4.3(b) compares two of the most widely used approaches, the hourly and the daily degree day calculation.

As long as the heating base temperature is lower than the cooling base temperature, the method works without further considerations. This is described in figure 4.2(a).



(a) Each outdoor air temperature is clearly attributed to the heating or cooling season. It is possible that it is neither heating nor cooling season.



(b) In the area where heating and cooling season are overlapping, the corresponding outdoor air temperature is only attributed to one season, namely the one of the previous value.

Figure 4.2: *Different scenarios for the attribution to HDD and CDD*

In this case heating and cooling are never needed at the same time in regard to the theory and the system is simply off for any outdoor air temperature between the two values. However, if the heating base temperature is higher than the cooling base temperature, any outdoor air temperature between these two values would contribute both to HDD and CDD. As both heating and cooling at the same time does not make any sense, figure 4.2(b) is applicable. For any outdoor air temperature between heating base temperature and cooling base temperature, it is only attributed to the same category as the previous value. This means that if the system is in heating mode, it will only switch to cooling once the outdoor air temperature exceeds the heating base temperature. At the same time it will only switch from cooling mode to heating mode once the outdoor air temperature drops below the cooling base temperature.

Hourly degree day calculation

Figure 4.3(a) illustrates an hour by hour approach. In this case the difference between outdoor and base temperature is evaluated for each hour (or possibly even smaller intervals). As can be seen in the magnification, the difference between base- and air temperature is taken. For each hour of the day, the air temperature is compared to the base temperature. All instances in which the base temperature is higher than the air temperature are added together. A separate sum is created for all hours when the values are reversed. Each of the resulting sums are then divided by 24 to get a daily value. During a single day, both heating and cooling may be

required. Equations 4.2 and 4.3 are the corresponding mathematical expressions for the calculation of HDDs and CDDs following this approach.

$$HDD = \sum_{d=1}^{365} \frac{\sum_{h=1}^{24} (\theta_{b,HDD} - \theta_{d,h})^+}{24} \quad (4.2)$$

$$CDD = \sum_{d=1}^{365} \frac{\sum_{h=1}^{24} (\theta_{d,h} - \theta_{b,CDD})^+}{24} \quad (4.3)$$

where

HDD	Heating degree days [-]
CDD	Cooling degree days [-]
$\theta_{b,HDD}$	base temperature for heating degree days [°C]
$\theta_{b,CDD}$	base temperature for cooling degree days [°C]
$\theta_{d,h}$	outdoor temperature during of the d th day of a year on the h th hour [°C]

Daily degree day calculation

In the second approach as shown in figure 4.3(b), each day can either be a cooling or a heating day. In a first step, the mean air temperature for the day is calculated and its difference to the base temperature is either contributing to the HDD or CDD. This approach suggests that there is only ever cooling or heating needed during one day. Equations 4.4 and 4.5 are the corresponding mathematical expressions for the calculation of HDD and CDD using this approach.

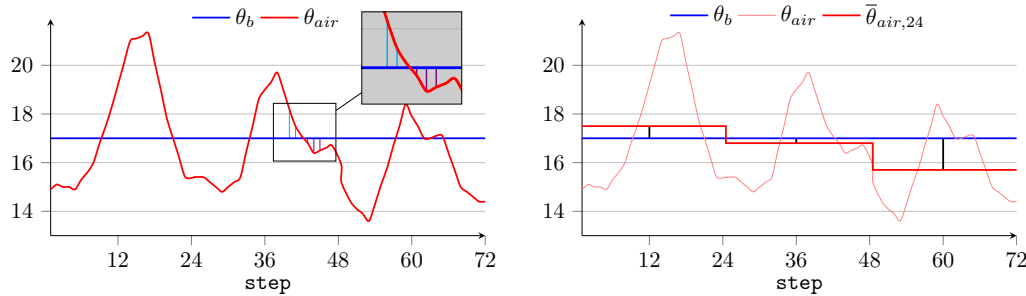
$$HDD_h = \sum_{d=1}^{365} \left(\theta_{b,HDD} - \frac{\sum_{h=1}^{24} \theta_{d,h}}{24} \right)^+ \quad (4.4)$$

$$CDD_h = \sum_{d=1}^{365} \left(\frac{\sum_{h=1}^{24} \theta_{d,h}}{24} - \theta_{b,CDD} \right)^+ \quad (4.5)$$

where

HDD_h	Number of heating degree day hours [-]
CDD_h	Number of heating degree day hours [-]
$\theta_{b,HDD}$	base temperature for heating degree days [°C]
$\theta_{b,CDD}$	base temperature for cooling degree days [°C]
$\theta_{d,h}$	outdoor temperature during of the d th day of a year on the h th hour [°C]

The results of either approach cannot be compared as they can differ greatly. For



(a) Degree day calculation based on hourly values. (b) Degree day calculation based on average (24h) values.

Figure 4.3: *Comparison of degree day calculation methods. The example shows data for Copenhagen, Denmark from July 28th to July 31st.*

the three days displayed in figure 4.3, the CDD based on hourly evaluation is 2.9 whereas it is only 1.5 if the daily evaluation is used. The HDD are 1.9 for the hourly calculation and only 0.5 for the second system. Even over such a short period the values for the hourly values are significantly higher. The difference between the two systems derives from the fact that the averaging done in the second approach compensates heat requirements during part of the day with cooling demands during the remaining hours. Transferred to a building, this is represented by storing part of the load in the building's thermal mass. This makes the daily approach the best solution for calculating reliable CDD and HDD for buildings using TABS.

Seasonal degree day approach

In order to prevent a system from switching from heating to cooling mode and back on a daily basis during the transition phase between seasons, the method has been further extended. For this an additional parameter, the inertness parameter (d_{inert}), has been introduced. It specifies the number of days that are required to switch from one mode to the other. While being in transition, the system is simply considered to be off.

For example if the inertness parameter is set to 3 and we are currently in heating mode, the system would switch off as soon as the test in equation 4.6 detects the need for cooling. However, it would only switch to cooling mode once the test has detected a cooling requirement for three consecutive days (i -days). In case the test detects a heating requirement during this period, heating is immediately reengaged. Equation 4.6 illustrates how the testing is done.

$$\text{Mode switched to} = \begin{cases} \text{heating} & \text{if } \sum_d^{d+n} \frac{\sum_{h=1}^{24} (\theta_b - \theta_{d,h})}{24} < 0 \text{ for last } d_{inert}\text{-days} \\ & \text{or after } d_{inert} - 1 \text{ days in off mode} \\ \text{cooling} & \text{if } \sum_d^{d+n} \frac{\sum_{h=1}^{24} (\theta_b - \theta_{d,h})}{24} > 0 \text{ for last } d_{inert}\text{-days} \\ & \text{or after } d_{inert} - 1 \text{ days in off mode} \\ \text{off} & \text{otherwise} \end{cases} \quad (4.6)$$

where

θ_b base temperature [$^{\circ}\text{C}$]
 $\theta_{d,h}$ outdoor temperature during of the d^{th} day of a year on the h^{th} hour [$^{\circ}\text{C}$]

For the Climate Classifications the results of the test in equation 4.6 have been used to extend the method for the calculation of HDD and CDD. The equations 4.4 and 4.5 have been altered to only count HDD and CDD if the system is in heating mode or cooling mode as indicated in equations 4.7 and 4.8.

$$\text{HDD} = \sum_{d=1}^{365} \begin{cases} \frac{\sum_{h=1}^{24} (\theta_{b,HDD} - \theta_{d,h})^+}{24} & \text{if heating mode} \\ 0 & \text{otherwise.} \end{cases} \quad (4.7)$$

$$\text{CDD} = \sum_{d=1}^{365} \begin{cases} \frac{\sum_{h=1}^{24} (\theta_{d,h} - \theta_{b,CDD})^+}{24} & \text{if cooling mode} \\ 0 & \text{otherwise.} \end{cases} \quad (4.8)$$

where

HDD Heating degree days [-]
 CDD Cooling degree days [-]
 $\theta_{b,HDD}$ base temperature for heating degree days [$^{\circ}\text{C}$]
 $\theta_{b,CDD}$ base temperature for cooling degree days [$^{\circ}\text{C}$]
 $\theta_{d,h}$ outdoor temperature during of the d^{th} day of a year on the h^{th} hour [$^{\circ}\text{C}$]

It is also possible to set the inertness parameter to $i = 0$ in which case the cooling season starts on March 1st and ends on September 30th with the remaining months considered as cooling season. The system is then operating in the respective mode regardless of the test described in equation 4.6.

Setting the inertness parameter to $i = 1$ causes the Climate Classifications to behave as if equations 4.4 and 4.5 were used.

4.2.3 Dew point hours

For cooling with TABS it is important to consider the possibility of condensation on the controlled surfaces in the room. The highest risk for condensation occurs in hot humid climate conditions and/or high internal heat and humidity loads. Under such circumstances the operation of TABS has to be carefully considered. Floor surface temperatures below 19°C and ceiling- and wall surface temperatures lower than 17°C should be avoided due to comfort requirements (ISO, 2005) as well as dew-point concerns (Babiak et al., 2007a). Supply temperatures are therefore often limited to a few degrees below these values. In this thesis the critical temperature (θ_{crit}) was set to 14°C unless otherwise specified. To determine the DPH, any incidence when the dew point temperature (θ_{dp}) exceeds the critical temperature is counted as described by the following equation.

$$DPH = \sum_{h=1}^{8760} \begin{cases} 1 & \text{if } \theta_{dp}^h > \theta_{crit} \\ 0 & \text{otherwise.} \end{cases} \quad (4.9)$$

where

DPH	Number of dew point hours [-]
θ_{crit}	critical temperature [°C]
θ_{dp}^h	dew-point temperature of the h-th hour [°C]

Other than for the degree days however, the magnitude of the violation is not taken into account. In this case such an additional information in itself would not add any value to the final conclusion. In order to make use of the violation magnitude it would not only be necessary to verify if the violation occurred during cooling times as suggested by the degree days, but also if the applied control actually uses cooling. Since the configuration of the control at the very least is highly dependent on the building management, such information cannot be used for a climate classification.

Humidity induced problems for the building structure were also briefly considered. Literature suggests that the use of TABS may have significant influence on the building structure (Bangert et al., 2003). Michel et al. (2013) state that:

"No considerable impact of temperature and relative humidity on the corrosion rate of passively corroding reinforcement bars was found, which is in agreement with previously presented studies in the literature. Further, no considerable influence of the relative humidity and temperature on the electrochemical properties, i.e. free corrosion potential and polarization resistance, was observed for the passively corroding specimens. In contrast to passively corroding reinforcement bars, tem-

perature and moisture dependent behaviour was observed for corrosion current density, polarization, and ohmic resistance of actively corroding reinforcement bars.”

As this potential problem can however be avoided by choosing the appropriate reinforcement bars, no additional limitations are imposed on the classification.

4.3 Criteria for the climate classification

Each location in the Climate Classification for TABS falls into one thermal category and one humidity category. The combination of these two is then the location's Climate Classifications.

4.3.1 Thermal Classification

The thermal classification has four categories based on five parameters. For both, heating and cooling, a base temperature as well as the inertness parameter is set and then used to calculate the corresponding CDD and HDD as described in section 4.2.2. The resulting values are then compared to the corresponding CDD_L and HDD_L in order to evaluate the need for cooling and heating respectively.

- **Heating based Climate** – If the calculated HDD exceed the set HDD_L but at the same time CDD is below CDD_L , the location is considered to be heating based.
- **Combined Climate** – If both, the cooling and heating degree days exceed their respective limits the location is classified as a *combined climate*.
- **Moderate Climate** – Any location in which both, the HDD and CDD are below their respective limits is considered to be in a moderate climate. Heating and cooling requirements should be easy to satisfy.
- **Cooling based Climate** – A location is considered to have a cooling based climate, if CDD exceeds CDD_L while HDD remains below HDD_L .

4.3.2 Humidity Classification

The humidity classification consists of three categories based on three parameters. The DPH are determined by counting the incidences when the dew point temperature exceeds the critical dew point temperature as described in section 4.2.3. The resulting value is then compared to the *lower dew point hour limit* ($DPH_{L,L}$) and the *upper dew point hour limit* ($DPH_{L,U}$). Any location can consequently be associated with one of the following humidity categories.

- **No dehumidification** – In this case humidity levels are not likely to cause any problems, even without any dehumidification. A location falls in this category if the DPH do not exceed the lower dew point hour limit.
- **Intermittent dehumidification** - The installation of a dehumidification unit is required. However the unit will not need to be operated throughout the cooling season. A location falls in this category if the DPH are between the lower dew point hour limit and the upper dew point hour limit.
- **Continuous dehumidification** - During the cooling period the indoor humidity needs to be controlled most of the time. A location falls in this category if DPH exceed the upper dew point hour limit.

4.3.3 The combined classification

The resulting European Climate Classification for TABS is based on a combination of one thermal- and one humidity category, delivering a total of 12 climate zones in theory. However, any thermal category that does not require cooling will also never need dehumidification as no condensation will occur on heated surfaces under normal conditions. It is therefore likely that some combinations may not be found at all. Depending on the setup of the Climate Classifications, the number of different climates actually found varies. Also, depending on the setup, locations will change their associated classification. Most commonly, 8 of the 12 classes can be found.

4.4 Locations included in the climate classification database

The original classification presented in Behrendt and Christensen (2013) consisted of 54 locations spread relatively evenly throughout Europe. While the northern part of Europe was consistently classified as a heating based climate without the need for dehumidification, the southern parts were found to be far less homogenous. Thus, additional locations, primarily located in southern Europe, have been added to the classification. As can be seen in figure 4.4, the highest concentration of cities in the classification can be found in the north-west of Spain. This is the result of an early parameter study, in which some locations in this area switched from one climate class to another, while the cities around it would remain in their previous categories.

The above hints at an inherent problem of any climate classification. They tend to create the illusion of clear borders between the different climate zones (especially if illustrated in a map). This is however not the case. In fact it is impossible to predict where one zone ends and the next one begins. Also, one location might for

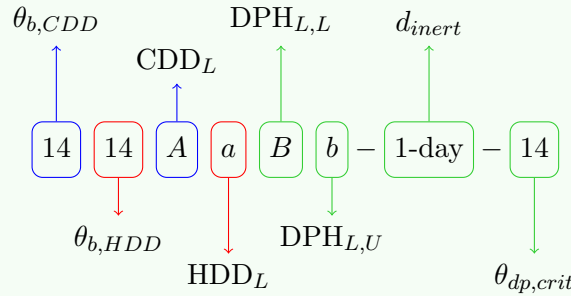


- | | | | |
|------------------------------|------------------------------|---------------------------------|--|
| 1. Porto, Portugal | 27. Brest, France | 49. Stuttgart, Germany | 73. Minsk, Belarus |
| 2. Bragança, Portugal | 28. Paris, France | 50. Munich, Germany | 74. Kosice, Slovakia |
| 3. Coimbra, Portugal | 29. Nancy, France | 51. Prague, Czech Republic | 75. Kiev, Ukraine |
| 4. Lisbon, Portugal | 30. Strasbourg, France | 52. Geneva, Switzerland | 76. Odessa, Ukraine |
| 5. La Coruña, Spain | 31. Dijon, France | 53. Innsbruck, Austria | 77. Debrecen, Hungary |
| 6. Pontevedra, Spain | 32. Bordeaux, France | 54. Vienna, Austria | 78. Belgrade, Serbia |
| 7. Lugo, Spain | 33. Clermont-Ferrand, France | 55. Torino, Italy | 79. Banja Luka, Bosnia and Herzegovina |
| 8. Oviedo, Spain | 34. Toulouse-Blagnac, France | 56. Milan, Italy | 80. Timisoara, Romania |
| 9. Santander, Spain | 35. Montpellier, France | 57. Venice, Italy | 81. Cluj-Napoca, Romania |
| 10. Ourense, Spain | 36. Nice, France | 58. Bologna, Italy | 82. Gelati, Romania |
| 11. Leon, Spain | 37. Brussels, Belgium | 59. Olbia-Costa Smeralda, Italy | 83. Bucharest, Romania |
| 12. San Sebastian, Spain | 38. Amsterdam, Netherlands | 60. Cagliari, Italy | 84. Podgorica, Montenegro |
| 13. Valladolid, Spain | 39. Bergen, Norway | 61. Rome, Italy | 85. Sofia, Bulgaria |
| 14. Salamanca, Spain | 40. Oslo, Norway | 62. Bari-Palese, Italy | 86. Plovdiv, Bulgaria |
| 15. Madrid, Spain | 41. Kiruna, Sweden | 63. Crotone, Italy | 87. Varna, Bulgaria |
| 16. Zaragoza, Spain | 42. Stockholm, Sweden | 64. Gela, Italy | 88. Thessaloniki, Greece |
| 17. Barcelona, Spain | 43. Tampere, Finland | 65. Ljubljana, Slovenia | 89. Athens, Greece |
| 18. Valencia, Spain | 44. Helsinki, Finland | 66. Tallinn-Hatku, Estonia | 90. Istanbul, Turkey |
| 19. Palma, Spain | 45. Copenhagen, Denmark | 67. Ventspils, Latvia | 91. Izmir, Turkey |
| 20. Sevilla, Spain | 46. Hamburg, Germany | 68. Riga, Latvia | 92. Larnaca, Cyprus |
| 21. Algiers, Algeria | 47. Berlin, Germany | 69. Kaunas, Lithuania | |
| 22. Tunis, Tunisia | 48. Frankfurt, Germany | 70. Koszalin, Poland | |
| 23. Reykjavik, Iceland | | 71. Warsaw, Poland | |
| 24. Dublin, Ireland | | 72. Zamosc, Poland | |
| 25. Aberdeen, United Kingdom | | | |
| 26. London, United Kingdom | | | |

Figure 4.4: Map showing the zones used throughout the ECC. The shape and size of each zone have been chosen arbitrarily.

Naming convention for the Climate Classification for TABS

As the Climate Classification for TABS is dependent on the initial setup, a naming convention has been established that reflects all 8 available parameters. The following scheme explains which part of the case name represents which parameter.



Numbers are given in degree celsius except for the inertness parameter which is given in days as also indicated in the case name. The letters represent corresponding values that can be found below.

Letter	CDD _L	HDD _L	DPH _{L,L}	DPH _{L,U}
A/a	250	1500	900	3800
B/b	500	1750	1100	4000
C/c	750	2000	1300	4200
D/d	1000	2250	1500	4400
next Letter	+250	+250	+200	+200

If the critical dew point temperature is not specified in the case name, it has been set to $\theta_{dp,crit} = 14^{\circ}\text{C}$ which is also the default value for most cases in this report.

example be considered as heating based without the need for dehumidification but still be more comparable to a city in a different zone than to another neighbouring city that is in the same climate zone. This is due to the hard limits that are used to determine in which climate class any location is included. In theory, a difference of just one HDD could turn a heating based– into a moderate climate. It is therefore important to use the obtained information with caution. For instance in the case shown in figure 4.5, it is likely that Nancy, France (location 29) is well within the specifications of a combined climate that does not need dehumidification, whereas Sofia, Bulgaria (location 85) might just barely be a combined climate with the need for intermittent dehumidification as it is surrounded by a number of different climate classes. Increasing the number of locations used for the classification, as done here, reduces uncertainties as the ares per location are (on average) smaller.

Figure 4.4 displays the areas associated with each of the 92 zones. These areas have been selected without regard to geographic characteristics. Instead, the zone borders are drawn to mostly divide the distance between two locations evenly. As a result, the user has to be aware that the location he should look out for is not necessarily the closest one to his area of interest. He should also consider geographical differences. Because it would be impossible to determine the exact geographical borders where the climate categories are actually changing from one to another, this rougher zoning is more appropriate for our purpose.

Figure 4.5 shows the results of the Climate Classification for TABS for case 1414AaBb-1day. This means that the cooling base temperature and heating base temperature are both set to 14°C, the CDD_L is set to 250 and the HDD_L to 1500. The lower dew point hour limit and upper dew point hour limit are set to 1100 and 4000 respectively, the inertness parameter is one day and the critical dew point temperature is at the default (14°C).

For this configuration, all of northern Europe is classified as a heating based climate without the need for dehumidification. If buildings in these areas should be supplied with active cooling, TABS could be operated without problems. Towards the center of the map, cooling becomes more important and mostly a combined climate can be found. Locations around the Mediterranean Sea are mostly cooling based but do need intermittent dehumidification. Moderate climate can be found in Portugal and along the Atlantic coast of Spain and France.

It has to be pointed out that the presented classification is one of many possible classifications. As the used lower dew point hour limit is equivalent to 1100 hours - or roughly 12% of the year - this value might seem too high. Lowering this limit would certainly increase the number of locations in which dehumidification would be necessary. However, due to the very conservative critical dew point temperature at 3°C below the lowest acceptable surface temperatures, there is a considerable safety margin justifying this seemingly high limit. The user of the classification should set the available parameters to best reflect his use-case. In the following section the impact of each parameter is discussed.

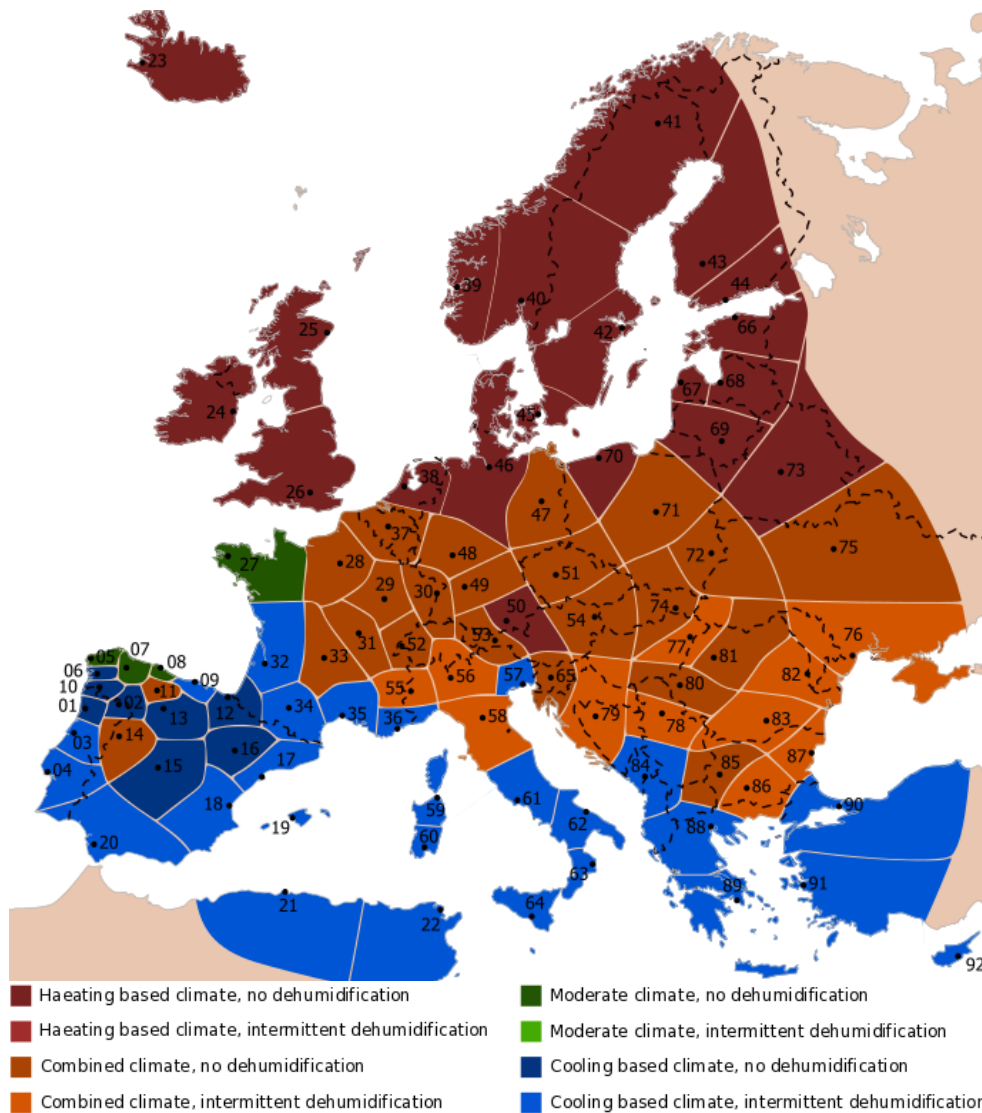


Figure 4.5: Map of Europe based on the new climate classification system. Case: 1414AaBb-1day

4.5 New and pre-defined Climate Classifications

A number of different Climate Classifications have been created and are available in appendix D and a few are discussed in the following. It is also possible to create new customized classifications as needed with the help of an Excel tool that can be obtained through DTU.

In figure 4.6, three different setups of the Climate Classifications with different are shown. With increasing values for CDD_L , the different locations start to change

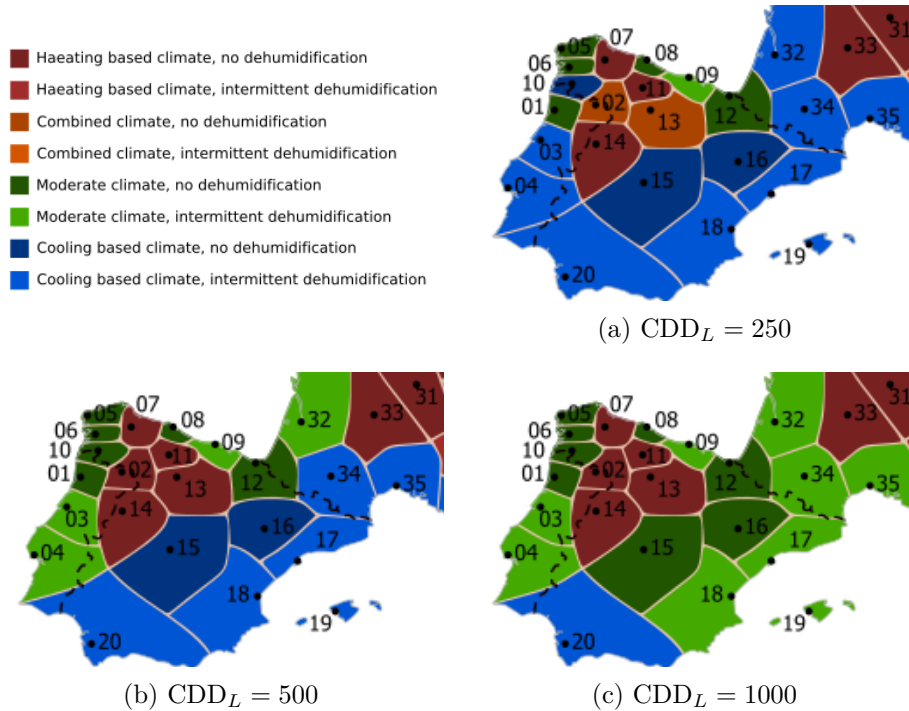


Figure 4.6: *Influence of changing on the Climate Classifications. The used setup is 1818XcBb-1day for all cases.*

from cooling based climate (e.g. location 17) to a moderate climate. The same happens for combined climates (e.g. location 13) which change to a heating based climate.

As expected, changes to the CDD_L did not have any effect on either the need for heating or dehumidification. This shows that the evaluation of the cooling need works independently of the other parameters (except for the base temperature as explained below). Whether or not a location required heating did not change between the cases presented which was to be expected.

In figure 4.7, two different setups of the Climate Classifications with different CDD_L are shown. As for the previous comparison it can be seen that increasing the limit reduces the number of zones that require heating. As before, the changes are however independent from the other parameters except the base temperature.

In Figure 4.8, three different setups of the Climate Classifications with different lower dew point hour limit and upper dew point hour limit are shown. As can be seen, with increasing limits the number of locations that require intermittent dehumidification is reduced. With the lowest upper limit already being 3800 none of the locations would be considered to constantly need dehumidification. Increasing

4.5 New and pre-defined Climate Classifications

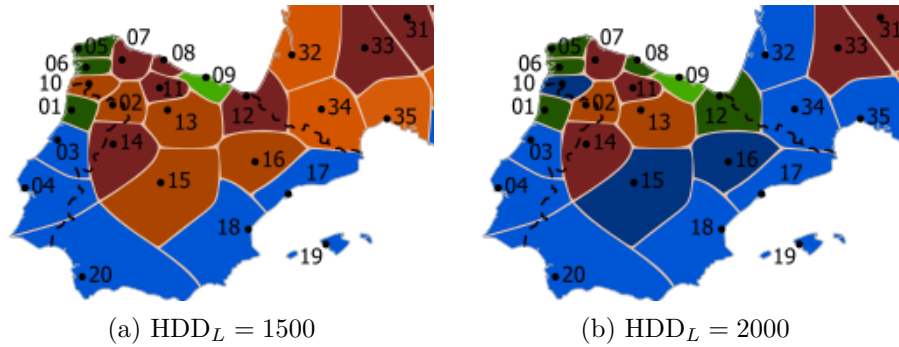


Figure 4.7: *Influence of changing HDD_L on the Climate Classifications. The used setup is 1818AxBb-1day for all cases.*

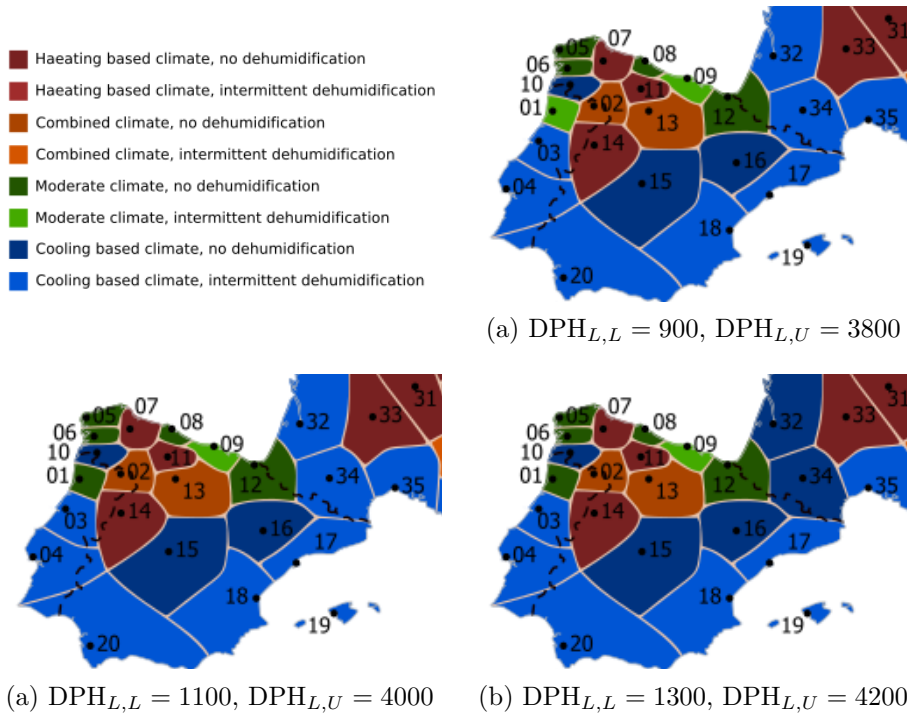


Figure 4.8: *Influence of changing upper dew point hour limit and lower dew point hour limit on the Climate Classifications. The used setup is 1818AcXx-1day for all cases.*

this level further consequently does not cause any changes in the classification. In figure 4.9, four different setups of the Climate Classifications are shown. Comparing these four cases, it can be seen that the impact of changing the base tem-

peratures is dependent on the location. The northern most locations (e.g. Scandinavia, England, the northern part of Germany as well as the Baltic states) are considered to be heating based climate with no need for dehumidification regardless of the base temperature. On the other hand, the southern most regions included in the classification also seem unaffected by the changing base temperatures. With the exception of Munich, Germany (location 50) all other locations change their climate category at least once.

For those locations in which the classification does not change, the building design (within reasonable limitations) will not change the location from being predominantly heating based to cooling based or vice versa. Nonetheless, bad design will of course have a great impact on the overall energy consumption of a building. In locations where the category is however changed, the building design has a greater impact on the required heating and cooling capacities to maintain a proper indoor climate.

As the base temperatures are used to calculate the HDD and CDD, any changes to them will cause changes to the thermal classification of the locations as well.

4.5 New and pre-defined Climate Classifications

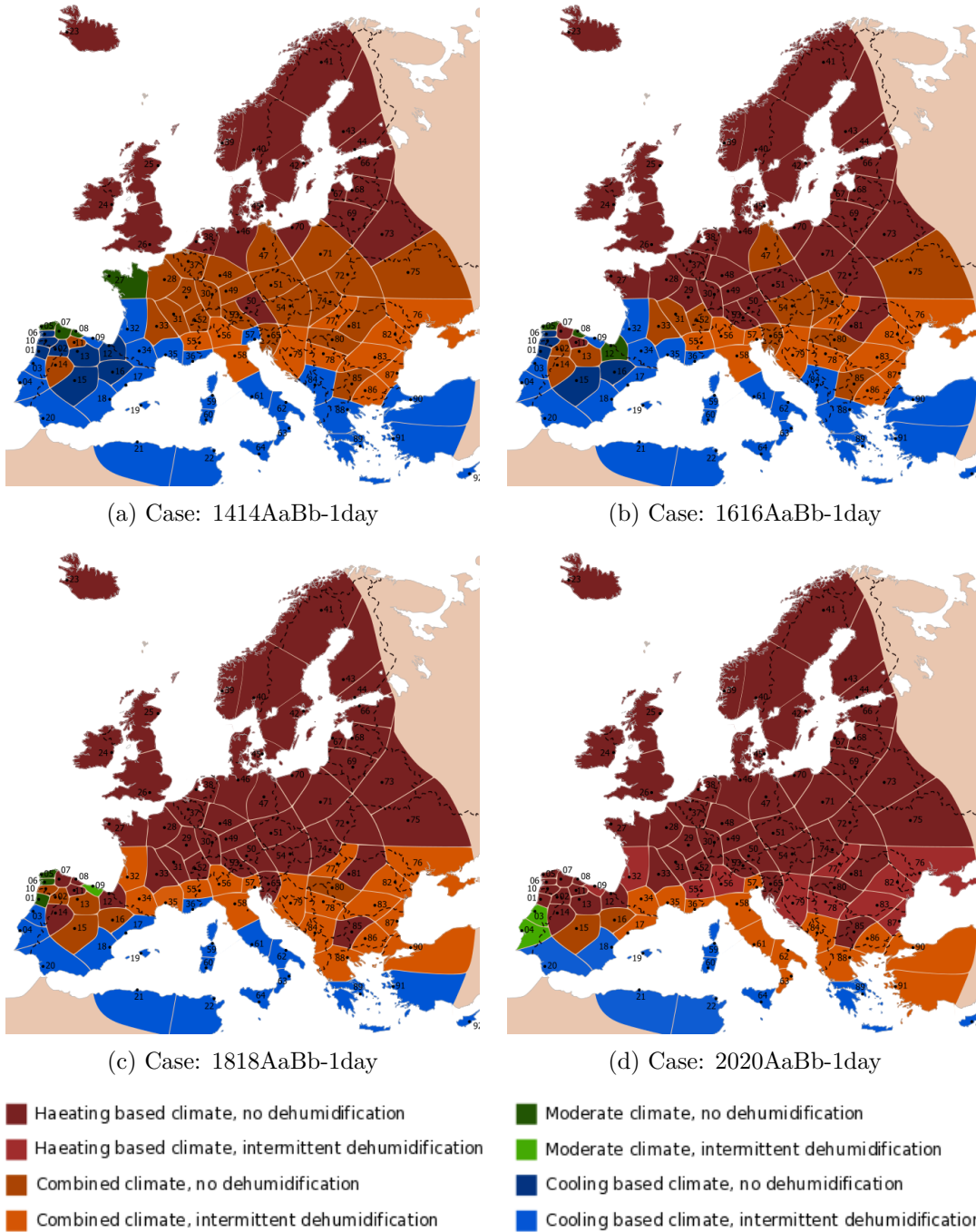


Figure 4.9: Influence of changing the base temperatures for heating and cooling in 2°C increments

4.6 System Validation

The basic principles of this extended Climate Classification for TABS are identical to those used in Behrendt and Christensen (2013). The change between the two versions are primarily a focus on the details of the classification as well as a tighter location network in areas that have previously seemed to be inconsistent. Thus the presented classification is validated in the same manner as the classification presented by Behrendt and Christensen (2013).

The used Climate Classifications setup was 1318DcBb-1day ($\theta_{b,CDD} = 16^\circ\text{C}$, $\theta_{b,HDD} = 18^\circ\text{C}$, $CDD_L = 1000$, $HDD_L = 2000$, $DPH_{L,L} = 1100$, $DPH_{L,U} = 4000$, $d_{inert} = 1$ and $\theta_{dp,crit} = 14^\circ\text{C}$). One of each available climate classifications was selected for the comparison.

Further used for the validation was a simple building with four zones as illustrated in figure 4.10. Zones A and B are regular offices and zone C is a conference room. Zone D is the hall connecting zones A and B. The loads and system configuration are described in table 4.6.

The results of the simulations have been evaluated according to DS/EN 15251. The system was considered to be acceptable if the operative temperature remained in

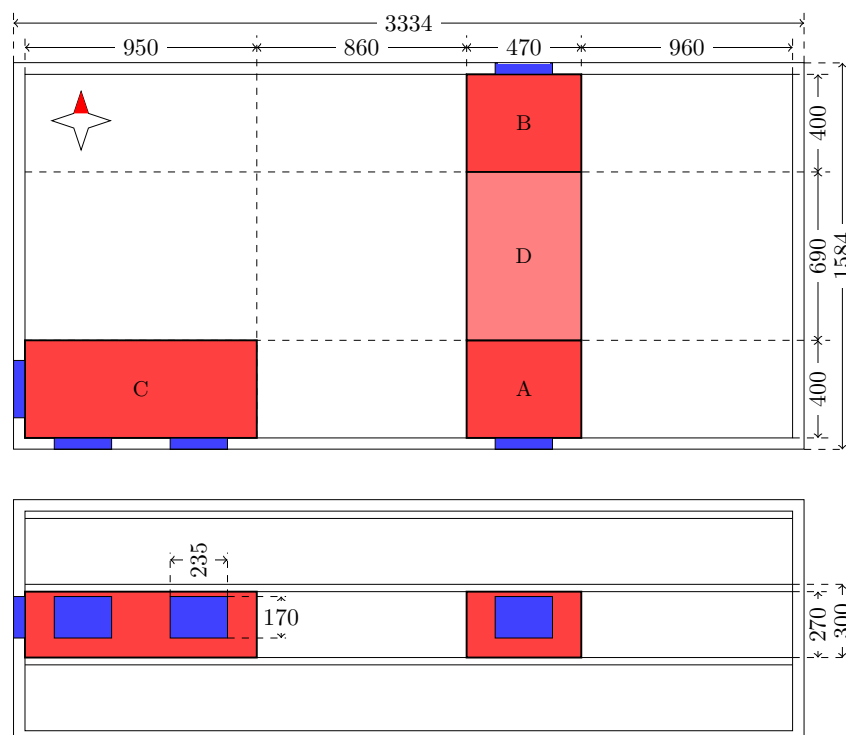


Figure 4.10: *Building Data - Measurements*

Table 4.6: *Building Data - Ventilation, TABS and loads*

		Zone A & B		Zone C		Zone D
Ventilation rate	[ACH]	1.9		1.9		0.9
TABS installed	[-]	Yes		Yes		No
Loads		sensible	latent	sensible	latent	sensible
Occupants	[W]	140	100	280	200	-
Equipment	[W]	160	-	320	-	-
Lighting	[W]	93	-	190	-	159
Schedules						
Ventilation	[h]	Weekdays from 8:00 to 17:00 else 10%				
Loads	[h]	Weekdays from 8:00 to 17:00				
Seasons						
Heating	[-]	1 st of October to 30 th of April				
Cooling	[-]	1 st of May to 31 st of September				
<ul style="list-style-type: none"> • During the heating season, the minimal supply air temperature is 20°C (no cooling). • During the cooling season, the maximal supply air temperature is 25°C (no heating). Additional dehumidification is applied as needed. • The ventilation system is using a heat recovery unit with an efficiency of 80%. • Building envelope constructed to current standards. 						

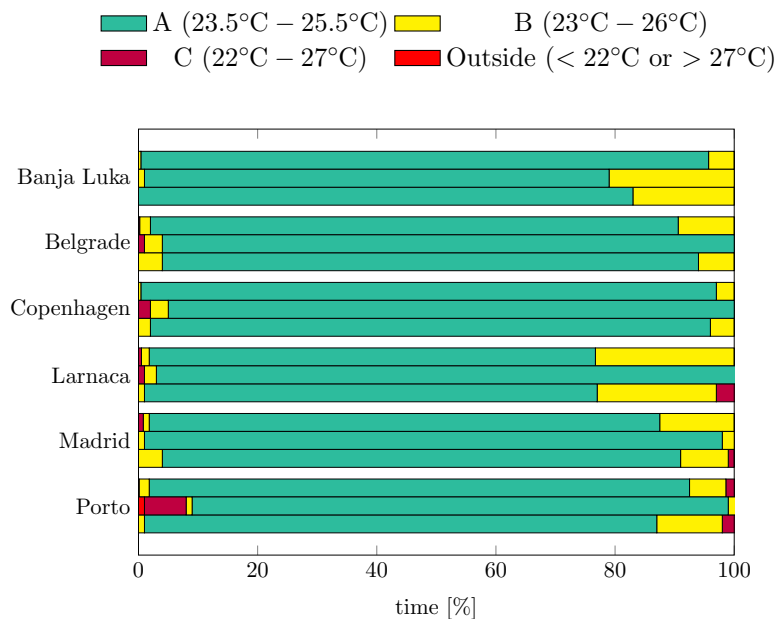
category B or better, for at least 90% of the time.

During heating season, the thermal comfort is usually category B or better for any location. There are however occasions when the indoor temperature falls too low or in some cases the room is even overheated as shown in figure 4.11(a). Considering however that only the dead-band for the heating and cooling operation are adjusted between locations, this had been expected.

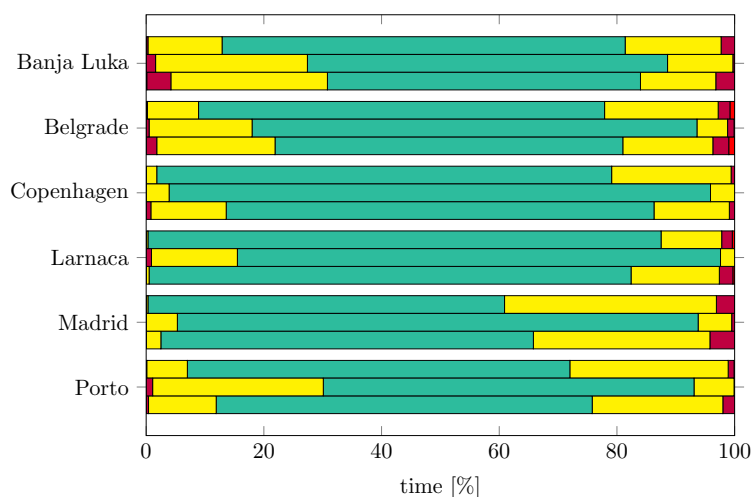
During cooling season, the building does not perform quite as well, but for the most part indoor temperatures still remain within category B or better as shown in figure 4.11(b). However, both undercooling as well as insufficient cooling are more common than during the heating season.

The performance differences between the heating and cooling season can also be seen in the simulation results obtained with the help of IES Virtual Environment. In general, the cooling system uses considerably more energy than the heating system. This is regardless of the location of the building. However, there is a clear correlation between the amount of heating and cooling for all locations. Keeping this in mind, the results of the IES Virtual Environment simulations generally support the findings of the Climate Classification for TABS.

The results of the Climate Classifications and the IES Virtual Environment simulations are presented in boxes 4.7 to 4.12. In the top part, the results of the Climate Classifications for the case 1318DcBb are given. The difference between



(a) Heating Season



(b) Cooling Season

Figure 4.11: *Thermal comfort categories for select locations*

the two lines is that the first has a dynamic season adaptation whereas the other has fixed cooling and heating seasons identical to those used in IES VE. The lower part of the table provides key results of the IES VE simulations. Below, the used dead-band for each location is illustrated.

Heating based climate without the need for dehumidification

According to the Climate Classifications, Copenhagen (Denmark) is clearly a heating based location with the HDD far exceeding the set HDD_L . The number of CDD is far below the set CDD_L and suggests that cooling will not be an issue. Also the DPH is very low suggesting that humidity will not have a significant impact on the building operation should cooling be applied.

The results from IES VE support this assessment. There is no water removed through the ventilation system throughout the entire year. From all locations tested, Copenhagen by far has the highest heating demand and at the same time the lowest cooling demand.

All relevant results are summarised in table 4.7.

Table 4.7: Data for Copenhagen, Denmark (Location 45)

Climate Classifications	HDD	CDD	DPH	Category
1318DcBb-1day	3431	117	122	11
1318DcBb fixed season	3562	308	298	11

IES Virtual Environment	Unit	zone A	zone B	zone C
Water removed	[kg/y]	0.0	0.0	0.0
TABS Heating	[kWh/m ² y]	5.1	7.5	9.9
TABS Cooling	[kWh/m ² y]	12	7.3	15.1
Ventilation Heating	[kWh/m ² y]	2.5	3.1	3.9
Ventilation Cooling	[kWh/m ² y]	0.0	0.0	0.0

TABS dead-band

$\theta_{air} = 17$ 19 21 23 25 27°C

Heating based climate with the need for intermittent dehumidification

In the Climate Classifications, Banja Luka (Bosnia and Herzegovina) is within a heating based climate but may require intermittent dehumidification if cooling is to be applied. The HDD is by far exceeding the set HDD_L . The number of CDD is below the set CDD_L , but considerably higher than for Copenhagen. As the DPH has exceeded the lower dew point hour limit, the Climate Classifications suggests that dehumidification should be installed. However, as upper dew point hour limit is not exceeded, it will only need to be operated occasionally.

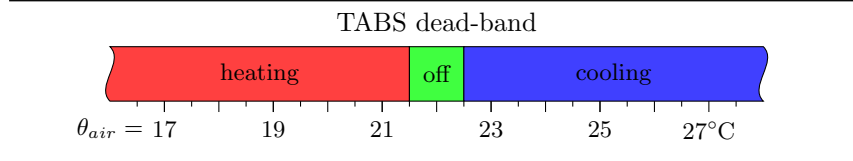
The results from IES VE support this assessment. The amount of water removed is not very high. However, not applying dehumidification may either lead to overheating due to limited cooling or even condensation on the controlled surfaces. The heating demand is considerably lower than for Copenhagen but still substantial, especially for the north facing zone B. The cooling demand has also about doubled compared to Copenhagen, but is still low by comparison with other locations considered to be cooling based.

All relevant results are summarised in table 4.8.

Table 4.8: Data for Banja Luka, Bosnia and Herzegovina (Location 79)

Climate Classifications	HDD	CDD	DPH	Category
1318DcBb-1day	2749	716	1282	12
1318DcBb fixed season	2897	917	1599	12

IES Virtual Environment	Unit	zone A	zone B	zone C
Water removed	[kg/y]	6.3	6.3	12.7
TABS Heating	[kWh/m ² y]	1.5	3.8	4.4
TABS Cooling	[kWh/m ² y]	21.0	13.4	25.1
Ventilation Heating	[kWh/m ² y]	2.6	3.3	3.6
Ventilation Cooling	[kWh/m ² y]	1.2	1.2	1.2



Combined climate with the need for intermittent dehumidification

Belgrade, Serbia is within a combined climate (both heating and cooling needed) and will require intermittent dehumidification during the cooling season. The HDD exceeds the HDD_L noticeably. The CDD narrowly exceeds the set CDD_L by only 2.5%. This is a close call but having a fixed limit as in this classification, this is bound to happen on occasion. The DPH has exceeded the lower dew point hour limit but is below the upper dew point hour limit. As a result, intermittent dehumidification will be required during the cooling period.

The results from IES VE support this assessment. The amount of water removed is not very high. However not applying dehumidification may either lead to overheating due to limited cooling or even condensation on the controlled surfaces. The heating demand is considerably lower than that for Copenhagen but comparable to Banja Luka. The cooling load has increased by more than 11% if compared to Banja Luka.

All relevant results are summarised in table 4.9.

Table 4.9: *Data for Belgrade, Serbia (Location 78)*

Climate Classifications	HDD	CDD	DPH	Category
1318DcBb-1day	2699	1025	1599	22
1318DcBb fixed season	2794	1146	1784	22

IES Virtual Environment	Unit	zone A	zone B	zone C
Water removed	[kg/y]	9.9	9.9	19.9
TABS Heating	[kWh/m ² y]	2.0	3.4	4.4
TABS Cooling	[kWh/m ² y]	23.8	14.9	29.2
Ventilation Heating	[kWh/m ² y]	2.9	3.5	4.0
Ventilation Cooling	[kWh/m ² y]	2.0	2.0	2.0

TABS dead-band

$\theta_{air} = 17 \quad 19 \quad 21 \quad 23 \quad 25 \quad 27^\circ\text{C}$

Moderate climate without the need for dehumidification

According to the Climate Classifications, Porto (Portugal) is located in a moderate climate where no dehumidification will be needed. Both HDD and HDD are well below their respective limits. The DPH are also just below the lower dew point hour limit. Only moderate heating and/or cooling should be needed in this location.

The results from the IES VE support this assessment for the most part. In the case of Porto, the simulation does not apply any heating to the building and only cooling is required. However, the amount of cooling actually exceeds the one applied in Belgrade. The difference between the evaluation of the Climate Classifications and IES VE is in this case based on the flexible approach to calculate HDD and CDD. If fixed seasons is used instead, especially the CDD rises considerably. All relevant results are summarised in table 4.10.

Table 4.10: Data for Porto, Portugal (Location 01)

Climate Classifications	HDD	CDD	DPH	Category
1318DcBb-1day	1292	486	1028	31
1318DcBb fixed season	1492	883	2106	32

IES Virtual Environment	Unit	zone A	zone B	zone C
Water removed	[kg/y]	0.5	0.5	1.0
TABS Heating	[kWh/m ² y]	0.0	0.0	0.0
TABS Cooling	[kWh/m ² y]	26.4	18.6	32.2
Ventilation Heating	[kWh/m ² y]	0.0	0.0	0.0
Ventilation Cooling	[kWh/m ² y]	0.0	0.0	0.0

TABS dead-band

Cooling based climate without the need for dehumidification

In the Climate Classifications, Madrid (Spain) has a cooling based climate where no dehumidification is needed. The HDD is below the HDD_L and the CDD exceeds the CDD_L . The DPH is one of the lowest overall and well below the lower dew point hour limit.

The results from the IES VE support this assessment. The heating load is very low or even non existent for Zone A, but the cooling needs are considerably higher than for any of the previous cases. Also the ventilation system is running more often than in the previous cases despite the fact that only very limited water is removed from the air. In fact, the values are low enough to run the system without dehumidification and instead reduce cooling for those few instances when a condensation problem could arise.

All relevant results are summarised in table 4.11.

Table 4.11: *Data for Madrid, Spain (Location 15)*

Climate Classifications	HDD	CDD	DPH	Category
1318DcBb-1day	1896	1174	358	41
1318DcBb fixed season	1964	1408	415	41

IES Virtual Environment	Unit	zone A	zone B	zone C
Water removed	[kg/y]	1.3	1.3	2.6
TABS Heating	[kWh/m ² y]	0.0	0.2	0.3
TABS Cooling	[kWh/m ² y]	30.7	18.6	35.4
Ventilation Heating	[kWh/m ² y]	0.0	1.3	1.5
Ventilation Cooling	[kWh/m ² y]	2.9	2.9	2.9

TABS dead-band

$\theta_{air} = 17$ 19 21 23 25 27°C

Cooling based climate with need for intermittent dehumidification

The final location included in the validation is Larnaca, Cyprus. According to the evaluation done in the Climate Classifications, it has a cooling based climate with the need for intermittent dehumidification. The HDD is well below the HDD_L and the CDD is well above the CDD_L . Also the DPH is very close to the set upper dew point hour limit.

The results from the IES VE support this assessment. There is no heating required at all in Larnaca but on the other hand, the cooling load is the highest of all the included cases. In addition, the ventilation system removes a considerable amount of water from the supply air in order to avoid condensation on the controlled surfaces.

All relevant results are summarised in table 4.12.

Table 4.12: *Data for Larnaca, Cyprus (Location 92)*

Climate Classifications	HDD	CDD	DPH	Category
1318DcBb-1day	551	2298	3760	42
1318DcBb fixed season	759	2457	3837	42

IES Virtual Environment	Unit	zone A	zone B	zone C
Water removed	[kg/y]	225.9	225.9	456.8
TABS Heating	[kWh/m ² y]	0.0	0.0	0.0
TABS Cooling	[kWh/m ² y]	40.8	26.4	53.9
Ventilation Heating	[kWh/m ² y]	0.0	0.0	0.0
Ventilation Cooling	[kWh/m ² y]	6.1	6.1	6.0

TABS dead-band

$\theta_{air} = 17 \quad 19 \quad 21 \quad 23 \quad 25 \quad 27^\circ\text{C}$

Chapter 5

Conclusion

Each of the tools can contribute to the early design of buildings using TABS in their own way. With the help of both tools it is possible to easily assess if a building at a certain location will be able to provide a good thermal comfort. While the Climate Classification for TABS provides the information about possible condensation risks the Simply TABS provides information on the thermal development inside the building.

Conclusion

Chapter 6

Further studies

For the Simply TABS additional validations of the added components is needed. Especially the heat loss model and the simulated connection to the environment have not been tested extensively. A validation against measurements in buildings is also suggested.

At the moment only a text based user interface is available for Simply TABS. While easy and modular this may detour people from using the tool. Developing a graphical user interface, possibly with a database to store commonly used components, would increase the program's attractiveness.

Just like for the calculation of cooling and heating degree days the calculation of the dew point hours should be refined to distinguish heating and cooling season. In doing so the Climate Classification results concerning the need for dehumidification would become more reliable.

The Climate Classification for TABS should be further extended with additional locations within Europe and eventually world wide. Before this can however be done the evaluation process should be speed-up. While it is practically instantly possible to test any setup for a given location it takes a considerable amount of time to run the calculations for all included locations. In this case the main part of the time is spent on the - automatic - opening, saving and closing of files.

Ideally the Climate Classification for TABS would be integrated with Simply TABS. With this only the eight parameter would be needed as additional input and one of the available locations needs to be specified. The result file could then also contain information on possible limitations due to humidity problems.

Further studies

References

- Ali, A. H. H. Passive cooling of water at night in uninsulated open tank in hot and areas. *Energy Conversion and Management*, 48(1):93–100, JAN 2007.
- Armstrong, P. R., Jiang, W., Winiarski, D., Katipamula, S., Norford, L. K., and Willingham, R. A. Efficient low-lift cooling with radiant distribution, thermal storage, and variable-speed chiller controls-part i: Component and subsystem models. *Hvac&R Research*, 15(2):367–401, MAR 2009.
- Asada, H. and Boelman, E. C. Exergy analysis of a low temperature radiant heating system. *Building Service Engineering*, 25(3):197–209, /8/1 2004.
- ASHRAE. *Handbook – Fundamentals (S-I)*. American Society of heating, Refrigeration and Air-Conditioning Engineers, Inc., 2001.
- ASHRAE. *Handbook: Systems and Equipment*. ASHRAE, 2002.
- ASHRAE. *ASHRAE 90.1 Energy standard for buildings except low-rise residential buildings (S-I)*. American Society of heating, Refrigeration and Air-Conditioning Engineers, Inc., 2010.
- Babiak, J., Olesen, B. W., and Petrás, D. *Low Temperature Heating and High Temperature cooling - Embedded water based surface systems*, volume 7. rehva - Federation of European Heating and Air-conditioning Associations, 2007a.
- Babiak, J., Olesen, B. W., and Petrás, D. *REHVA Guidebook no. 7, Low Temperature Heating and High Temperature cooling - Embedded water based surface systems*. rehva - Federation of European Heating and Air-conditioning Associations, 2007b.
- Babiak, J., Olesen, B. W., and Petrás, D. *Low Temperature Heating and High Temperature Cooling - Thermally activated building system*. PhD thesis, Technical University of Denmark - Department of Civil Engineering - International Center for Indoor Environment and Energy, August 2007c.

REFERENCES

- Babiak, J., Deecke, H., Geithe, O., and Nielsen, L. Cooling with thermally-active mass in extreme climatic conditions. Technical report, Uponor GmbH, 2010a.
- Babiak, J., Hansen, J., Nojd, K., Nielsen, L., Vuolle, M., and Rudolf, J. Heating and cooling with combined ventilation and radiant systems in residential low energy buildings. In *Clima 2010*. Clima 2010, 2010b.
- Bangert, F., Grasberger, S., Kuhl, D., and Meschke, G. Environmentally induced deterioration of concrete: physical motivation and numerical modeling. *ENGINEERING FRACTURE MECHANICS*, 70(7-8):891–910, 2003. ISSN 00137944, 18737315.
- Behrendt, B. and Christensen, J. E. Climate classification for the simulation of thermally activated building systems (TABS). *Proceedings of BS2013*, pages 3614–3621, 2013.
- Behrendt, B. and Olesen, B. Thermische behaglichkeit und energieaufwand bei flächenheizungen in bürogebäuden. In *BAUSIM 2010*, 2010.
- Behrendt, B., Raimando, D., Zhang, Y., Schwarz, S., Christensen, J. E., and Olesen, B. W. A system for the comparison of tools for the simulation of water-based radiant heating and cooling systems. In *12th Conference of International Building Performance Simulation Association*, pages 1025–1032, 2011.
- Cappelen, J. Graddage hører vinteren til, March 2012.
- Causone, F., Corgnati, S. P., Filippi, M., and Olesen, B. W. Solar radiation and cooling load calculation for radiant systems: Definition and evaluation of the direct solar load. *Energy and Buildings*, 42(3):305–314, 2010. ISSN 03787788.
- Chungpaibulpatana, S. and Praditsmanont, A. Performance analysis of the building envelope: A case study of the main hall, shinawatra university. *Energy and Buildings*, 40(9):1737–1746, 2008.
- Corgnati, S. P. Heat flows and air distribution in rooms cooled by radiant panels, 2002.
- Corgnati, S. P., Fracastoro, G. V., and Perino, M. Un metodo di calcolo per il dimensionamento dei soffitti radianti per il raffrescamento estivo, cda 7. Technical report, unknown, 2000.
- Crawley, D. B., Hand, J. W., Kurnmert, M., and Griffith, B. T. Contrasting the capabilities of building energy performance simulation programs. *BUILDING AND ENVIRONMENT*, 43(4):661–673, 2008.

- Deecke, Günter, and Olesen. *Die Betonkernaktivierung*. Velta, 2003.
- DS/EN 15251. *DS/EN 15251 - Indoor environmental input parameters for design and assessment of energy performance of buildings addressing indoor air quality, thermal environment, lighting and acoustics*. DS, 2007.
- El Ahwany, C. Achieving high energy efficiency through concrete core activation, energieeffizient mit betonkernaktivierung. *Betonwerk Und Fertigteil-Technik/Concrete Plant and Precast Technology*, 80(3):36–39, 2014. ISSN 03734331.
- Energy Lens. Degree days - handle with care!, March 2012.
- European Union (EU). Directive 2010/31/eu of the european parliament and of the council of 19 may 2010 on the energy performance of buildings. *Official Journal of the European Union*, 53(L153):13ff, 06 2010a. URL <http://eur-lex.europa.eu/legal-content/EN/TXT/HTML/?uri=OJ:L:2010:153:FULL&from=EN>.
- European Union (EU). New energy labels for household appliances; low-energy buildings from 2020. Technical report, European Parliament, 2010b.
- Finke, U., Zeidler, O., and Fitzner, K. *10 Goldene Regeln für gute Lüftung, Klima und Behaglichkeit*, chapter Kühllasten, Zuluftvolumenströme und Raumluftgeschwindigkeiten minimieren, pages 75–89. Manfred Stahl, 1. edition, 2006.
- Gwerder, M., Tödtli, J., Lehmann, B., Dorer, V., Güntensperger, W., and Renggli, F. Control of thermally activated building systems (tabs) in intermittent operation with pulse width modulation. *Applied Energy*, 86(9):1606–1616, 2009.
- Gwerder, M., Lehmann, B., Tödtli, J., Dorer, V., and Renggli, F. Control of thermally-activated building systems (tabs). *Applied Energy*, 85(7):565–581, 2008.
- IEA. *Technology Roadmap - Energy efficient building envelopes*. IEA Publications, December 2013.
- DS/EN ISO 7730 - *Ergonomics of the thermal environment - Analytical determination and interpretation of thermal comfort using calculation of the PMV and PPD*. ISO, 2005.
- ISO 11855-4. *ISO 11855 part 4 - Building Environment Design - Design, Dimensioning, Installation and Control of the Embedded Radiant Heating and Cooling Systems —Part 4: Dimensioning and calculation of the dynamic heating and cooling capacity for TABS*. ISO, 2011.

REFERENCES

- Jäger, A.-V. *10 Goldene Regeln für gute Lüftung, Klima und Behaglichkeit*, chapter Optimale Raumtemperaturen liegen zwischen 20°C und 26°C, pages 13–26. Manfred Stahl, 1. edition, 2006.
- Kalz, D. E. *Heating and Cooling Concepts Employing Environmental Energy and Thermo-Active Building Systems for Low-Energy Buildings- System Analysis and Optimization*. PhD thesis, Technical University of Karlsruhe, 2009.
- Karlson, H. Self-regulating floor heating systems in low energy buildings. In *Proceedings of the 8th Symposium on Building Physics in the Nordic Countries*, 2008.
- Karlsson, H. *Thermal Modelling of Water-Based Floor Heating Systems - supply temperature optimisation and self-regulating effects*. PhD thesis, Chalmers University of Technology, 2010.
- Koschenz, M. and Lehmann, B. *Thermoaktive Bauteilsysteme tabs*. EMPA, 2000.
- Kottek, M., Grieser, J., Beck, C., Rudolf, B., and Rubel, F. World map of the köppen-geiger climate classification updated. *Meteorologische Zeitschrift*, 15(3): 259–263, June 2006.
- Lehmann, B., Dorer, V., Gwerder, M., Renggli, F., and Toedtli, J. Thermally activated building systems (tabs): Energy efficiency as a function of control strategy, hydronic circuit topology and (cold) generation system. *APPLIED ENERGY*, 88(1):180–191, 2011. ISSN 03062619, 18729118.
- Lehmann, B., Dorer, V., and Koschenz, M. Application range of thermally activated building systems tabs. *Energy & Buildings*, 39(5):593–598, 2007.
- Michel, A., Nygaard, P., and Geiker, M. Experimental investigation on the short-term impact of temperature and moisture on reinforcement corrosion. *Corrosion Science*, 72:26, 2013.
- Olesen, B. W. and Dossi, F. C. Operation and Control of Activated Slab Heating and Cooling Systems. In *58. Congresso Annuale ATI*, page 11, Padova e S. Martino di Castrozza, 8.-12. September 2003.
- Olesen, B. W. and Pittarello, E. The cooling capacity of the thermo active building system combined with acoustic ceiling. In *Nordic Symposium on Building Physics*, 2008.
- Rijksen, D. O., Wisse, C. J., and van Schijndel, A. W. M. Reducing peak requirements for cooling by using thermally activated building systems. *Energy and Buildings*, 42(3):298–304, 3 2010.

REFERENCES

- Santos, H. R. and Leal, V. M. Energy vs. ventilation rate in buildings: A comprehensive scenario-based assessment in the european context. *Energy and Buildings*, 54:111, 2012. ISSN 03787788.
- Tian, Z. and Love, J. Application of radiant cooling in different climates: Assessment of office buildings through simulation. In *11th International IBPSA Conference*, pages 2220–2227, 2009.
- Tyagi, V. V. and Buddhi, D. Pcm thermal storage in buildings: A state of art. *Renewable and Sustainable Energy Reviews*, 11(6):1146–1166, 8 2007.
- Vangtook, P. and Chirarattananon, S. Application of radiant cooling as a passive cooling option in hot humid climate. *Building and Environment*, 42(2):543–556, FEB 2007.

REFERENCES

List of Symbols

Symbol	Description	Unit
A_F	floor area	m^2
A_W	internal wall area	m^2
CDD_L	Number of cooling degree days needed to be in the associated thermal category	–
CDD	Cooling degree days	–
CDD_h	Number of heating degree day hours	–
$c \frac{d\theta}{dt}$	internal energy storage	W
c_F	specific heat of the fluid, typically water	$J/(kg \cdot K)$
c_j	specific heat of the j-th layer of the slab	$J/(kg \cdot K)$
c_P	specific heat of the respective layer of the slab	$J/(m^2 \cdot K)$
c_{IW}	average specific heat of internal walls	$J/(m^2 \cdot K)$
c_W	specific heat of the fluid in the circuit	$J/(kg \cdot K)$
d_e	external pipe diameter	m
DPH	Number of dew point hours	–
f_P^h	fraction of the maximum cooling power that is used	%
f_Q^h	fraction of the heat load actually impacting the room	%
h_{A-C}	convective heat transfer coefficient between air and ceiling	$W/(m^2 \cdot K)$
h_{A-F}	convective heat transfer coefficient between air and floor	$W/(m^2 \cdot K)$
h_{A-W}	convective heat transfer coefficient between air and internal walls	$W/(m^2 \cdot K)$
h_C	convective heat transfer coefficient between ceiling and other surfaces	$W/(m^2 \cdot K)$
h_{C-A}	convective heat transfer coefficient between ceiling and air	$W/(m^2 \cdot K)$
h_{C-F}	convective heat transfer coefficient between ceiling and floor	$W/(m^2 \cdot K)$

REFERENCES

Symbol	Description	Unit
h_{C-W}	convective heat transfer coefficient between ceiling and internal walls	$W/(m^2 \cdot K)$
HDD	Heating degree days	—
HDD_h	Number of heating degree day hours	—
HDD_L	Number of heating degree days needed to be in the associated thermal category	—
h_F	convective heat transfer coefficient between floor and other surfaces	$W/(m^2 \cdot K)$
h_{F-A}	convective heat transfer coefficient between floor and air	$W/(m^2 \cdot K)$
h_{F-C}	convective heat transfer coefficient between floor and ceiling	$W/(m^2 \cdot K)$
h_{F-W}	convective heat transfer coefficient between floor and internal walls	$W/(m^2 \cdot K)$
J_{LS}	Number of material layers in lower part of slab	—
J_{US}	Number of material layers in upper part of slab	—
$\dot{m}_{H,sp}$	specific fluid mass flow in the circuit	$kg/(m^2 \cdot s)$
$n^{actual,day}$	current iteration	—
$n^{max,day}$	maximum number of allowed iterations	—
$n^{actual,step}$	current iteration	—
$n^{max,step}$	maximum number of allowed iterations	—
m_j	number of nodes within the respective construction layer	—
$P_{circ}^{h,max}$	maximum cooling capacity of the circuit in the h^{th} hour	W
$P_{circ}^{h,max,new}$	maximum cooling capacity of the circuit in the h^{th} hour for follow-up simulations	W
l	pipe length	m
T	pipe spacing	m
Q_A^h	heat flow to from air node	W
Q_C^h	heat flow to from ceiling node	W
Q_{circ}^h	delivered cooling capacity of the circuit	W
Q_{con}^h	convective heat gains for each h^{th} hour	W
Q_{con}^h	total convective heat gains for each h^{th} hour	W
Q_F^h	heat flow to from floor node	W
Q_{Inf}^h	infiltration based heat gains and losses for each h^{th} hour	W
Q_i^h	total internal heat gains for each h^{th} hour	W

Symbol	Description	Unit
$Q_{con,i}^h$	internal convective heat gains for each h^{th} hour	W
$Q_{rad,i}^h$	internal radiant heat gains for each h^{th} hour	W
Q_{IW}^h	heat flow from internal wall node	W
Q_{IWS}^h	heat flow from wall surface node	W
Q_{P+1}^h	heat flow from the next node	W
Q_{P-1}^h	heat flow from the previous node	W
Q_{pa}^h	primary air convective heat gains for each h^{th} hour	W
Q_{rad}^h	total radiant heat gains for each h^{th} hour	W
$Q_{rad,C}^h$	total radiant heat gains at ceiling node for each h^{th} hour	W
$Q_{rad,F}^h$	total radiant heat gains at floor node for each h^{th} hour	W
$Q_{rad,IWS}^h$	total radiant heat gains at internal wall surface node for each h^{th} hour	W
Q_{rad}^h	total radiant heat gains for each h^{th} hour	W
Q_{Sun}^h	solar heat gains in the room for each h^{th} hour	W
Q_t^h	total convective heat gains for each h^{th} hour	W
Q_{Tran}^h	transmission heat gains for each h^{th} hour	W
$R_{add,F}$	additional thermal resistance covering the floor	$(m^2 \cdot K)/W$
$R_{add,W}$	wall surface thermal resistance	$(m^2 \cdot K)/W$
RD_P	conduction thermal resistance connecting node (p) with the previous node ($p - 1$)	$(m^2 \cdot K)/W$
RD_{P-1}	conduction thermal resistance connecting the previous node ($p - 1$) with the current node (p)	$(m^2 \cdot K)/W$
Re	Reinolds number	—
R_r	thermal resistance through pipe	$(m^2 \cdot K)/W$
R_t	total thermal resistance of the active layer	$(m^2 \cdot K)/W$
RU_P	conduction thermal resistance connecting node (p) with the previous node ($p - 1$)	$(m^2 \cdot K)/W$
RU_{P+1}	conduction thermal resistance connecting the next node ($p + 1$) with the current node (p)	$(m^2 \cdot K)/W$
R_w	thermal resistance on the pipe inner side	$(m^2 \cdot K)/W$
R_X	fictive pipe level thermal resistance	$(m^2 \cdot K)/W$
R_Z	fictive thermal resistance for water circuit	$(m^2 \cdot K)/W$
s_{LS}	thickness of the slab construction below the active layer	m
s_r	pipe wall thickness	m
s_{US}	thickness of the slab construction above the active layer	m

REFERENCES

Symbol	Description	Unit
U_{LS}	heat transfer coefficient of the lower part of the slab	$W/(m^2 \cdot K)$
U_{US}	heat transfer coefficient of the upper part of the slab	$W/(m^2 \cdot K)$
δ_P	half of the thickness of the material represented by the p-th node $\delta_P = \frac{\delta_j}{2m_j}$	m
δ_{P+1}	half of the thickness of the material represented by the next (p+1)-th node	m
δ_{P-1}	half of the thickness of the material represented by the previous (p-1)-th node	m
Δt	calculation time step ($\Delta t = 3600$ for hourly simulations)	s
λ_b	thermal conductivity of the material of the layer the pipe is embedded in	$W/(m \cdot K)$
λ_j	thermal conductivity of the j-th layer of the slab	$W/(m \cdot K)$
λ_P	thermal conductivity of the material represented by the p-th node	$W/(m \cdot K)$
λ_r	pipe material thermal conductivity	$W/(m \cdot K)$
λ_{P+1}	thermal conductivity of the material represented by the p+1-th node	$W/(m \cdot K)$
λ_{P-1}	thermal conductivity of the material represented by the p-1-th node	$W/(m \cdot K)$
ρ_j	density of the j-th layer of the slab	kg/m^3
θ_b	base temperature	$^{\circ}C$
$\theta_{b,CDD}$	base temperature for cooling degree days	$^{\circ}C$
$\theta_{b,HDD}$	base temperature for heating degree days	$^{\circ}C$
θ_{crit}	critical temperature	$^{\circ}C$
$\theta_{d,h}$	outdoor temperature during of the d th day of a year on the h th hour	$^{\circ}C$
θ_A^h	temperature of the air thermal node in the h th hour	$^{\circ}C$
$\bar{\theta}_{AL}^h$	average active layer temperature at the h th hour	$^{\circ}C$
θ_C^h	temperature of the ceiling surface thermal node in the h th hour	$^{\circ}C$
θ_{dp}^h	dew-point temperature of the h-th hour	$^{\circ}C$
θ_F^h	temperature of the floor surface thermal node in the h th hour	$^{\circ}C$
θ_I^h	temperature of the I th slab thermal node in the h th hour	$^{\circ}C$
θ_{I+1}^h	temperature of the below the I th slab thermal node in the h th hour	$^{\circ}C$

Symbol	Description	Unit
θ_{I-1}^h	temperature of the node above the I th slab thermal node in the h th hour	°C
θ_{IW}^h	temperature of the internal wall thermal node in the h th hour	°C
θ_{IW}^{h-1}	temperature of the internal wall node in the previous time step	°C
θ_{IWS}^h	temperature of the internal wall surface thermal node in the h th hour	°C
$\theta_{op,max}^h$	internal temperature at which simulated heat loss starts to take effect	°C
θ_{P+1}^h	temperature of the next node	°C
θ_P^h	temperature of node P at the current step of this iteration	°C
$\theta_P^{h'}$	temperature of node P at the previous step of this iteration	°C
$\theta_P^{h_{prevDay}}$	temperature of node P at the same step during previous iteration	°C
θ_{op}^h	operative temperature in the h th hour in the room	°C
$\theta_{op,min}^h$	internal temperature at which heat load reduction takes effect	°C
$\theta_{op,os}^h$	can be used to offset $\theta_{op,range}^h$	K
$\theta_{op,range}^h$	temperature range in which the reduction takes place	K
θ_{P-1}^h	temperature of the previous node	°C
θ_I^{h-1}	temperature of the I th slab thermal node in the previous hour	°C
$\theta_{f,In}^{h,set}$	water inlet set-point temperature in the h th hour (also minimal supply temperature)	°C
$\theta_{f,In}^h$	water inlet temperature in the h th hour	°C
ξ^{day}	current deviation between calculation iterations	K
$\xi^{max,day}$	maximum tolerance allowed in iterative calculation	K
ξ^{step}	current deviation between calculation steps	K
$\xi^{max,step}$	maximum tolerance allowed in calculation step	K

REFERENCES

Appendices

Appendix A

Simply TABS Project Setup

As any other simulation tool *Simply TABS* requires a number of inputs in order to start a simulation. As *Simply TABS* is however designed without a dedicated graphical user interface a simple but at the same time flexible way to feed the required data to the tool was thought of. The immediate requirements of the *Simply TABS* is a set of text based input files. The generation of these files can be done completely independent of the *Simply TABS*.

Tables A.7 through A.4 show the content of example input files for the *Simply TABS* with explanations of each input value. The example project is based on the values specified in ISO 11855 part 4.

A.1 Configuration File

In addition to the mentioned input files the *Simply TABS* also needs a configuration file. This file should however only be changed by advanced users and is not explained here.

A.2 Start File

The first thing the *Simply TABS* does once it is started is to open a file called "SSTe.start". Table A.1 illustrates the typical content of the file. It usually only contains one project name. It is however possible to write as many projects (one per line) into this file as desired. The *Simply TABS* will then execute all of them one after the other. For each of the projects the results are saved in a corresponding output file.

A.3 Project File

Once the *Simply TABS* has the list of projects it should simulate it opens the first project file on the list. All project files contain the names of the five input files that make up the actual simulation configuration. For the project "11855-4.proj" these are mentioned in Table A.1. Separating a single project in to five independent files was done to be able to simply exchange just one of the files while the rest of the simulation stays unchanged. In this way it is easy to make parameter studies. As can be seen here it is possible that all input files have the same name. To make this possible each type of input is stored in its individual sub folder. Like most of the input files there are no optional inputs available.

Table A.1: File: *P_Files/Example.proj* → This file contains the names of the input files needed for this project.

Name	File Name	Description
InputFiles - START		Signals the SSTe that the following data are the requiered input files.
BoundaryData	11855-4.inp	Boundary input file name
CircuitData	11855-4.inp	Circuit input file name
PipeData	11855-4.inp	Pipe input file name
RoomData	11855-4.inp	Room input file name
SlabData	11855-4.inp	Slab input file name
InputFiles - END		Signals the SSTe the end of the input file list.

A.4 Boundary File

The boundary data input files contain any information that is not part of the building itself. The first five values found in Table A.2 determine the length of the simulation and the minimal tolerance that is required for a successful simulation. For the simulation to be considered successful the results must differ less than the corresponding values "tolDayMax" and "tolHourMax" after at most "nSub-TimeStep". The remaining data defines the environment and system setup for each of the "nTimeSteps". This illustrates that the data given in Table A.2 is not complete as only eight out of 24 data sets are provided. In the example the first eight hours would have the exact same conditions. As the remaining 16 hours are however not defined the *Simply TABS* would abort the simulation explaining that to few boundary data sets are defined.

As all heat exchange with the environment is defined with only three values, the convective heat flux ($Q_{rad,i}^h$), the radiant heat flux ($Q_{rad,i}^h$) and the maximum cool-

Table A.2: File: *I_Files/Boundary/11855_4.inp* → This file contains all relevant boundary informations for the simulation. There can be multiple "TimeStepData" sets.

Name	Value	Unit	Description
BoundaryData - START			Signals the SStE that the following data is part of the boundary data.
nTimeSteps	24	–	The number of time steps for the simulation. Standard is 24, one for each hour of the day.
lTimeStep	3600	s	Length of one time step.
nSubTimeStep	500	–	Number of allowed calculation iterations between two reported time steps (nTimeSteps)
tolDayMax	0.0001	–	Total allowed tolerance during one day (or over all time steps nTimeStep)
tolHourMax	0.00001	–	Allowed tolerance between two time steps (nTimeSteps)
TimeStepData - START			Signals the SStE that the following data is part of a time step. Multiple of these TimeStepData sets have to be defined.
nHours	8	–	Number of time steps (nTimeSteps) using the same boundary conditions. In total the same amount of hours as nTimeSteps have to be defined. $\sum nHours_{TimeStepData} = nTimeStep$
convHeatFlux	30	W	Total convective heat load during the time step
radHeatFlux	10	W	Total radiant heat load during the time step
runningMode	1	–	TABS operation: 1=ON; 0=OFF
tWater	20	°C	Minimum supply temperature
maxCoolPower	1000	W	Maximum cooling power per time step
TimeStepData - END			Signals the SStE the end of the current time step data.
BoundaryData - END			Signals the SStE the end of the boundary data input.

ing capacity ($P_{circ}^{h,max}$), it is evident that *Simply TABS* is greatly simplifying. Compared to a full building simulation programs (BSPs) the heat balance of the zone has less parameters. The full heat balance for *Simply TABS* is illustrated in Figure 3.1(b).

The two heat fluxes include all gains and losses that occur within the zone due to usage (occupants, equipment, lighting, etc.) and the environment (solar radiation, heat transfer through the building envelope, etc.). The heat fluxes for each time step can be calculated using Equations 3.2 and 3.3.

The TABS are the only active system available in the *Simply TABS* that can be used to transfer heat to and from the zone. In its current configuration the

Simply TABS however should only be used for cooling. In the boundary file the three operational parameters of the TABS are defined. The running mode (f_{rm}^h) is used to turn the entire system on (1) or off (0). The minimal supply temperature ($\theta_{f,In}^{h,set}$) and the maximum cooling power ($P_{circ}^{h,max}$) limit the system capability. If operational the chiller will always try to cool the return water to the minimal supply temperature but not extract more heat than its maximum capacity allows.

A.5 Room File

The *Simply TABS* calculates a single room only. There are however no limitations as to the dimensions of the room. It can be as big or small as desired. The only two dimensional properties are the floor area and the (internal) wall area. The geometry of the room is defined through the provided view factors.

In a real office building the most common room typically has a ceiling, a floor, three internal walls and one external wall. This is also the type¹ of room the *Simply TABS* can calculate. The floor and ceiling are both part of the slab and modelled in detail. Their construction is defined in a separate input file (see below) that is discussed separately. The definition of the internal walls only includes the total area, the heat capacity and the heat transfer resistance of the wall surface. The heat capacity should be provided based on halve of the real construction thickness per square meter as internal walls are considered to be adiabatic hence any heat that is transferred to the internal walls also needs to be removed from them during the simulation period. The heat capacity can be calculated according to Equation A.1 for symmetric internal walls.

$$c_{IW} = \frac{\sum_{j=1}^n c_{j,IW} \cdot \rho_{j,IW} \cdot s_{j,IW}}{2} \quad (\text{A.1})$$

The two view factors included in the input file are used to internally calculate the missing view factor between internal wall and slab.

The values for the radiant heat exchange between the surfaces and the air

All room data inputs are listed in Table A.3. The number of "nTimeSteps" has to be equal to the sum of all "nHours" defined in the "TimeStepData" section.

¹in theory the *Simply TABS* can be used to simulate any cubical room that has an internal ceiling and floor. If all walls should be external the remaining input values simply need to be adjusted accordingly. In practice at least a small internal wall area has to exist due to stability issues.

Table A.3: File: *I_Files/Room/11855_4.inp* → This file contains all relevant room informations.

Name	Value	Unit	Description
RoomData - START			Signals the SSTe that the following data is part of the room data.
FloorArea	30	m^2	Total floor area of the simulated zone
WallArea	48	m^2	Total area of internal walls (external wall area excluded)
FvFloorToCeiling	0.21	–	View factor between floor and ceiling node
FvSlabToExtWall	0.35	–	View factor between slab and external wall
hAirToFloor	1.5	$W/(m^2 \cdot K)$	Radiant heat exchange between air and floor node
hAirToCeiling	5.5	$W/(m^2 \cdot K)$	Radiant heat exchange between air and ceiling node
hAirToWalls	2.5	$W/(m^2 \cdot K)$	Radiant heat exchange between air and internal wall node
FloorResistance	0.1	$(m^2 \cdot K)/W$	Additional heat transfer resistance on the floor surface
CeilingResistance	0	$(m^2 \cdot K)/W$	Additional heat transfer resistance on the ceiling surface
WallResistance	0.05	$(m^2 \cdot K)/W$	Additional heat transfer resistance on the internal wall surface
CWalls	10600	$J/(m^2 \cdot K)$	Heat capacity of halve of the internal walls (as the other halve would be attributed to adjacent zones)
RoomData - END			Signals the SSTe the end of the room data input.
The following values are calculated internally. It is not possible to use them as input values			
FvSlabToIntWall	0.44	–	View factor between slab and internal wall $FvSlabToIntWall = 1 - \frac{FvFloorToCeiling - FvSlabToExtWall}{FvFloorToCeiling - FvSlabToExtWall}$

A.6 Slab File

The slab is defined as illustrated in Table A.4. The slab may consist of any number of layers. Each layer has to be defined individually. For the definition of a layer the physical properties, thermal conductivity (λ_j), specific heat (c_j) and density (ρ_j) have to be provided. Additionally the thickness (δ_j) of the layer has to be specified and "nDevisions" has to be provided. Within each layer "nDevisions" + 1 nodes are used for the calculation of the temperature distribution in the slab. A large number of nodes increases the simulation accuracy as well as time. It is therefore important to find a good compromise between accuracy and time consumption.

Table A.4: File: *I_Files/Slab/11855_4.inp* → This file contains the name of the project that should be simulated.

Name	Value	Unit	Description
SlabData - START			Signals the SSTe that the following data is part of the slab data.
nLayers	4	–	The number of physical layers in the slab construction
Active-Layer_depth	0.19	<i>m</i>	Distance between top of slab and active layer
Layer - START			Signals the SSTe that the following data is part of a slab layer. Multiple of these slab layers can be defined.
nDevison	1	–	Number of devisons that are made within a physical layer. The number of virtual layers is $nDevison + 1$
Thickness	0.02	<i>m</i>	thickness of the physical layer
ThCond	0.17	$W/(m \cdot K)$	Thermal conductivity of the maerial
SpecHeat	2300	$J/(kg \cdot K)$	Spesivic heat of the material
Density	700	kg/m^3	density of the material
Layer - END			Signals the SSTe the end of the current layer.
SlabData - END			Signals the SSTe the end of the slab data input.

Due to the way the slab data is provided the active layer could be located in five different spaces. The *Simply TABS* will automatically identify each case and act accordingly. Should the active layer be located outside or on the surface of the construction the simulation will end with an error suggesting a wrong slab definition. In all other cases additional test are run to determine if the geometry is within the parameters required for the *Simply TABS* to deliver results. If the active layer is located between two defined layers, as shown in Figure A.1(a), the *Simply TABS* will not change the construction. This is however an unusual case as the pipes are commonly embedded in the concrete layer. In case the active layer coincides with a defined devison within a material layer, as shown in Figure A.1(b), it is used as the active layer node. Should neither of the previous two cases be true one more devison is inserted into the layer in which the pipes are embedded. As illustrated in Figure A.1(c) only one layer is effected by this. Other than the ISO 11855-4 the *Simply TABS* does not require individual layers above and below the active layer. It is for instance possible to provide a slab definition containing just one layer. As long as the above mentioned limitations regarding the location of the active layer are met the *Simply TABS* will automatically split the defined slab into the appropriate number of layers. After the input data is

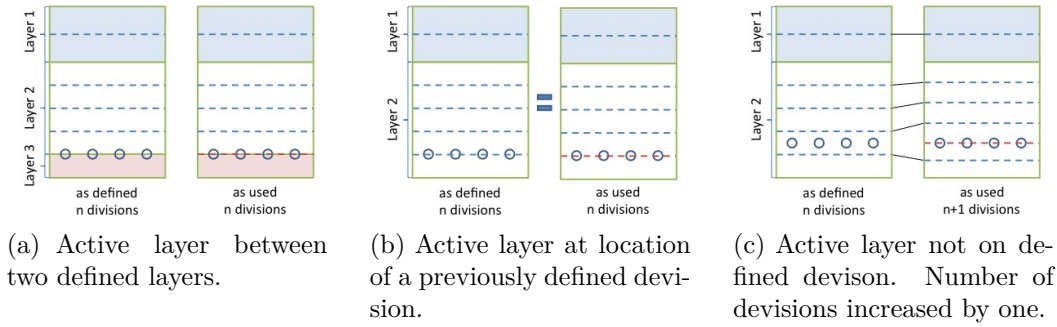


Figure A.1: *Different scenarios for location of active layer within slab construction.*

converted Equations A.2 and A.3 are met.

$$s_{US} = \sum_{j=1}^{J_{US}} \delta_j \quad (\text{A.2})$$

$$s_{LS} = \sum_{j=J_{US}+1}^{J_{US}+J_{LS}} \delta_j \quad (\text{A.3})$$

A.7 Circuit File

The pipe circuit is defined in Table A.5. The required data is set up in a way that it can be combined with any slab construction. This was done to make it easy to evaluate differences in the slab construction while using the same circuit geometry. This is also the reason why the area is defined as a percentage of the floor area rather than a total value.

In most TAB systems water is used to extract heat from the room. It is however possible to use any other liquid with *Simply TABS* as only the fluid density and heat capacity need to be provided.

A.8 Pipe File

The properties of the pipes are defined as illustrated in Table A.6. *Simply TABS* can only be used for the calculation of circular pipes directly. However if oval or square pipes should be of interest there equivalent characteristics could be provided.

Simply TABS Project Setup

Table A.5: File: *I_Files/Circuit/11855_4.inp* → This file contains the name of the project that should be simulated.

Name	Value	Unit	Description
CircuitData - START			Signals <i>Simply TABS</i> that the following data is part of the circuit data.
pipe_spacing	0.1	<i>m</i>	average distance between pipes in the slab.
area_perc	1	%	part of total floor area that is covered by the TAB system.
mass_flow_mm	36	$kg/(m^2 \cdot s)$	specific mass flow in the pipes
fluid_char_rho	1000	kg/m^3	fluid density
fluid_c_w	4187	$J/(kg \cdot K)$	fluid heat capacity
CircuitData - END			Signals <i>Simply TABS</i> the end of the circuit data input.
Optionally <i>r_t</i> can be provided directly as input value. In this case the internal calculation is bypassed and the given value used instead.			
<i>r_t</i>	0.073	$(m^2 \cdot K)/W$	total thermal resistance of the active layer

Table A.6: File: *I_Files/Pipe/11855_4.inp* → This file contains the name of the project that should be simulated.

Name	Value	Unit	Description
PipeData - START			Signals the SSTe that the following data is part of the pipe data.
diameter_ext	0.02	<i>m</i>	external diameter of the pipes
wall_thickness	0.0023	<i>m</i>	wall thickness of the pipes
thermal_cond	0.35	$W/(m \cdot K)$	thermal conductivity of the pipe material (total)
PipeData - END			Signals the SSTe the end of the pipe data input.

A.9 Start conditions

At the start of any simulation the *Simply TABS* requires to have initial temperatures and heat fluxes for all nodes. These are currently set within the code and can not be changed. The initial temperature is $20^\circ C$ and all heat fluxes are set to $0W$.

Table A.7: *File: SSt.e.start* → *This file contains the name of the project that should be simulated.*

Project	Description
11855-4.proj	The project the SSt.e should simulate. If multiple projects are listed (one per line) the simulation tool will consecutively run all specified projects.

Simply TABS Project Setup

Appendix B

List of all cases used in this paper

Table B.1: *List of all simulations created with Simply TABS included in this thesis*

Case Name	Description
RT	Standard case used in this report. It is used to validate the SSTe as discussed in Section 3.2. The input data can be found in tables A.2, A.5, A.6, A.3 and A.4 in section A.
RT_3days	Same as RT but data defined for 3 days.
RT_3days_OH01-03	Same as RT_3days but using the simulated environmental heat loss described in section 3.1.8. For details see table B.3.
RT_3days_UC01-06	Same as RT_3days but using the extended control function discussed in section 3.1.9 with using the values specified in table B.2.
RT_6days	Same as RT_3days but extended to 6 days.
RT_6days_OH01-03	Same as RT_3days_OH01-03 but extended to 6 days. For details see table B.3.
RT_NoAddRes	Identical with case RT but $R_{add,F} = 0$ ($m^2 \cdot K$)/W
RT_UCFlex16	Long simulation with varying values. First 10 days are additional startup phase. The following 33 days the minimal permissible operative temperature rises each third day by one degree. For details see table B.2

Table B.1 – continues on next page

Table B.1 – continued from previous page

Case Name	Description
RT_UCFlex19	Long simulation with varying values. First 10 days are additional startup phase. The following 33 days the minimal permissible operative temperature rises each third day by one degree. For details see table B.2

Table B.2: *Setting used in cases with cooling limitation [°C]*

Case	$\theta_{op,min}^h$	$\theta_{op,os}^h$	$\theta_{op,range}^h$	$\theta_{f,In}^{h,set}$
RT_3days_UC01	22	2	2	16
RT_3days_UC02	21	2	2	16
RT_3days_UC03	20	2	2	16
RT_3days_UC04	22	2	2	19
RT_3days_UC05	21	2	2	19
RT_3days_UC06	20	2	2	19
RT_UCFlex16	14 – 24	2	2	16
RT_UCFlex19	14 – 24	2	2	19

Table B.3: *Setting used in cases simulated environmental heat loss [°C]*

Case	$\theta_{op,max}^h$	$\theta_{op,os}^h$	$\theta_{op,range}^h$
RT_3days_OH01	24	1	2
RT_3days_OH02	26	1	4
RT_3days_OH03	28	1	6
RT_6days_OH01	24	1	2
RT_6days_OH02	26	1	4
RT_6days_OH03	28	1	6

Table B.4: *List of all simulations created with IDA ICE 4.5 included in this thesis*

Case Name	Description
RT	Standard case used in this report. The input data can be found in section A. It is used to validate the SSTe as discussed in Section 3.2.

List of all cases used in this paper

Appendix C

Data for Validation with ISO 11855 - 4

Table C.1: *Expected results as given in ISO 11855-4*

Step	T_f	T_c	T_a	Q_f	Q_c	Q_s	$Q_{circuit}$
1	22.7	22.3	22.7	-1	109	-68	770
2	22.5	22.1	22.4	-8	94	-46	716
3	22.3	22.0	22.2	-11	85	-34	666
4	22.2	21.8	22.1	-12	79	-27	620
5	22.0	21.7	21.9	-12	75	-23	577
6	21.9	21.6	21.8	-12	71	-20	537
7	21.8	21.5	21.7	-11	68	-18	501
8	21.6	21.4	21.6	-10	66	-16	467
9	22.5	21.8	23.4	124	442	134	0
10	22.7	22.1	23.8	147	472	81	0
11	22.9	22.3	24.1	161	485	54	0
12	23.1	22.5	24.3	170	490	39	0
13	23.3	22.7	24.5	176	492	32	0
14	23.5	22.9	24.7	179	493	28	0
15	23.6	23.1	24.9	181	493	26	0
16	23.8	23.3	25.0	182	493	25	0
17	24.0	23.4	25.2	183	493	24	0
18	24.1	23.6	25.4	184	493	24	0
19	24.3	23.8	25.5	184	492	23	0
20	23.8	23.5	24.3	89	246	-85	871
21	23.6	23.2	24.0	69	236	-55	915
22	23.4	23.0	23.8	55	234	-40	926

Table C.1 – continued from previous page

23	23.3	22.8	23.6	47	234	-32	878
24	23.1	22.6	23.4	42	234	-26	826

Table C.2: *SSTe results based on input data from ISO 11855-4*

Step	θ_A^h	θ_C^h	θ_F^h	Q_C^h	Q_F^h	Q_{IWS}^h	Q_{circ}^h
0	23.4	22.6	23.1	234	43	-27	803
1	22.6	22.3	22.6	106	-1	-65	750
2	22.4	22.1	22.4	93	-7	-46	698
3	22.2	21.9	22.3	85	-10	-35	649
4	22.0	21.8	22.1	79	-11	-28	604
5	21.9	21.7	22.0	74	-11	-23	562
6	21.8	21.5	21.8	71	-11	-20	524
7	21.7	21.4	21.7	68	-10	-18	489
8	21.6	21.3	21.6	65	-9	-16	456
9	23.4	21.8	22.4	449	127	123	0
10	23.8	22.1	22.7	473	148	79	0
11	24.1	22.3	22.9	484	161	55	0
12	24.3	22.5	23.1	489	170	41	0
13	24.5	22.7	23.3	491	175	33	0
14	24.7	22.9	23.4	492	179	29	0
15	24.8	23.1	23.6	493	181	27	0
16	25.0	23.2	23.8	493	182	25	0
17	25.2	23.4	23.9	492	183	24	0
18	25.3	23.6	24.1	492	184	24	0
19	25.5	23.7	24.2	492	184	24	0
20	24.2	23.4	23.7	243	86	-79	1,000
21	23.9	23.1	23.5	238	67	-55	975
22	23.7	22.9	23.4	237	54	-41	908
23	23.5	22.7	23.2	236	47	-32	851
24	23.4	22.6	23.1	234	43	-27	803

Table D.1 – continued from previous page

Location	0d	1d	2d	3d	4d	5d	6d	7d
019. Palma, Spain.xlsx	42	42	42	42	42	42	42	42
020. Sevilla, Spain.xlsx	42	42	42	42	42	42	42	42
021. Algiers, Algeria.xlsx	42	42	42	42	42	42	42	42
022. Tunis, Tunisia.xlsx	42	42	42	42	42	42	42	42
023. Reykjavik, Iceland.xlsx	11	11	11	11	11	11	11	11
024. Dublin, Ireland.xlsx	11	11	11	11	11	11	11	11
025. Aberdeen, United Kingdom.xlsx	11	11	11	11	11	11	11	11
026. London, United Kingdom.xlsx	21	11	11	11	11	11	11	11
027. Brest, France.xlsx	31	31	31	31	31	31	31	31
028. Paris, France.xlsx	21	21	21	21	21	21	11	11
029. Nancy, France.xlsx	21	21	21	21	21	21	11	11
030. Strasbourg, France.xlsx	22	21	21	21	21	21	11	11
031. Dijon, France.xlsx	22	21	21	21	21	21	11	11
032. Bordeaux, France.xlsx	42	42	41	41	41	41	41	41
033. Clermont-Ferrand, France.xlsx	21	21	21	21	21	21	21	21
034. Toulouse-Blagnac, France.xlsx	42	42	42	42	42	42	41	41
035. Montpellier, France.xlsx	42	42	42	42	42	42	42	42
036. Nice, France.xlsx	42	42	42	42	42	42	42	42
037. Brussels, Belgium.xlsx	21	21	11	11	11	11	11	11
038. Amsterdam, Netherlands.xlsx	21	11	11	11	11	11	11	11
039. Bergen, Norway.xlsx	11	11	11	11	11	11	11	11
040. Oslo, Norway.xlsx	11	11	11	11	11	11	11	11
041. Kiruna, Sweden.xlsx	11	11	11	11	11	11	11	11
042. Stockholm, Sweden.xlsx	11	11	11	11	11	11	11	11
043. Tampere, Finland.xlsx	11	11	11	11	11	11	11	11
044. Helsinki, Finland.xlsx	11	11	11	11	11	11	11	11
045. Copenhagen, Denmark.xlsx	11	11	11	11	11	11	11	11
046. Hamburg, Germany.xlsx	21	11	11	11	11	11	11	11
047. Berlin, Germany.xlsx	21	21	21	21	21	21	11	11
048. Frankfurt, Germany.xlsx	21	21	21	21	21	21	21	21
049. Stuttgart, Germany.xlsx	21	21	21	21	21	21	11	11
050. Munich, Germany.xlsx	21	11	11	11	11	11	11	11
051. Prague, Czech Republic.xlsx	21	21	11	11	11	11	11	11
052. Geneva, Switzerland.xlsx	21	21	21	21	21	21	21	21
053. Innsbruck, Austria.xlsx	21	21	21	21	21	21	11	11
054. Vienna, Austria.xlsx	21	21	21	21	21	21	21	21
055. Torino, Italy.xlsx	22	22	22	22	22	22	22	22

Table D.1 – continued from previous page

Location	0d	1d	2d	3d	4d	5d	6d	7d
056. Milan, Italy.xlsx	22	22	22	22	22	22	22	22
057. Venice, Italy.xlsx	42	42	42	42	42	42	42	42
058. Bologna, Italy.xlsx	22	22	22	22	22	22	22	22
059. Olbia-Costa Smeralda, Italy.xlsx	42	42	42	42	42	42	42	42
060. Cagliari, Italy.xlsx	42	42	42	42	42	42	42	42
061. Rome, Italy.xlsx	42	42	42	42	42	42	42	42
062. Bari-Palese, Italy.xlsx	42	42	42	42	42	42	42	42
063. Crotone, Italy.xlsx	42	42	42	42	42	42	42	42
064. Gela, Italy.xlsx	42	42	42	42	42	42	42	42
065. Ljubljana, Slovenia.xlsx	21	21	21	21	21	21	21	21
066. Tallinn-Harku, Estonia.xlsx	11	11	11	11	11	11	11	11
067. Ventspils, Latvia.xlsx	11	11	11	11	11	11	11	11
068. Riga, Latvia.xlsx	21	11	11	11	11	11	11	11
069. Kaunas, Lithuania.xlsx	21	11	11	11	11	11	11	11
070. Koszalin, Poland.xlsx	11	11	11	11	11	11	11	11
071. Warsaw, Poland.xlsx	21	21	21	21	21	21	11	11
072. Zamosc, Poland.xlsx	21	21	21	21	21	21	11	11
073. Minsk, Belarus.xlsx	21	11	11	11	11	11	11	11
074. Kosice, Slovakia.xlsx	21	21	21	21	21	21	21	21
075. Kiev, Ukraine.xlsx	21	21	21	21	21	21	11	11
076. Odessa, Ukraine.xlsx	22	22	22	22	22	22	21	21
077. Debrecen, Hungary.xlsx	22	22	22	22	22	22	22	22
078. Belgrade, Serbia.xlsx	22	22	22	22	22	22	22	22
079. Banja Luka, Bosnia and Herzegovina.xlsx	22	22	22	22	22	22	21	21
080. Timisoara, Romania.xlsx	22	21	21	21	21	21	21	21
081. Cluj-Napoca, Romania.xlsx	22	21	21	21	21	21	11	11
082. Galati, Romania.xlsx	22	22	22	22	22	22	22	22
083. Bucharest, Romania.xlsx	22	22	22	22	22	22	22	22
084. Podgorica, Montenegro.xlsx	42	42	42	42	42	42	42	42
085. Sofia, Bulgaria.xlsx	21	21	21	21	21	21	21	21
086. Plovdiv, Bulgaria.xlsx	22	22	22	22	22	22	22	22
087. Varna, Bulgaria.xlsx	22	22	22	22	22	22	22	22
088. Thessaloniki, Greece.xlsx	42	42	42	42	42	42	42	42
089. Athens, Greece.xlsx	42	42	42	42	42	42	42	42
090. Istanbul, Turkey.xlsx	42	42	42	42	42	42	42	42
091. Izmir, Turkey.xlsx	42	42	42	42	42	42	42	42

Table D.1 – continued from previous page

Location	0d	1d	2d	3d	4d	5d	6d	7d
092. Larnaca, Cyprus.xlsx	42	42	42	42	42	42	42	42

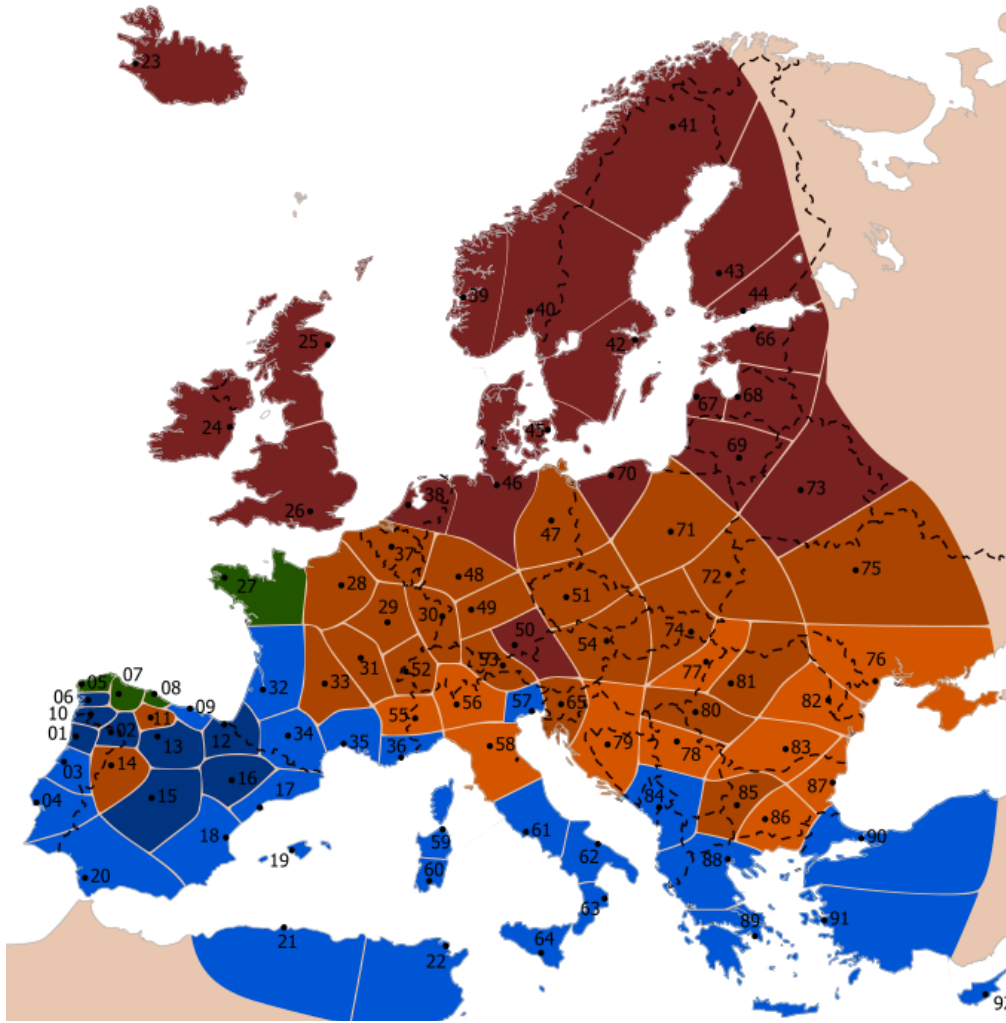


Figure D.1: *Climate map for case 1414AaBb-1day*

Table D.2: *Case: 1616AaBb – $CDD_L = 250$, $HDD_L = 1500$, $DPH_{L,L} = 1100$, $DPH_{L,U} = 4000$*

Location	0d	1d	2d	3d	4d	5d	6d	7d
001. Porto, Portugal.xlsx	42	42	41	31	31	31	31	31
002. Braganca, Portugal.xlsx	21	21	21	21	21	21	21	21
003. Coimbra, Portugal.xlsx	42	42	42	42	42	42	42	42
004. Lisbon, Portugal.xlsx	42	42	42	42	42	42	42	42
005. La Coruna, Spain.xlsx	42	42	31	31	31	31	31	31
006. Pontevedra, Spain.xlsx	41	41	41	41	41	41	41	41

Table D.2 – continued from previous page

Location	0d	1d	2d	3d	4d	5d	6d	7d
007. Lugo, Spain.xlsx	11	11	11	11	11	11	11	11
008. Oviedo, Spain.xlsx	31	31	31	31	31	31	31	31
009. Santander, Spain.xlsx	42	42	42	42	31	31	31	31
010. Ourense, Spain.xlsx	41	41	41	41	41	41	41	41
011. Leon, Spain.xlsx	21	21	11	11	11	11	11	11
012. San Sebastian, Spain.xlsx	32	32	31	31	31	31	31	31
013. Valladolid, Spain.xlsx	21	21	21	21	21	21	21	21
014. Salamanca, Spain.xlsx	21	21	21	21	21	21	21	21
015. Madrid, Spain.xlsx	21	21	41	41	41	41	41	41
016. Zaragoza, Spain.xlsx	41	41	41	41	41	41	41	41
017. Barcelona, Spain.xlsx	42	42	42	42	42	42	42	42
018. Valencia, Spain.xlsx	42	42	42	42	42	42	42	42
019. Palma, Spain.xlsx	42	42	42	42	42	42	42	42
020. Sevilla, Spain.xlsx	42	42	42	42	42	42	42	42
021. Algiers, Algeria.xlsx	42	42	42	42	42	42	42	42
022. Tunis, Tunisia.xlsx	42	42	42	42	42	42	42	42
023. Reykjavik, Iceland.xlsx	11	11	11	11	11	11	11	11
024. Dublin, Ireland.xlsx	11	11	11	11	11	11	11	11
025. Aberdeen, United Kingdom.xlsx	11	11	11	11	11	11	11	11
026. London, United Kingdom.xlsx	11	11	11	11	11	11	11	11
027. Brest, France.xlsx	11	11	11	11	11	11	11	11
028. Paris, France.xlsx	21	21	11	11	11	11	11	11
029. Nancy, France.xlsx	21	21	11	11	11	11	11	11
030. Strasbourg, France.xlsx	22	22	11	11	11	11	11	11
031. Dijon, France.xlsx	22	22	21	21	21	11	11	11
032. Bordeaux, France.xlsx	42	42	42	41	41	41	41	31
033. Clermont-Ferrand, France.xlsx	21	21	21	21	11	11	11	11
034. Toulouse-Blagnac, France.xlsx	22	22	42	42	42	41	41	41
035. Montpellier, France.xlsx	42	42	42	42	42	42	42	42
036. Nice, France.xlsx	42	42	42	42	42	42	42	42
037. Brussels, Belgium.xlsx	11	11	11	11	11	11	11	11
038. Amsterdam, Netherlands.xlsx	11	11	11	11	11	11	11	11
039. Bergen, Norway.xlsx	11	11	11	11	11	11	11	11
040. Oslo, Norway.xlsx	11	11	11	11	11	11	11	11
041. Kiruna, Sweden.xlsx	11	11	11	11	11	11	11	11
042. Stockholm, Sweden.xlsx	11	11	11	11	11	11	11	11
043. Tampere, Finland.xlsx	11	11	11	11	11	11	11	11

Table D.2 – continued from previous page

Location	0d	1d	2d	3d	4d	5d	6d	7d
044. Helsinki, Finland.xlsx	11	11	11	11	11	11	11	11
045. Copenhagen, Denmark.xlsx	11	11	11	11	11	11	11	11
046. Hamburg, Germany.xlsx	11	11	11	11	11	11	11	11
047. Berlin, Germany.xlsx	21	21	21	11	11	11	11	11
048. Frankfurt, Germany.xlsx	21	21	11	11	11	11	11	11
049. Stuttgart, Germany.xlsx	11	11	11	11	11	11	11	11
050. Munich, Germany.xlsx	11	11	11	11	11	11	11	11
051. Prague, Czech Republic.xlsx	11	11	11	11	11	11	11	11
052. Geneva, Switzerland.xlsx	21	21	21	21	21	21	21	21
053. Innsbruck, Austria.xlsx	11	11	11	11	11	11	11	11
054. Vienna, Austria.xlsx	21	21	21	21	21	21	21	11
055. Torino, Italy.xlsx	22	22	22	22	22	22	22	22
056. Milan, Italy.xlsx	22	22	22	22	22	22	22	22
057. Venice, Italy.xlsx	22	22	22	22	22	22	22	22
058. Bologna, Italy.xlsx	22	22	22	22	22	22	22	22
059. Olbia-Costa Smeralda, Italy.xlsx	42	42	42	42	42	42	42	42
060. Cagliari, Italy.xlsx	42	42	42	42	42	42	42	42
061. Rome, Italy.xlsx	42	42	42	42	42	42	42	42
062. Bari-Palese, Italy.xlsx	42	42	42	42	42	42	42	42
063. Crotone, Italy.xlsx	42	42	42	42	42	42	42	42
064. Gela, Italy.xlsx	42	42	42	42	42	42	42	42
065. Ljubljana, Slovenia.xlsx	21	21	21	21	21	21	21	11
066. Tallinn-Harku, Estonia.xlsx	11	11	11	11	11	11	11	11
067. Ventspils, Latvia.xlsx	11	11	11	11	11	11	11	11
068. Riga, Latvia.xlsx	11	11	11	11	11	11	11	11
069. Kaunas, Lithuania.xlsx	11	11	11	11	11	11	11	11
070. Koszalin, Poland.xlsx	11	11	11	11	11	11	11	11
071. Warsaw, Poland.xlsx	11	11	11	11	11	11	11	11
072. Zamosc, Poland.xlsx	11	11	11	11	11	11	11	11
073. Minsk, Belarus.xlsx	11	11	11	11	11	11	11	11
074. Kosice, Slovakia.xlsx	21	21	21	21	21	21	21	21
075. Kiev, Ukraine.xlsx	21	21	21	21	11	11	11	11
076. Odessa, Ukraine.xlsx	22	22	22	22	21	21	21	21
077. Debrecen, Hungary.xlsx	22	22	22	22	22	22	22	21
078. Belgrade, Serbia.xlsx	22	22	22	22	22	22	22	22
079. Banja Luka, Bosnia and Herzegovina.xlsx	22	22	22	22	22	22	21	21

Table D.2 – continued from previous page

Location	0d	1d	2d	3d	4d	5d	6d	7d
080. Timisoara, Romania.xlsx	22	22	21	21	21	21	21	21
081. Cluj-Napoca, Romania.xlsx	22	22	11	11	11	11	11	11
082. Galati, Romania.xlsx	22	22	22	22	22	22	22	22
083. Bucharest, Romania.xlsx	22	22	22	22	22	22	22	22
084. Podgorica, Montenegro.xlsx	42	42	42	42	42	42	42	42
085. Sofia, Bulgaria.xlsx	21	21	21	21	21	11	11	11
086. Plovdiv, Bulgaria.xlsx	22	22	22	22	22	22	22	22
087. Varna, Bulgaria.xlsx	22	22	22	22	22	22	22	22
088. Thessaloniki, Greece.xlsx	42	42	42	42	42	42	42	42
089. Athens, Greece.xlsx	42	42	42	42	42	42	42	42
090. Istanbul, Turkey.xlsx	42	42	42	42	42	42	42	42
091. Izmir, Turkey.xlsx	42	42	42	42	42	42	42	42
092. Larnaca, Cyprus.xlsx	42	42	42	42	42	42	42	42

Appendix E

Appended Papers

Appended Papers

Paper I

*"Climate Classification for the Simulation of Thermally Activated
Building Systems (TABS)"*

B. Behrendt & J. E. Christensen

Published in: *Proceedings of Building Simulation, 2013*

Appended Papers

CLIMATE CLASSIFICATION FOR THE SIMULATION OF THERMALLY ACTIVATED BUILDING SYSTEMS (TABS)

Benjamin Behrendt, Jørgen Christensen
Department of Civil Engineering
Technical University of Denmark

ABSTRACT

Thermally activated building systems (TABS) provide high temperature cooling and low temperature heating which has a better efficiency compared to traditional heating and cooling solutions. Additionally the moderate required temperature levels for heating and cooling create the opportunity to use alternative (sustainable) energy sources that would otherwise be insufficient.

The design of TABS is however challenging and most often requires a complete simulation of the building. The standard ISO 11855-4 (2011) suggests a simplified sizing method for TABS. The results however omit condensation risk entirely. The proposed climate classification should fill this gap by providing the missing data in a simple manner.

INTRODUCTION

TABS are low temperature heating and high temperature cooling systems. This has a number of advantages if compared to conventional systems. The required temperature levels are more favorable for the use in conjunction with sustainable energy sources such as for instance ground heat exchangers, solar energy (collectors), heat pumps, low temperature district heating and others. The use of TABS can considerably decrease the primary energy demand of a building while at the same time maintaining or even improve the comfort in the building.

The utilization of TABS for cooling of buildings introduces one problem that is mostly foreign to air based cooling systems: Condensation within occupied space. Even though in office buildings the internal humidity load is mostly within acceptable limits the problem could still arise depending on the external environment.

During the design of TABS it is therefore important to evaluate the risk of condensation within the building. If a complete building simulation is undertaken most building simulation tools today recognize potential condensation risks and notify the user. Since simulations of the like are however time consuming it is of considerable value if the usability of TABS could be quickly assessed in a simplified approach. To this end the ISO 11855-4 (2011) suggests the use of a simplified simulation method. This type of simulation however does not consider humidity at all but focuses solely on thermal performance. A possible result of

a simulation with such tool could be that the building may be sufficiently cooled by TABS, a full building simulation would however reveal that the system would likely cause condensation on the controlled surfaces.

To identify this risk it would be beneficial if a climate classification for the use of TABS would exist. This is however not the case as most available climate classifications consider precipitation but not humidity (relative or total). The Köppen-Geiger (Kottek et al., 2006) or the ASHRAE Climate classification (ASHRAE, 2010) are to examples for well established systems, in terms of simulating TABS they are however not quite fitting the needs.

The suggested climate classification is greatly simplified if compared with other established systems such as the Köppen-Geiger or the ASHRAE classification but it incorporates the two important key variables for TABS. The proposed system is based on a combination of degree days and the outside dew point temperature. Compared to the afore mentioned classifications it offers less climatic zones but in return they are closer modeled to the problem at hand.

The current classification is only based on 54 locations in Europe hence its resolution is still too low in some areas. It can however already be used to get a first estimate of what should be expected of a TABS system used in the area.

The method had been tested on a simple office building that has been simulated in various locations (e.g. climate zones) and it has been found that the method works as intended.

Problem statement

The intention is to create a simple climate classification to determine the usability of TABS for a modern building (in accordance to current building standards) throughout Europe (and eventually worldwide). The following points should be answered through the classification. The classification should provide a quick answer to the questions:

Does the building need ...

- ... a heating system?
- ... a cooling system?
- ... a heating and cooling system?
- ... no dehumidification?
- ... intermittent dehumidification?
- ... continuous dehumidification?

In conjunction with the simplified approach for the sizing of TABS as suggested in ISO 11855-4 (2011) this will provide a method to evaluate the usability of tabs.

EXISTING CLIMATE CLASSIFICATIONS

A number of already existing climate classifications have been considered but due to different shortcomings they could not be used.

One of the most promising climate classifications was the Köppen-Geiger system. In the end this system could not be used due to high differences within one climatic zone making it impossible to use it for the evaluation of TABS. It also had shortcomings in relation to the provided humidity data.

Another system that had been considered is the ASHRAE Climate Zones. However in this case insufficient data was provided as climate data only includes precipitation in the USA and humidity is completely omitted. However the ASHRAE Climate Zones have been used in a previous study (Love and Tian, 2009) comparing the use of TABS to a VAV and radiator based system with regard to energy savings. Only US cities have been included in this study.

The degree day method has been used in previous. Since the operation of TABS can be greatly limited by humidity it is important to have a system that pays attention to this aspect. The new introduced system as a combination of heating and cooling degree days as well as humidity can achieve this.

THE NEW CLIMATE CLASSIFICATION

Degree days are defined as the difference of the base temperature and the average daily or hourly outdoor temperature. After both, heating and cooling degree day calculations are explained, the used base temperature is discussed in detail.

Heating Degree Days

Heating Degree Days (HDD) are calculated by defining a base temperature, from which the average daily or hourly outdoor temperature is subtracted. If the value is positive, it is added to the sum of heating degree days. This is repeated for every day or hour throughout the year. Equation 1 shows the heating degree day calculation using average daily temperatures based on hourly temperatures. Equation 2 shows the heating degree day calculation using hourly temperatures. Thus the key difference is that Equation 1 only adds to the HDD if the daily average outdoor temperature is below the base temperature whereas Equation 2 adds to the HDD every time the hourly outdoor temperature is below the base temperature.

The high thermal mass of TABS causes the system to have a high time constant. This high time constant makes it practically impossible to actively react to short term changes in heating demand. For this reason Equation 1 is the appropriate choice. Short term changes in heating demand are compensated through self regulation of TABS. This self regulation is a com-

ination of two things. First the difference in heat capacity of air and typical building materials (e.g. concrete) and second the changing temperature difference between the air and the active surfaces.

$$HDD = \sum_{j=1}^{365} \left(T_b - \frac{\sum_{i=1}^{24} T_{j,i}}{24} \right)^+ \quad (1)$$

$$HDD = \sum_{j=1}^{365} \frac{\sum_{i=1}^{24} (T_b - T_{j,i})^+}{24} \quad (2)$$

Cooling Degree Days

Cooling Degree Days (CDD) are calculated very similar to heating degree days. A base temperature is defined which is then subtracted from the average daily or hourly outdoor temperature. If the value is positive it is added to the sum of cooling degree days. This is repeated for every day or hour throughout the year. Equation 3 shows the cooling degree calculation using average daily temperatures based on hourly temperatures. Equation 4 shows the cooling degree day calculation using hourly temperatures.

For calculating CDD Equation 3 has been used. The argument is the same as for the calculation of HDD.

$$CDD = \sum_{j=1}^{365} \left(\frac{\sum_{i=1}^{24} T_{j,i}}{24} - T_b \right)^+ \quad (3)$$

$$CDD = \sum_{j=1}^{365} \frac{\sum_{i=1}^{24} (T_{j,i} - T_b)^+}{24} \quad (4)$$

Base Temperature

In general, the base temperature - or balance point temperature - is the outside air temperature at which weather-related energy demand would be zero including any gains from occupants, solar radiation, lighting, equipment, etc. - i.e. the average gains are equal to the average heat loss of the building in the given period. Or in simpler terms: No system (heating or cooling) is required, if the outside temperature is equal to the base temperature. This can also be seen from Equation 5 (ASHRAE, 2001).

$$q_{gain} = h \cdot (T_i - T_b) \quad (5)$$

$$T_b = T_i - \frac{q_{gain}}{h} \quad (6)$$

This shows that it is impossible to have one standardized base temperature as buildings vary in their construction (heat loss coefficient), location and use (average gains from equipment, occupants, solar radiation, etc.) as well as desired indoor temperature (thermal comfort requirements).

In addition different base temperatures are currently used in different countries. In Denmark 17°C are commonly used as base temperature for heating degree days with a minimum indoor temperature of 20°C. The remaining 3°C are assumed to be provided through internal and external heat gains. (ASHRAE, 2001; Cap-pelen, 2002) The same base temperature is used in some European countries, in others, like the United Kingdom and Germany the used base temperatures are with 15.5°C and 15°C respectively considerably lower. The USA on the other hand use a higher base temperature of 18.3°C (Energy Lens n.d.; Butala & Prek 2010) for the calculation of cooling degree days less countries have set a base temperature. ASHRAE uses a base temperature of only 10°C, assuming that the remaining heat to reach thermal comfort is supplied through a combination of internal and external gains (ASHRAE, 2001).

For the new climate classification the base temperature used for heating degree days is 18°C and for cooling degree days is 13°C. Compared to the suggestion by Laustsen (2008) only four climatic zones have been defined as illustrated in Table 1.

Table 1: Criteria for the four different thermal climates, based on heating and cooling degree days with a base temperature of 18°C for HDD and 13°C for CDD, based on Laustsen (2008).

Climate	Heating	Cooling
Heating based	$2000 \leq HDD$	$CDD < 1000$
Combined	$2000 \leq HDD$	$1000 \leq CDD$
Moderate	$HDD < 2000$	$CDD < 1000$
Cooling based	$HDD < 2000$	$1000 \leq CDD$

Humidity considerations

For cooling with TABS it is important to consider the possibility of condensation on controlled surfaces as well as inside of the construction. Where the first is easily spotted, the latter is not as easy to observe. Condensation inside of the slab might lead to future problems and should therefore be avoided. This makes low dew-point temperatures of 14°C interesting. Under extreme conditions it could otherwise happen that mold starts to grow on the controlled surfaces.

Due to thermal comfort requirements (neglecting possible radiant asymmetries) the floor surface temperatures should not be lower than 19°C and wall surfaces should not be cooled below 17°C (Babiak et al., 2007). The presented climate classification distinguishes three different humidity scenarios.

- **No dehumidification** - In this case humidity levels are not likely to cause any problems, even without any dehumidification.
- **Intermittent dehumidification** - The installation of a dehumidification unit is required. However the unit will not need to be operated throughout the cooling season.

- **Continuous dehumidification** - During the cooling period the indoor humidity needs to be controlled most of the time.

Within the 54 evaluated cities (52 in Europe, 2 in North-Africa) no case has been found where continuous dehumidification would be necessary. As can be seen in Table 2 there are however locations like Abu Dhabi, United Arab Emirates, that do require continuous dehumidification.

Degree Days and humidity combined

The new system is now a combination of the four thermal zones with the three humidity scenarios. This generates a theoretical total of twelve climate zones. Based on the 54 European cities that have been evaluated for the classification not all of these zones can be found in Europe. Table 2 shows an example city for each of the climate zones. If no example is given no occurrence of this combination has been found so far.

Table 2: Example cities for each defined category (if any) using base temperatures of 18°C for HDD and 13°C for CDD

Climate	No Dehumidification
Heating based	Copenhagen, Denmark HDD: 3562, CDD: 308
Combined	Bucharest, Romania HDD: 3029, CDD: 1071
Moderate	Porto, Portugal HDD: 1506, CDD: 870
Cooling based	Madrid, Spain HDD: 1964, CDD: 1407
Climate	Intermittent Dehumidification
Heating based	Strasbourg, France HDD: 2947, CDD: 650
Combined	Milan, Italy HDD: 2640, CDD: 1064
Moderate	-
Cooling based	Athens, Greece HDD: 1112, CDD: 2120
Climate	Continues Dehumidification
Heating based	-
Combined	-
Moderate	-
Cooling based	Abu Dhabi, UAE HDD: 24, CDD: 5159

SYSTEM VALIDATION

In order to validate the established system a number of simulations have been done in BSim. The reference Building used for this study is the same as has been used for an earlier simulation tool comparison by Behrendt et al. (2011). Its dimensions can be seen in figure 1. The building is well insulated and has good glassing and external shading.

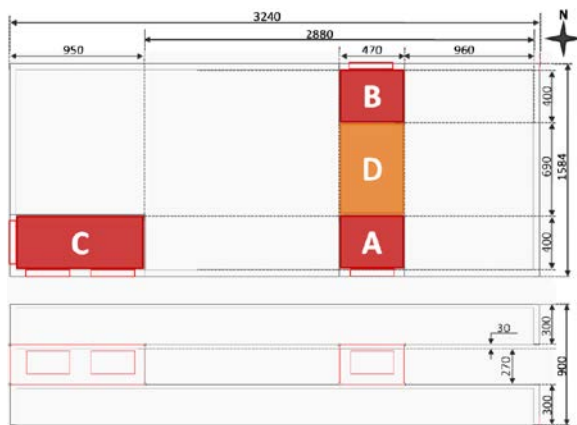


Figure 1: Zone division in the reference building

Table 3 summarizes key values for the building. All loads were present only on weekdays from 8:00 to 17:00 and ventilation was only operating during these hours as well. There is no system operation or internal loads present on weekends. The ventilation system contains a heat recovery system with an efficiency of 80% and during the heating season the supply air is heated to 20°C if the outdoor temperature drops below 16°C (no cooling). During the cooling season the supply air is cooled to 25°C if necessary (no heating). Additional dehumidification is applied as necessary. The heating season was set from 1st of October to 30th of April and from 1st of March to September 30th was considered to be cooling season.

Between the investigated locations only the supply water temperatures as well as used dead-bands have been adjusted to reflect the local demands.

Table 3: Reference building data

		Zone		
		A & B	C	D
Floor area	$[m^2]$	18.6	38	31.9
Glazing area	$[m^2]$	4	12	—
Ventilation rate	$[l/s]$	27	54.6	22.3
TABS installed		yes	yes	no
Loads		A & B	C	D
Occupants	$[W]$	240	480	—
Equipment	$[W]$	160	320	—
Lighting	$[W]$	93	190	159
Total	$[W]$	493	990	159

The indoor environment was then evaluated according to DS/EN 15251 (2007). The system was considered to be sufficient if the operative temperature remained in category B, or better, for at least 95% of the time. For the validation calculations for all locations have been done. However only a selection is presented in this paper.

Madrid, Spain

According to table 2 Madrid is in a cooling based climate without the need for dehumidification. The simulations done in BSim (see table 4 and 5 for information TABS setup) to verify this show that TABS will be

able to provide adequate cooling throughout the cooling season. As can be seen in figure 2 the operative temperature only exceeds 26°C for about 1% of the time in Zone C. Apart from that there is a slight problem with under-cooling in zones A and B where temperatures drop below 23°C for about 1% of the time.

Table 4: TABS operation key values - part 1

		Season	
		Cooling	Heating
T_s	$[^{\circ}\text{C}]$	21.5	21.5
Dead-band			
Zone A	$[^{\circ}\text{C}]$	23 – 24	20.5 – 21.5
Zone B	$[^{\circ}\text{C}]$	22 – 24	20.5 – 21.5
Zone C	$[^{\circ}\text{C}]$	23 – 23.5	20.5 – 21.5

Table 5: TABS operation key values - part 2

		Zone		
		A	B	C
Pump on	$[H]$	5441	4377	5541
Solar gains	$[kWh]$	969	538	2742
H ₂ O removed	$[kg]$	0.3	0.3	0.6

As table 5 shows only very little (in total 1.2kg) water was removed from the supply air in order to avoid condensation through the entire cooling season. With this it is very unlikely that actual condensation would have occurred, as the surface temperature is usually considerably higher than the supply temperature, thus introducing a considerable safety margin. This was not surprising as can be seen from figure 3 where all hours with dew point temperatures above 14°C are shown. As can be seen the dew point temperature barely exceeds 16°C .

In the case of Madrid most of the cooling is achieved through TABS. The ventilation system is primarily used to supply fresh air to the zones. This can also be seen from table 6 where, during the cooling period, ventilation consumes about 10% of the energy that is used by TABS. In general only limited heating is needed.

Table 6: Yearly energy consumption for Madrid, Spain

	Zone		
	A	B	C
TABS Heating	0.1	1.4	0.6
TABS Cooling	48.4	33.6	51.2
Ventilation Heating	0.9	1.5	1.1
Ventilation Cooling	4.7	4.7	4.7
Total	54.1	41.2	57.6
	$[kWh/m^2 \text{ per year}]$		

Abu Dhabi, United Arab Emirates

According to table 2 Abu Dhabi is in a cooling based climate with the need for continuous dehumidification. The simulations done in BSim (see table 7 and 8 for information TABS setup) to verify this show that TABS will be able to provide adequate cooling throughout

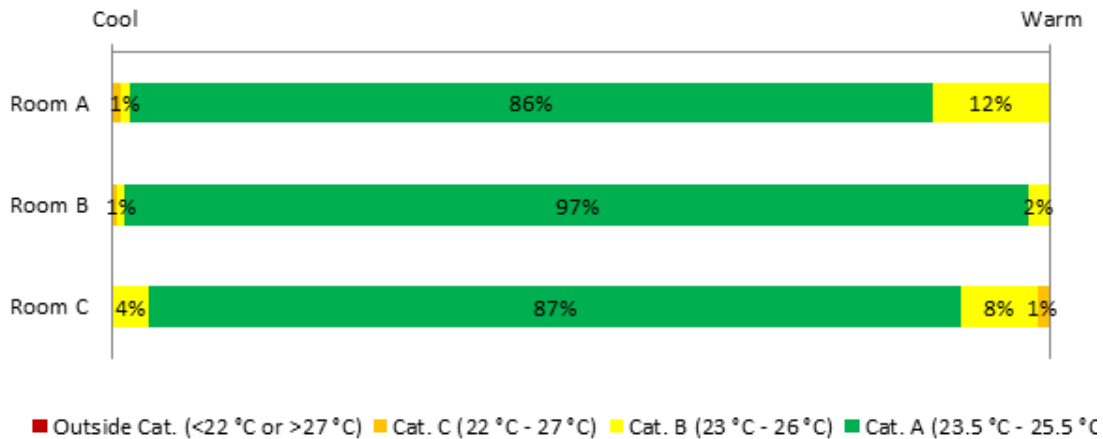


Figure 2: Operative temperature distribution according to the comfort categories for Madrid, Spain

the cooling season. As can be seen in figure 4 the operative temperature only exceeds 26°C for about 2% of the time in Zone C. Also in zone C there is a substantial amount of time (34%) in which temperatures are between 25.5°C and 26°C (cat. B). This is however acceptable for the aim of this validation.

Table 7: TABS operation key values - part 1

	Season	
	Cooling	Heating
T_s [°C]	19.5	21
Dead-band		
Zone A [°C]	23 – 24	20 – 24
Zone B [°C]	23 – 24	20 – 24
Zone C [°C]	23 – 24	23 – 24

Table 8: TABS operation key values - part 2

		Zone		
		A	B	C
Pump on [H]		3769	3706	4840
Solar gains [kWh]		1003	550	2912
H ₂ O removed [kg]		366	366	742

As table 8 shows that there is a significant amount of water (in total 1474kg removed from the supply air

over the course of the year. Without a continuous dehumidification this would result in considerable condensation on the controlled surfaces. This was also expected from the climate classification and can also be seen from figure 4. In this case the dew point temperature well exceeds 16°C most of the time, making continuous dehumidification during the cooling season necessary.

In Abu Dhabi the TABS are removing roughly three fourth of the heat from the zones, with the remaining energy being removed by the ventilation system. Table 9 shows that there is a considerable cooling load but no heating is required at any time.

Table 9: Yearly energy consumption for Abu Dhabi, United Arab Emirates

	Zone		
	A	B	C
TABS Heating	0.0	0.0	0.0
TABS Cooling	102.1	85.9	116.8
Ventilation Heating	0.0	0.0	0.0
Ventilation Cooling	36.6	36.6	37.0
Total	138.6	122.5	153.9
	[kWh/m ² per year]		

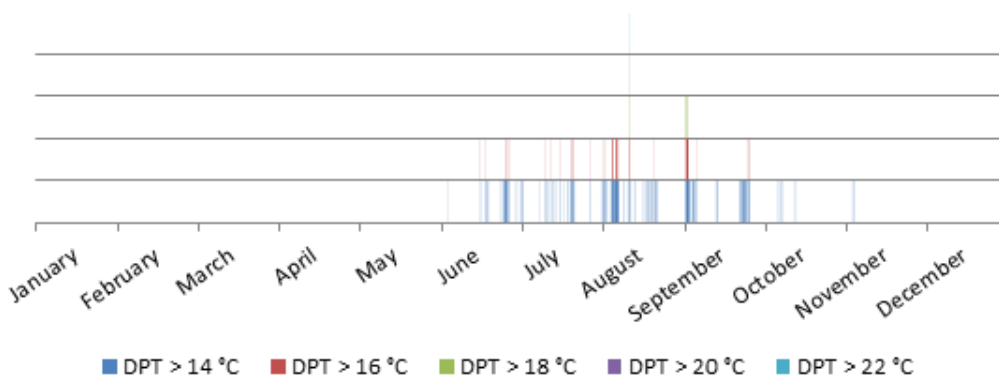


Figure 3: Dew point temperature diagram for Madrid, Spain as example for a cooling based climate without need for dehumidification

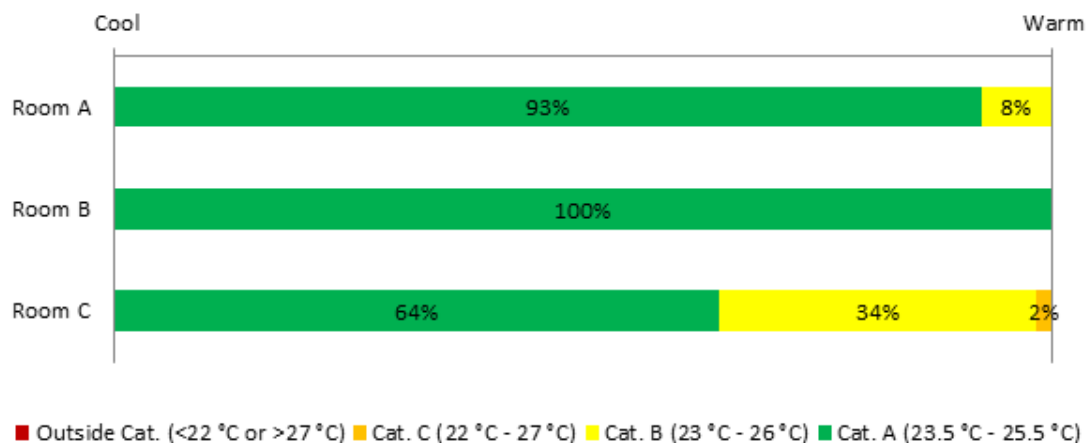


Figure 4: Operative temperature distribution according to the comfort categories for Abu Dhabi, United Arab Emirates

DISCUSSION AND RESULT ANALYSIS

Due to insufficient humidity informations, both the Köppen-Geiger, as well as the ASHRAE climate classification have been rejected. Extending either one of the systems to include humidity levels would likely have resulted in further zone fragmentation (even higher amount of different climatic zones), making them complicated to use.

The new classification offers a considerably simpler method, leaving less room for mix-ups while using the system.

The validation has shown that it is possible to use the new system to predict the need for dehumidification. However as the comparison of the energy consumption of Madrid and Abu Dhabi shows it is not possible to predict what percentage of the load will be removed by TABS and how much the ventilation system has to take care of. In extreme cases it is possible that the air handling unit is removing the biggest part of the load do to dehumidification requirements.

Within Europe only seven out of twelve possible climatic zones have been found. This was not surprising as a heating based climate will only require very lit-

tle cooling (if any) and in turn have very little need for dehumidification. There might however be circumstances where even a heating base climate requires continuous dehumidification during cooling periods. It is however questionable that cooling would be installed in such cases.

Based on the data for the 54 cities Figure 6 has been created. As can be seen most of Europe is either heating (north) or cooling (south) based. However there are some locations within otherwise uniform areas that indicate that the current resolution might not be high enough. As can be seen by Strasbourg (France - No. 15) climatic zones might be completely enclosed by just one other zone. This suggests that is very well possible that an increase on resolution (analysis of more locations/cities) could reveal that the current zoning is imprecise. The included map should therefore only be used with caution but it should reveal good results in close proximity to any of the indicated cities.

The new classification can also be used to evaluate the usability of other systems. Since the system is however set up for the evaluation of TABS additional precautions have to be considered.

The minimum permissible dew point temperature may

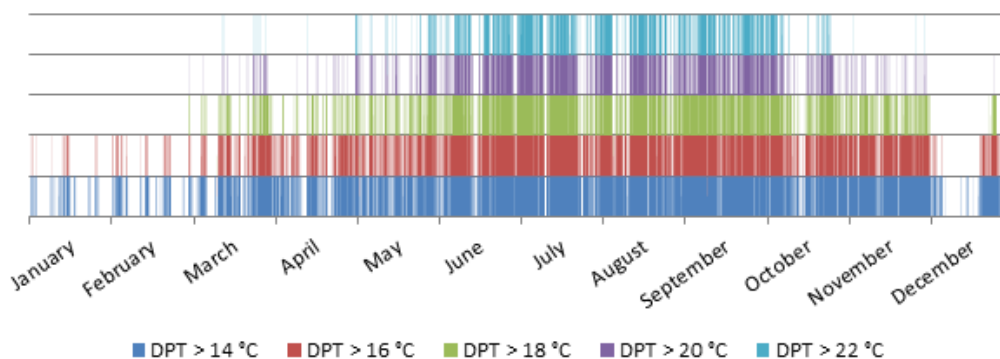
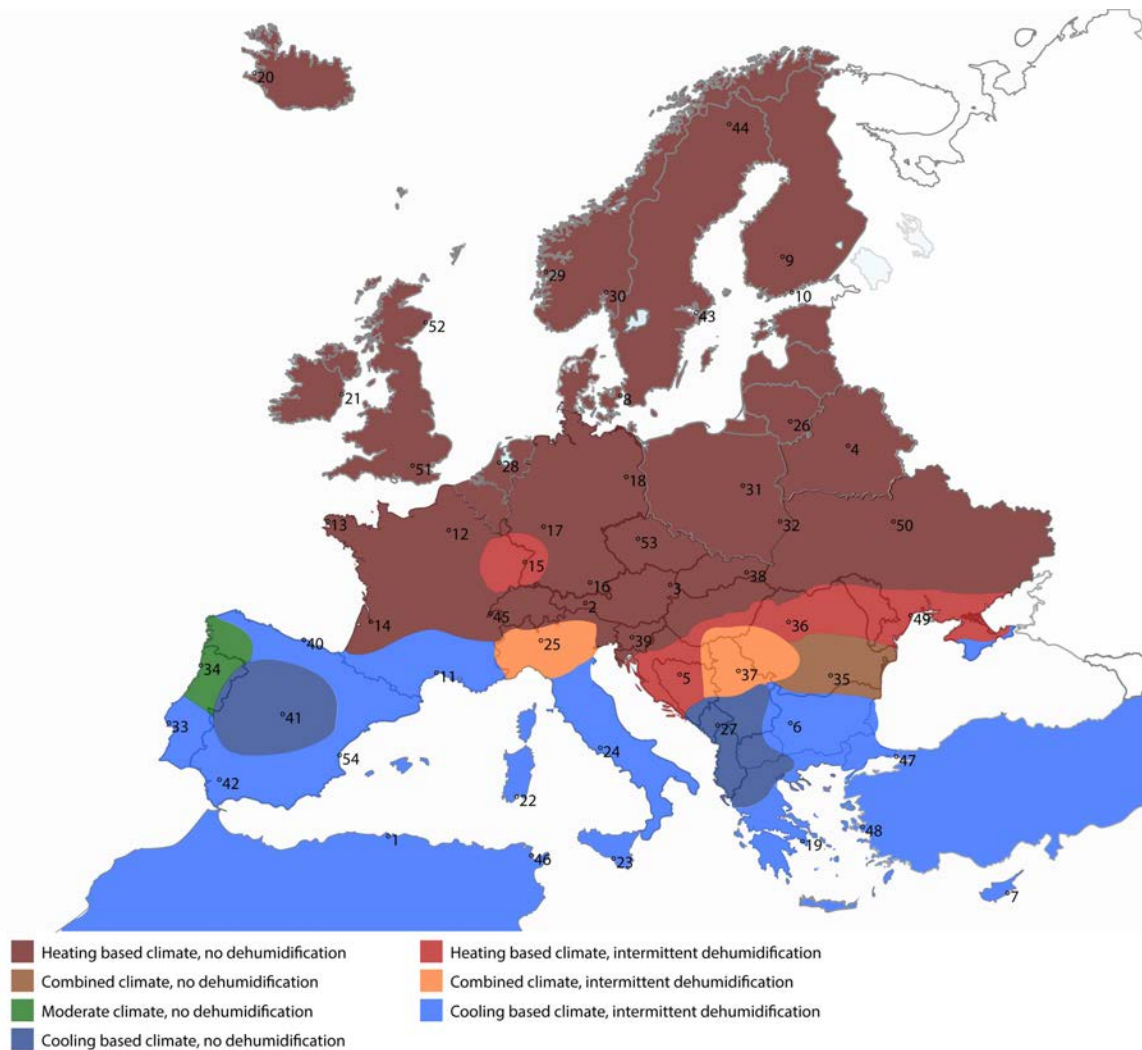


Figure 5: Dew point temperature diagram for Abu Dhabi, United Arab Emirates as example for a cooling based climate without need for dehumidification



- | | | |
|---------------------------------------|----------------------------|------------------------------|
| 1. Algiers, Algeria | 19. Athens, Greece | 37. Belgrade, Serbia |
| 2. Innsbruck, Austria | 20. Reykjavík, Iceland | 38. Kosice, Slovakia |
| 3. Vienna, Austria | 21. Dublin, Ireland | 39. Ljubljana, Slovenia |
| 4. Minsk, Belarus | 22. Cagliari, Italy | 40. Santander, Spain |
| 5. Banja Luka, Bosnia and Herzegovina | 23. Gela, Italy | 41. Madrid, Spain |
| 6. Sofia, Bulgaria | 24. Rome, Italy | 42. Sevilla, Spain |
| 7. Larnaca, Cyprus | 25. Milan, Italy | 43. Stockholm, Sweden |
| 8. Copenhagen, Denmark | 26. Kaunas, Lithuania | 44. Kiruna, Sweden |
| 9. Tampere, Finland | 27. Podgorica, Montenegro | 45. Geneva, Switzerland |
| 10. Helsinki, Finland | 28. Amsterdam, Netherlands | 46. Tunis, Tunisia |
| 11. Montpellier, France | 29. Bergen, Norway | 47. Istanbul, Turkey |
| 12. Paris, France | 30. Oslo, Norway | 48. Izmir, Turkey |
| 13. Brest, France | 31. Warsaw, Poland | 49. Odessa, Ukraine |
| 14. Bordeaux, France | 32. Zamosc, Poland | 50. Kiev, Ukraine |
| 15. Strasbourg, France | 33. Lisbon, Portugal | 51. London, United Kingdom |
| 16. Munich, Germany | 34. Porto, Portugal | 52. Aberdeen, United Kingdom |
| 17. Frankfurt, Germany | 35. Bucharest, Romania | 53. Prague, Czech Republic |
| 18. Berlin, Germany | 36. Cluj-Napoca, Romania | 54. Valencia, Spain |

Figure 6: Map of Europe based on the new climate classification system.
Based on vector map by Dill (2012)

differ greatly from one system to another. For example a chilled beam might already cause condensation on its surfaces while no condensation occurs for TABS when operated at the same supply temperature. However, in this case chilled beams would (with otherwise equivalent geometric properties) have a higher cooling capacity due to its better heat transfer.

Another problem for the use with systems other than TABS could be the choice made for the calculation of HDD and CDD. For systems with low thermal inertia Equations 2 and 4 would be more appropriate to calculate HDD and CDD rather than the here used Equations 1 and 3.

CONCLUSION

For evaluating the use of TABS in different climates, a method for classifying the climates involving heating and cooling degree days and the outdoor dew-point temperature has been put forward and a map of Europe divided into 7 of 12 possible climate zones has been created. The method is simple and works as intended. In conjunction with a simplified sizing method for TABS as suggested in ISO 11855-4 (2011) it is possible to estimate the capabilities of TABS under the given circumstances without the need of a full blown building simulation. This can save time and money as it can be done at early design stages with very little effort.

The current classification should however be further refined. The currently used base temperatures might not be the best choice for modern buildings. The improved insulation and glazing that is required due to current building codes in many countries has a significant influence on the buildings base temperature. Due to different valid building standards around the world it might be necessary to adjust the base temperature accordingly to get the best results.

NOMENCLATURE

- h = heat loss coefficient of the building envelope [W/K]
 T_b = base temperature [°C]
 T_i = average indoor temperature [°C]
 $T_{j,i}$ = outdoor temp. of hour i on day j [°C]
 T_s = Supply water temperature [°C]
 q_{gain} = average gains from equipment, occupants, the sun, etc. [W]
 $\sum(\dots)^+$ = only add to sum if bracket positiv

REFERENCES

- ASHRAE 2001. *ASHRAE Handbook Fundamentals (S-I)*. American Society of heating, Refrigeration and Air-Conditioning Engineers, Inc.
- ASHRAE 2010. *ASHRAE 90.1 Energy standard for*

buildings except low-rise residential buildings (S-I). American Society of heating, Refrigeration and Air-Conditioning Engineers, Inc.

- Babiak, J., Olesen, B. W., and Petrs, D. 2007. *Low temperature heating and high temperature cooling*. REHVA.
- Behrendt, B. M., Raimando, D., Zhang, Y., Schwarz, S., Christensen, J. E., and Olesen, B. W. 2011. A system for the comparison of tools for the simulation of water-based radiant heating and cooling systems. In *12th Conference of International Building Performance Simulation Association*, pages 1025–1032.
- Cappelen, J. 2002. Graddage hører vinteren til @ONLINE Available at: http://www.dmi.dk/dmi/graddage_horer_vinteren_til [Accessed March 29, 2012].
- Dill, E. 2012. Vector maps of europe @ONLINE Available at: <http://www.vecteezy.com/map-vector/5918-vector-maps-of-europe> [Accessed July 23, 2012].
- DS/EN 15251 2007. Indoor environmental input parameters for design and assessment of energy performance of buildings addressing indoor air quality, thermal environment, lighting and acoustics.
- ISO 11855-4 2011. Building environment design — design, dimensioning, installation and control of the embedded radiant heating and cooling systems —part 4: Dimensioning and calculation of the dynamic heating and cooling capacity for tabs.
- Kottek, M., Grieser, J., Beck, C., Rudolf, B., and Rubel, F. 2006. World map of the köppen-geiger climate classification updated. *Meteorologische Zeitschrift*.
- Laustsen, J. 2008. Energy efficiency requirements in building codes, energy efficiency policies for new buildings: Iea information paper. Technical report, International Energy Agency.
- Love, J. and Tian, Z. 2009. Application of radiant cooling in different climates: Assessment of office buildings through simulation. In *11th International IBPSA Conference*, page 2220–2227.

Paper II

*"A system for the comparison of tools for the simulation of
water-based radiant heating and cooling systems"*

B. Behrendt, D. Raimondo, Y. Zhang, S. Schwarz, J. E. Christensen & B. W. Olesen

Published in: *Proceedings of Building Simulation, 2011*

Appended Papers

A SYSTEM FOR THE COMPARISON OF TOOLS FOR THE SIMULATION OF WATER-BASED RADIANT HEATING AND COOLING SYSTEMS

Benjamin M. Behrendt¹, Daniela Raimondo², Ye Zhang³,
Stephanie Schwarz¹, Jørgen E. Christensen¹, Bjarne W. Olesen¹

¹ Technical University of Denmark*, ² Politecnico di Torino**,
³ BeiJing University of Technology*

* Department of Civil Engineering, ** Department of Energetics

ABSTRACT

Low temperature heating and high temperature cooling systems such as thermally activated building systems (TABS) offer the chance to use low exergy sources, which can be very beneficial financially as well as ecologically when using renewable energy sources.

The above has led to a considerable increase of water based radiant systems in modern buildings and a need for reliable simulation tools to predict the indoor environment and energy performance.

This paper describes the comparison of the building simulation tools IDA ICE, IES <VE>, EnergyPlus and TRNSYS. The simulation tools are compared to each other using the same room and boundary conditions.

The results show significant differences in predicted room temperatures, heating and cooling degree hours as well as thermal comfort in winter and summer.

INTRODUCTION

Over the past years, building simulation has become more and more important for the design of new buildings. Building simulation can be used to (i) increase comfort, (ii) decrease energy consumption and at the same time (iii) lower the overall costs for heating and cooling.

Providing better comfort can increase productivity and reduce sickness or other problems of the occupants. Reducing the energy consumption in buildings can contribute greatly towards the goal of a sustainable society. From 2006 to today, the delivered energy for residential and commercial buildings has risen and its share has increased from 15 to 20 per cent (U.S. Energy Information Administration, 2009, 2010). The use of low temperature heating and high temperature cooling systems, such as thermally activated building systems (TABS) can help to reduce this share. TABS can be operated using temperature levels close to the desired room temperature due to the use of large heat transfer areas. The consequential decrease of the temperature difference leads to the opportunity to use renewable energy sources, many of which can also be considered as low exergy sources. In this way not only energy consumption can be reduced but also exergy

destruction can be minimized.

A transition from current heating and cooling systems to low temperature heating and high temperature cooling is also needed to be able to decrease losses in the distribution systems of centralized energy supply like district heating and cooling plants and increase energy performance of decentralized energy systems like heat pumps, chillers, boilers, co-generation etc..

Compared to full air conditioning systems the use of water based cooling may reduce investment costs in equipment, lower operation costs and reduce building height (building materials). Reducing the overall first costs of a building increases its attractiveness to investors. Whereas reducing the running costs is attractive for the user. It is however, important in future cost analysis to look both at investment and running costs, when evaluating the cost benefits of different concepts.

Whereas the simulation of air based heating and cooling systems is supported by most simulation tools, not all of them support the use of thermally activated building systems (TABS)(Crawley et al., 2005b). In most cases the simulation of TABS requires the installation of an additional module to the regular simulation tool or can only be performed by some questionable modification like simulating the TABS as an additional space.

In the end, the question remains how reliable the simulation of TABS is and how the results compare to an actually existing building. This paper is trying to answer this question for a selection of simulation tools.

PROGRAM OVERVIEW

Different commercial available simulation tools have been used to model a modern office building using TABS for heating and cooling purposes. These simulation tools are IDA ICE (4.101), IES <VE> (6.3 April 2011), Energy Plus (6.0.0) and TRNSYS (16.01.0003).

IDA ICE 4

URL: www.equa.se/ice

The modular dynamic multi-zone simulation tool, IDA Indoor Climate and Energy (IDA ICE), is a commercial program which was first released in May 1998. It can be used for the study of the thermal indoor climate of individual zones as well as the energy consumption

of the entire building. IDA has been programmed in the simulation languages Neutral Model Format and Modelica using symbolic equations. Depending on the experience of the user and the complexity of the problem at hand, three different, but integrated user levels are available: Wizard, Standard and Advanced.

The Wizard level can be used to make fast and easy simulations of a single room. It can be used to calculate heating and cooling loads. Both, the Standard as well as the Advanced level are capable of simulating multiple zones within a building. The Standard level is used to build the general simulation model using the available domain specific concepts and objects, such as zones, heating devices or windows. The Advanced level can then be used to edit the mathematical model of the system.

The modular nature of IDA ICE makes it possible to write individual models extending its capabilities as needed by the individual user. (Crawley et al., 2008)

IES <VE>

URL: www.iesve.com

IES <VE> is a commercial simulation platform with the first major version 3.0 released in the late 1990's. The program combines several software components for different simulation tasks.

The main modelling tool in IES <VE> is ModelIT, where it is possible to construct a 3D model of rooms or a whole building. Additionally, CAD data can be imported using plug-ins (e.g. in Revit or SketchUp) or by importing CAD files (e.g. DFX).

For the dynamic thermal simulation, the component ApacheSim is used, whose calculations are based on first-principle mathematical models of heat transfer processes.

ApacheSim can be linked to other components of IES <VE> to include detailed results of shading devices and solar penetration (SunCast), airflow analysis (MacroFlow), component based HVAC systems (ApacheHVAC) and lighting (LightPro, RadianceIES). The results can also be exported for a more detailed CFD simulation by Microflow. (Crawley et al., 2005a; IES, 2011)

EnergyPlus

URL: <http://apps1.eere.energy.gov/buildings/energyplus/>

EnergyPlus is a new-generation building energy simulation program based on DOE-2 and BLAST, with numerous added capabilities. It was released in April 2001, and developed by several U.S. Universities with support from the U.S. Department of Energy, Office of Building Technology, State and Community Programs. EnergyPlus is actually a trademark of the U.S. Department of Energy and a new version of the tool is periodically available online.

EnergyPlus is a stand-alone simulation program without an (user friendly) graphical interface. EnergyPlus

is capable of making whole building energy simulations. It enables to model heating and cooling loads, levels of light, ventilation, other energy flows and water use. It allows to simultaneously model different kinds of embedded systems, obtaining simulation output as the real building would. It includes many innovative simulation capabilities, like, but not limited to, time-steps less than an hour, modular systems and plants with integrated heat balance-based zone simulation, multi-zone air flow, thermal comfort, water use, natural ventilation, and photovoltaic systems.

The building model and the input files can be made through the program itself or imported from different building design programs (EERE, 2011).

TRNSYS

URL: <http://sel.me.wisc.edu/trnsys/index.html>

TRNSYS, standing for transient system simulation program, is a complete and extensible simulation environment. It is commercially available since 1975 (Klein, 2006). It is a flexible tool designed to simulate the transient performance of thermal energy systems. TRNSYS was first developed in a joint project between the University of Wisconsin-Madison, Solar Energy Lab and Colorado State University, Solar Energy Applications Lab in the 1970's.

TRNSYS is an algebraic and differential equation solver in which components are connected graphically in the simulation studio. In building simulations, all HVAC components are solved simultaneously with the building envelope thermal balance and the air network at each time step. The simulation results are based on the individual component simulation performances which can be selected from the simulation studio. It is suitable for the simulation of complicated systems. Users can easily accomplish the desired system control strategies by writing the logical programming or use simple equations thanks to TRNSYS open source code.

TRNSYS also includes the program TRNEdit, which is an all-in-one editor for reading and writing TRNSYS input and output files. TRNEdit can also perform parametric TRNSYS simulations and plot data from the TRNSYS simulation output (Crawley et al., 2008; Klein, 2006; Price and Blair, 2003).

METHODS

In order to analyse the quality of the simulations, it was decided that they should start on a basic level. The complexity of the simulations has been increased from one stage to the next. At the final stage, which is not part of this paper, the simulations will represent a real building, for which extensive measurement data for multiple years is available. Through comparison of the simulation results with the genuine measurement data, it is then possible to evaluate the simulation quality. In the present paper only the results of the different tools are compared with one another.

Comparison of operative temperature

Through the analysis of the operative temperature it is possible to quickly assess the general correlation of the simulation results. If the trend of the lines is synchronized, it is possible to conclude that the programs react similar to the changing input data.

Deviation of operative temperature

By comparison of the average calculated operative temperature of all included tools with the individual operative temperature, it is possible to observe how the differences between the tools change over the course of the year.

Degree hours

Degree hours of overheating for summer as well as for insufficient heating in winter were calculated. In this case however they can naturally not be used to assess the quality of the installed system. Instead, they can be used to easily compare the programs.

Thermal comfort

The thermal environment can be assessed through the thermal comfort categories introduced by the standard EN 15251 (CEN, 2007). This method of representing the results describes the percentage of occupied hours when the operative temperature exceeds the specified ranges.

Other metrics

For the comparison of any heating or cooling system, a number of other metrics such as energy consumption or other comfort factors are of cause relevant. However, due to the nature of the simulation tools, parameters such as draught, vertical air temperature gradients, and radiant temperature asymmetry cannot be calculated.

In the present study the energy use for auxiliary equipment like fans and pumps are not included. Some of the tools can calculate this directly and in other tools the information for calculating this part of the total energy consumption will be available

Using default settings

As far as possible the different default settings of the tools have been used. This will likely result in a lower correlation between the results of the different tools. On the other hand, it is not likely that a user is adjusting any of the default values without any incentive. It was therefore decided that - rather than trimming all possible variables to unison in order to get the highest possible correlation - to leave them as they were to get a more realistic deviation.

TABS

For the final stage in this paper, TABS were modelled in all tools. In the following, the used approach for each of the tools is described.

- IDA allows for the simulation of TABS on both, the Standard and the Advanced level. The TABS

is hereby inserted as an additional layer in the slab construction.

On the Standard level, the input values are limited to design cooling and heating power, temperature difference for design power, controller (Pi, Proportional, Thermostat or always on), coil mass flow, depth in the slab and a heat transfer coefficient that should be selected in accordance to standard EN 15377-1 (CEN, 2008).

On the Advanced level, additional changes to the system can be made, including, but not limited to, changing the pipe length and inner diameter, the heat capacity of the liquid in the pipes or fine tune the control of the system.

In both cases the slab temperature is assumed to be constant over the entire area.

- In IES <VE>, TABS are simulated by splitting the internal ceilings into a ceiling - room - ceiling construction.

The ceiling construction should be divided at the pipe level. The room representing the slabs should be small and the surface resistances should be adjusted to give the construction a more realistic heat transfer behaviour.

The easiest way to obtain results for the thermal behavior of the office room is to use ApacheSim. Here, the temperature of the fictive room between the ceilings is set to the supply temperature of the real system. It can be controlled by either giving it absolute values or using a profile based on, for instance, the air or operative temperature of an office room, the outside air temperature or an equation including both.

A more complicated, but also more promising approach for evaluating TABS is ApacheHVAC. In which "radiators" or "cooled ceilings" should be introduced into the fictive room between the ceilings. In this case, care should be taken also of heat transfer coefficients, water flow rates and heating or cooling areas of the systems.

- EnergyPlus allows to simulate TABS including an internal source layer in the floor/ceiling construction. Water flow and internal diameter, length of the pipes and distance between the tubes are required. Supply water temperature in the system/tubes can be set, but the final system control has to be based on a set point temperature (here the indoor air temperature).
- TRNSYS simulates TABS by defining an active layer in the floor or ceiling. The definition process begins similarly to that of a normal wall. The parameters like pipe spacing, pipe outer diameter, pipe wall thickness and pipe wall conductivity are required when defining the active layer.

To ensure a correct calculation, a minimum mass flow rate (generally greater than $13 \text{ kg/m}^2\text{h}$) has to be set. The ordinary piping system has been modelled in two segments in this simulation.

The reasoning behind this approach

The comparison of computer tools is a laborious and time consuming business. Virtually all parameters have to be controlled and sometimes this might not even be completely possible. In any case, one can argue that this approach is valid and offers a high insight into the program at an academic level. On the other hand many of these adjustments might be omitted while "just" simulating a real building, simply because they are unknown. Consequently this means that many of the default values remain unchanged and influence the outcome of the simulation. For this reason it is important to see how the results are changing with increasing complexity of the simulations.

SIMULATION

As mentioned before, the comparison is made through a number of stages. In the following, the stages presented in this paper are explained in more detail. In the end, some fundamental differences between the tools are mentioned, that should also be controlled for further analysis.

Stage 1 - Basic building

As a first step of the comparison, a basic simulation has been made in the selected simulation tools. For this comparison, only the building envelope has been modelled and placed in the outdoor thermal environment. Internal loads as well as any installations (e.g. heating and cooling systems, lighting and others) have been neglected.

- Building dimensions and construction as reference building (see figure 1).
- Infiltration is at 0.2 *ACH*.
- Simulation of zones A, B, C and D as indicated in figure 1 (only zone A used).
- No HVC&H systems.
- No internal loads.
- Weather data for Brussels (TRY from ASHRAE 2001).

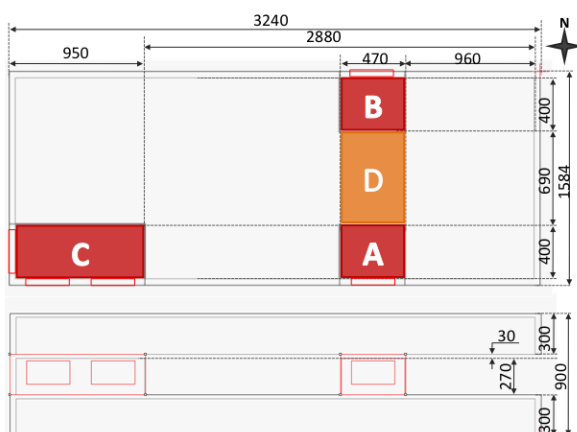


Figure 1: Reference building floor plan with indication of simulated zones - 2nd floor

Stage 2a and 2b - Shading

In the second stage of the simulations, the simple model was extended with shading. For Stage 2a internal shading and for Stage 2b external shading was used. In both cases the shading was modelled to represent Venetian blinds with an angle of 45°.

Stage 3a and 3b - Ventilation

Both stage 3a and 3b have been based on stage 2a. For both stages the air was supplied untreated from the outside and exhausted without heat recovery. In stage 3a 5.6 *l/s · person* and in stage 3b 10 *l/s · person* of outside air have been provided.

Stage 4 - Internal Loads

Starting from the model of stage 3b, internal loads were introduced for stage 4. The loads for stage 4 were:

- Occupants: 2 with 1 *MET* and summer: 0.5 *CLO*, winter: 1 *CLO*; Schedule: Workdays from 7:00 to 16:00 with break from 12:00 to 13:00, else not present.
- Lighting: 10 *W/m²*; Schedule: Workdays from 7:00 to 8:30 at 100 %, then linear decline to 0 % at 11:00, else off.
- Equipment: 75 *W/Occ* (Computer and Screen); Schedule: Workdays from 7:00 to 16:00, else off.

Stage 5 - TABS

For the modelling of TABS the data given in table 1 has been used as indicated for each program. For the comparison the default values from TRNSYS have been used except for the h-value (H-water-pipe-fin coefficient as defined in EN 15377-1) which is only used by IDA and suggested within the program.

Differences between tools

The following points are differences between the four programs that can have a considerable impact on simulation results. The different approaches for the calculation of a TABS system were introduced in the TABS section of the METHODS.

- All tools but IES <VE> have the possibility to model occupants based on MET and CLO values. In IES <VE> it is necessary to specify the heat generation in absolute values (e.g. *W/m²*). This means that in IES <VE> the heat delivered to the zones is constant for the entire year, whereas it depends on the room temperature when a real occupant model is used. Between IES <VE> and IDA, this difference can exceed 200W.
- In all simulation tools it is possible to adjust a number of parameters. These parameters can influence the run time of the simulation as well as its accuracy. Bad selection of these parameters can even lead to a premature termination of the simulation. This is especially true for IDA as it becomes more and more challenging to solve the

Table 1: Input data used for the simulation of TABS depending on the simulation tool

parameters	Values	IDA	IES	E+	TRNSYS
pipe conductivity	$1.26 \frac{kJ}{h \cdot m \cdot K}$	-	+	-	+
pipe spacing	150 mm	*	+	+	+
inner pipe diameter	12 mm	*	+	+	+
pipe wall thickness	2 mm	*	+	-	+
depth in slab	200 mm	+	+	-	+
constant water flow	350 kg/h	+	-	+	+
supply temp. summer	22 °C	+	+	+	+
supply temp. winter	24.5 °C	+	+	+	+
h-value	$30 \frac{W}{m^2 K}$	+	-	-	-

+ required; - not used by tool;
* optional on advanced level

system of differential equations the more complex it gets. For instance the by default existing heat recovery unit should be deleted if it is not used. It can otherwise prolong the simulation time considerably and in extreme cases even lead to the premature termination of the simulation.

- The warm-up phase is handled differently for all of the programs. The used settings are:

IDA: 14 days of periodic simulations with the first day of the simulation period.

IES: 30 days of dynamic simulations with the last days of the previous year.

EnergyPlus: Up to 100 days (default 25) of warm up. Iterations are aborted once the start-up temperature (23°C) converges with the ambient temperature.

TRNSYS: Two year simulation, first year as start-up phase.

If any of these times are set too short it will have a negative impact on, at least, the beginning of the simulation. Also the different approaches, periodic or dynamic, can have an influence since they will lead to different starting conditions for the simulations.

Apart from these points many other settings could have an influence on the outcome of the simulations.

RESULTS AND DISCUSSION

Stage 1

For the simulations at stage 1 the results for the operative temperature (T_{op}) are shown in figure 2. The development of T_{op} for all tools shows the same characteristic. The differences in the beginning of the sim-

ulations are a result of different start-up procedures between the programs. The lower peak temperatures for IDA and IES found in the summer time could be explained by a higher sensitivity to small infiltration rates, for EnergyPlus and TRNSYS it seems to be vice versa. For simulations without any infiltrations (not presented in this paper) the highest temperatures were found to be in a much closer range of one another. For reference the outdoor air temperature is included here.

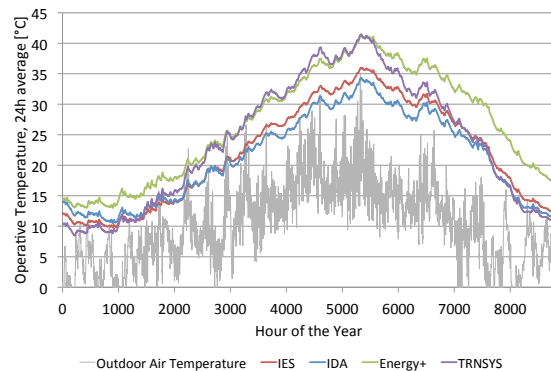


Figure 2: Operative temperature (24h moving average) for Stage 1

Figure 3 shows the deviation of the operative temperatures (T_{op}) for each simulation tool from their common average simulation result. For the basic building the deviation is very high. This deviation however decreases from here on as can be seen in figure 6b.

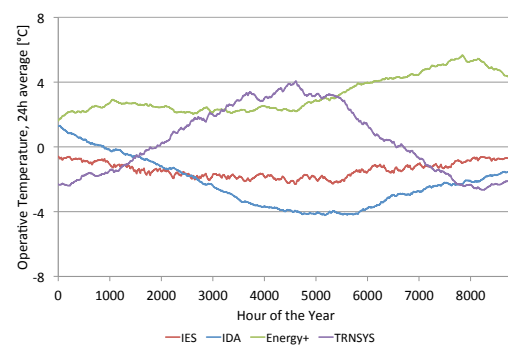
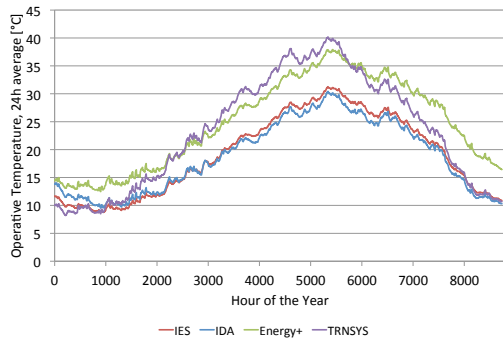


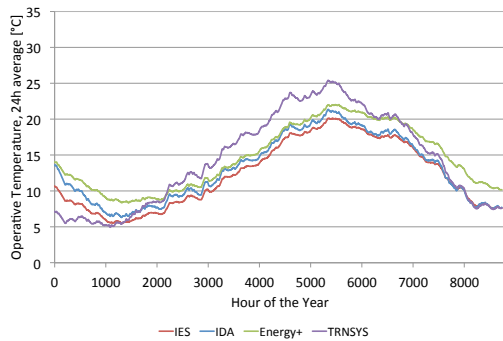
Figure 3: Operative temperature difference between average simulation results and indicated tool for stage 1. (24h moving average)

Stage 2

Introducing blinds (internal for stage 2a and external for stage 2b) lowers the temperature and results in a smoothed short term temperature fluctuation as can be found by comparing figures 2, 4a and 4b. Between the simulation of internal and external shading, the agreement between the tools is higher for external shading. The overall shape of the curve however remains unchanged.



(a) Stage 2a - Internal Blinds



(b) Stage 2b - External Blinds

Figure 4: Operative temperature for internal and external shading.

Stage 3

Through the introduction of ventilation the, results of the simulation tools are coming closer together. IES and IDA show significant lower temperatures during the summer for Stage 3a ($5.6 \text{ l/s} \cdot \text{person}$), compared to EnergyPlus and TRNSYS as seen in figure 5a. Looking at figure 5b for Stage 3b ($10 \text{ l/s} \cdot \text{person}$) all simulation tools are much closer to each other.

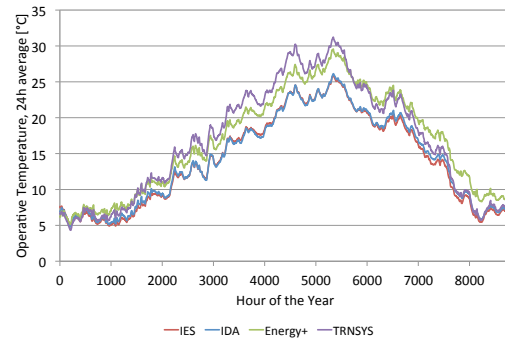
Stage 4

Starting from Stage 3b, the addition of internal loads increases T_{op} for all tools. Figure 6a shows that the agreement between the tools however remains high. The deviation of the operative temperature, from the average has its maximum at about 2 K as illustrated in figure 6b.

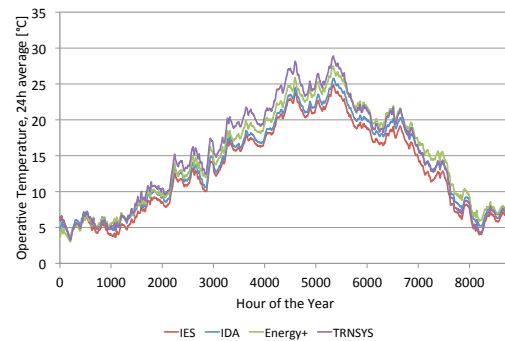
Stage 5

Finally TABS are added to the building simulation. As can be seen in figure 7, the calculated temperatures are fluctuating by around 5°C (based on a 24 h average) for all tools. However, the fluctuations are not, as on all previous stages, synchronous between the tools.

Figures 8a and 8b show the comfort categories achieved with the used rudimentary control for TABS. Both, for winter and summer the results are not the best. This is not due to the TABS itself but rather to the poor control of them. However, the results for each tool are quite different and would not necessarily trigger the same reactions by the engineer using the tool.



(a) Stage 3a (2a + Ventilation: $5.6 \text{ l/s} \cdot \text{person}$)



(b) Stage 3b (2a + Ventilation: $10 \text{ l/s} \cdot \text{person}$)

Figure 5: Operative temperature for two different ventilation rates.

Degree hours

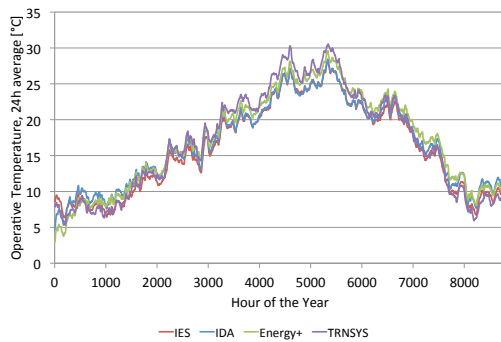
Tables 2 and 3 show the calculated degree hours of cooling and heating for each tool and stage for set-point temperatures of 24.5°C and 22°C respectively. As has been expected, the degree hours for each tool show the same consistent pattern.

For cooling (Table 2) they drop from stage 1 to stage 3a gradually with each building improvement. The increase from 3a to 3b is due to the higher ventilation rate. Especially for TRNSYS the higher air supply has an overall cooling effect, which is also reflected in the heating period. Naturally, the values for stage 4 are increasing again as additional loads are present in the zone. The addition of a cooling system (TABS) again reduces the remaining degree hours.

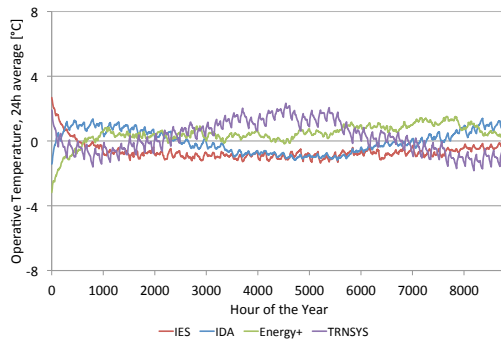
Comparing the different tools to one another, it is apparent that the results are significantly different for most stages. IDA shows for all stages the by far lowest cooling degree hours. EnergyPlus and TRNSYS calculate the highest cooling degree hours.

For heating (Table 3) the pattern is exactly reversed. This is of course only consequent. Shading reduces solar gains, the ventilation replaces warm indoor air with colder outside air and the internal loads provide heat. Regarding the heating degree hours, the results are closer together the more complex (higher stage number) the simulation becomes.

The degree hours presented in tables 2 and 3 show that results of each tool are too different to always draw



(a) Stage 4 (3b + Internal Loads)



(b) Stage 4 (3b + Internal Loads)

Figure 6: Operative temperature and temperature difference with internal loads.

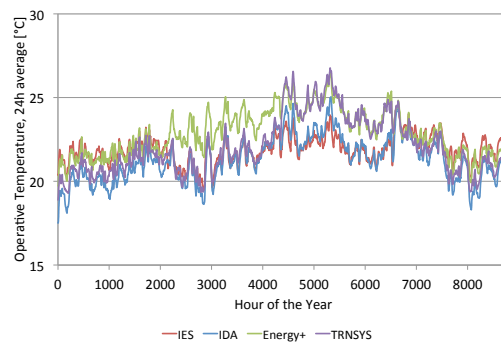


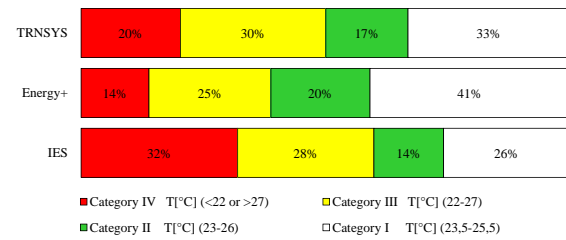
Figure 7: Operative temperature for Stage 5 (24h moving average)

the same conclusion from them. This shows the dangerous potential of building simulation. Depending on the used tool (and detail of the simulation), one might come to different conclusions depending rather on the choice of the tool than the building itself.

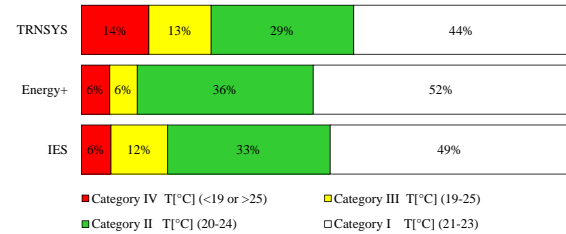
CONCLUSIONS

The present study has shown that different building simulation tools lead to essentially different results for building simulations under the given conditions. This result is not unexpected considering that not all possible settings were controlled. However the magnitude of the differences was higher than expected.

Part of these differences can be explained through the different detail between the models. The way occupants, shading, TABS and other things are modelled



(a) Stage 5 - Comfort Categories Summer



(b) Stage 5 - Comfort Categories Winter

Figure 8: Comfort categories with operating TABS.

differs greatly. For instance in IES occupants are more similar to equipment, having a constant heat production, in IDA this heat production is greatly depending on the air temperature.

A second reason for the differences between the tools are the default parameters that have not been adjusted. Using different parameters will consequently effect the outcome of the simulation.

Even though the tools did not predict the same results at each stage, the relative changes in the results new

Table 2: Calculated degree hours of cooling to 24.5°C from April through September

Stage	IDA	IES	Energy+	TRNSYS
	[degree hours in thousand] (cooling)			
1	14.2	20.3	36.1	34.9
2a	5.7	8.5	26.0	31.0
2b	0.0	0.0	0.0	0.2
3a	0.0	0.0	0.0	0.2
3b	0.2	0.2	3.3	5.6
4	1.4	1.4	3.1	4.7
5	0.1	0.1	1.7	1.2

Table 3: Calculated degree hours of heating to 22°C from October through March

Stage	IDA	IES	Energy+	TRNSYS
	[degree hours in thousand] (heating)			
1	28.3	29.0	16.3	31.0
2a	33.9	34.9	18.7	32.6
2b	50.7	54.0	41.4	53.2
3a	50.7	54.0	41.4	53.2
3b	54.0	55.8	46.0	50.6
4	42.9	46.9	43.5	47.6
5	6.2	1.9	2.6	4.4

input parameters (from stage to stage) are similar for all tools.

Inserting a TABS system in the model showed a reduction in operative temperature differences between the simulating tools.

Essentially the results show that the choice of the simulation tool can greatly influence the building evaluation through the simulation, since in a real world case not all variables are known.

The simulation of TABS has led to a much smaller deviation of simulation results than on any previous stage.

REFERENCES

- CEN 2007. Indoor environmental input parameters for design and assessment of energy performance of buildings addressing indoor air quality, thermal environment, lighting and acoustics. European Standard EN 15251:2007, European Committee for Standardization (CEN).
- CEN 2008. Heating systems in buildings – design of embedded water based surface heating and cooling systems – part 1: Determination of the design heating and cooling capacity. European Standard EN 15377-1:2008, European Committee for Standardization (CEN).
- Crawley, D. B., Hand, J. W., Kummert, M., and Griffith, B. T. 2005a. Contrasting the capabilities of building energy performance simulation programs. *Building Simulation*.
- Crawley, D. B., Hand, J. W., Kummert, M., and Griffith, B. T. 2005b. Contrasting the capabilities of building energy performance simulation programs (version 1.0). Technical report, U.S. Department of Energy, Washington DC, USA; Energy Systems Research Unit, University of Strathclyde, Glasgow, Scotland, UK; Solar Energy Laboratory, University of Wisconsin-Madison, USA; National Renewable Energy Laboratory, Golden, Colorado, USA.
- Crawley, D. B., Hand, J. W., Kummert, M., and Griffith, B. T. 2008. Contrasting the capabilities of building energy performance simulation programs. *Building and Environment*, 43(4):661–673.
- EERE 2011. EnergyPlus Energy Simulation Software. website, Office of Energy Efficiency and Renewable Energy (EERE), U.S. Department of Energy, Washington DC, USA. <http://apps1.eere.energy.gov/buildings/energyplus/> Accessed 27. May 2011.
- IES 2011. Introducing the <virtual environment>. manual, Integrated Environmental Solutions IES. <http://www.iesve.com/software> Accessed 28. May 2011.
- Klein, S. A. 2006. Trnsys, a transient system simulation program. manual, Solar Energy Laboratory, University of Wisconsin-Madison.
- Price, H. and Blair, N. 2003. Current tes capabilities in trnsys. presentation, National Renewable Energy Laboratory (NREL), Golden, CO.
- U.S. Energy Information Administration 2009. International energy outlook 2009. Technical Report DOE/EIA-0484(2009), Office of Integrated Analysis and Forecasting, U.S. Department of Energy, Washington, DC. <http://www.eia.gov/oiaf/ieo/pdf/0484%282009%29.pdf> Accessed 27. May 2011.
- U.S. Energy Information Administration 2010. International energy outlook 2010. Technical Report DOE/EIA-0484(2010), Office of Integrated Analysis and Forecasting, U.S. Department of Energy, Washington, DC. <http://www.eia.gov/oiaf/ieo/pdf/0484%282010%29.pdf> Accessed 27. May 2011.

Paper III

*”Thermische Behaglichkeit und Energieaufwand bei
Flächenheizungen in Bürogebäuden”*

B. M. Behrendt & B. W. Olesen

Published in: *Proceedings of BauSim, 2013*

Appended Papers

THERMISCHE BEHAGLICHKEIT UND ENERGIEAUFWAND BEI FLÄCHENHEIZUNGEN IN BÜROGEBÄUDEN

Benjamin M. Behrendt¹, Bjarne W. Olesen und Lorenzo Mattarolo
International Center for Indoor Environment,
Technical University of Denmark, Kgs. Lyngby, Denmark

Kontakt E-Mail: ¹benbe@byg.dtu.dk

KURZFASSUNG

Die vorliegende Studie befasst sich mit der Anwendbarkeit von Flächenstrahlungssystemen unter bestimmten kritischen Bedingungen.

Dem Risiko von Kondensation an den aktiven Flächen sowie den Leitungen während der Kühleisaison wurde dabei besonderes Augenmerk geschenkt.

Es wurde getestet, ob durch Kombination des Systems mit natürlicher Belüftung sichergestellt werden kann, dass eine thermisch akzeptable Umgebung erreicht wird.

Durch unterschiedliche Platzierung der Messstellen für Taupunkt und operative Temperatur soll der Einfluss einzelner interner Konditionen bewertet werden.

ABSTRACT

This report is concerned with the feasibility of radiant systems in certain critical environments.

A focus of the study was put on the condensation risk on active surfaces as well as on the pipes themselves.

It has been tested if natural ventilation in combination with the system can secure a thermal acceptable environment.

The influence of individual internal conditions was tested by placing the sensors for operative temperature and dew point to different locations.

Schlüsselwörter:

Kondensation, Kühlen, Energieaufwand, Computersimulation, thermische Behaglichkeit, Flächenheizung, Flächenkühlung

EINLEITUNG

Es wurden Simulationen mit IDA Indoor Climate and Energy (Version 3) und dem dazugehörigen Modul für Strahlungssysteme durchgeführt.

Es wurden insgesamt fünf Zonen simuliert, wobei der Fokus in dieser Arbeit auf den Zonen mit hohen latenten Wärmen, hier die Konferenzräume, lag.

Die folgenden Resultate beziehen sich daher auf die Konferenzräume.

Die Simulation wurde für vier Orte in Schweden durchgeführt: Malmö (mit Wetterdaten einer Messstation in Kopenhagen), Göteborg, Stockholm und Kiruna. Malmö, Göteborg und Stockholm liegen dabei im Süden Schwedens, wohingegen Kiruna die nördlichste Stadt Schwedens ist (rund 1000km nördlich von Stockholm).

SIMULATIONEN

Das Schema des simulierten Gebäudes ist in Abbildung 1 dargestellt. Tabelle 1 beinhaltet die wichtigsten Eckdaten für die Simulationen. Die hier genannten Werte wurden für alle durchgeführten Simulationen verwendet.

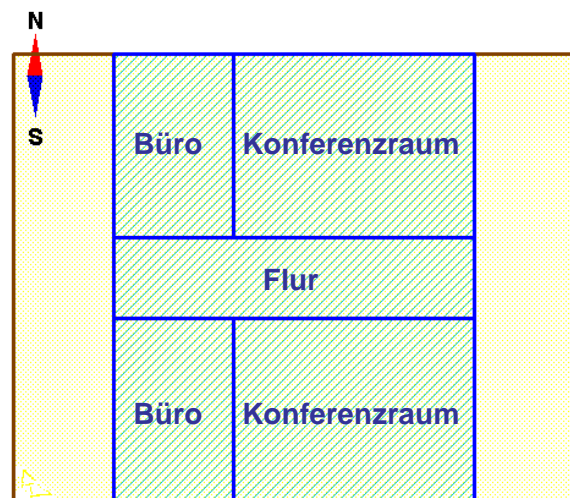


Abbildung 1 Schema des simulierten Gebäudes

Tabelle 1 Im Modell verwendete Annahmen und interne Bedingungen

	KONFERENZ- RAUM	BÜRO
Grundfläche	39,6 m ²	19,8 m ²
Personen	12 occ., 1,1 Met, 0,5 – 1 Clo	2 occ., 1,2 Met, 0,5 – 1 Clo
Licht	100 W	50 W
Equipment	350 W	
Infiltration	0,1 ACH	
Verschattungsfaktor	0,5 (wenn Top > 23°C)	
Lasten und Systeme	8:00 – 12:00 und 13:00 – 17:00	

Die Simulationen wurden sowohl für die Sommer- als auch die Wintersaison durchgeführt. Der Betrieb aller Anlagen richtet sich nach den in Tabelle 1 angegebenen Zeiten. Außerhalb dieser Zeiten sind die Systeme inaktiv.

Lüftung

In den Sommermonaten wurde mit Luft bei Umgebungstemperatur gelüftet. Zur Vermeidung von Zug wurde ein unteres Limit von 17°C eingehalten, auf das die Zuluft gegebenenfalls aufgeheizt wurde. Als Zulufraten wurden Kategorie C (entsprechend dem Standard EN ISO 15251; 4 l/s·pers + 0.4 l/sm²) und Kategorie „low“ (nicht im Standard enthalten; 2 l/s·pers + 0.4 l/sm²) untersucht. Der Fall „low“ stellt die Situation dar, in der sich mehr Personen in dem Raum befinden als ursprünglich vorgesehen.

Flächenstrahlungssystem – „Cooling Panel“

Cooling Panels wurden in allen Räumen modelliert. Sie bestehen aus MDF-Platten (Medium Density Fiberboard), einem EPS-Paneel (Expanded Polystyrene), einer geformten Aluminiumschicht, PEX-Rohren mit einem Innendurchmesser von 8mm und einer Wandstärke von 1,8mm sowie einem Verlegeabstand von 120mm. Der Aufbau ist in Abbildung 2 schematisch dargestellt. Die Paneele waren ganzjährig aktiv.



Abbildung 2 Schematische Darstellung eines "Cooling Panels"

Flächenstrahlungssystem – Bodensystem

In der zweiten Simulation kam ein Bodensystem zum Einsatz. Das System besteht aus Rohren mit einem Durchmesser von 17mm, die in eine 45mm Estrichschicht eingelassen sind. Direkt unter den Rohren ist eine 30mm starke Isolation vorgesehen. Der eigentliche Boden ist 150mm stark und besteht aus Beton. Abbildung 3 ist eine schematische Darstellung des Bodens.

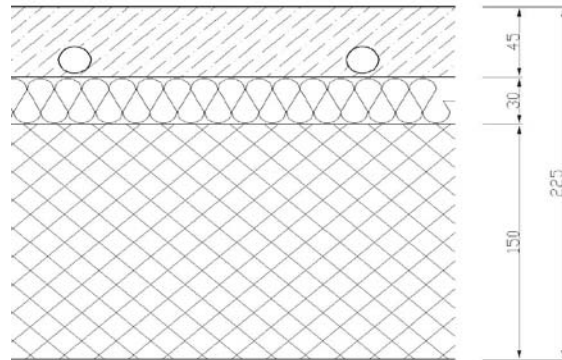


Abbildung 3 Schema des Bodensystems

Vorlauftemperaturkontrolle

Es wurden zwei unterschiedliche Funktionen für die Kontrolle der Vorlauftemperatur (T_s) untersucht. Beiden gemein ist, dass T_s immer größer als 17°C sein muss um Probleme durch Strahlungsasymmetrie zu vermeiden. Eine weitere Randbedingung ist, dass T_s die Taupunkttemperatur (T_{dp}) nie unterschreiten darf. Die erste Kontrolle ist sowohl von der Umgebungstemperatur (T_{ex}) als auch von der operativen Temperatur (T_{op}) abhängig, vgl. Gl. 1. Die zweite untersuchte Kontrollfunktion ist lediglich von T_{ex} abhängig, vgl. Gl. 2 (Olesen et al., 2004).

$$T_s = 0,52 \cdot (20 - T_{ex}) - 16 \cdot (T_{op} - 22) + k \quad (1)$$

$$T_s = 0,35 \cdot (18 - T_{ex}) + h \quad (2)$$

mit $k_0=20$; $h_0=18$.

Taupunktmessung

Weiterhin wurde untersucht welchen Einfluss auf die Performace unterschiedliche Orte für die Messung der Taupunkttemperatur haben. Zu diesem Zweck wurden Simulationen verglichen, bei denen die Taupunkttemperatur in einem Büro bzw. in einem Konferenzraum gemessen wurde.

ERGEBNISSE

Die Ergebnisse sind stark von den klimatischen Bedingungen abhängig. Für die hier untersuchten Orte sind diese vorwiegend moderate Luft- und niedrige Taupunkttemperaturen. Unter anderen Bedingungen können deutlich abweichende Ergebnisse festgestellt werden.

Das Kondensationsrisiko steigt an, wenn die Lüftung unter die Minimalanforderungen reduziert wird oder der Raum überladen ist.

Die Platzierung der Sensoren kann das Kondensationsrisiko deutlich beeinflussen. Es muss darauf geachtet werden, dass, sollte sich der Sensor nicht im Raum mit den höchsten latenten Lasten befinden, eine Minimaltemperatur für die Vorlauftemperatur eingehalten wird.

Zwischen den unterschiedlichen verwendeten Regelungsverfahren konnten nur geringe Unterschiede in Bezug auf Komfort und Kondensationsrisiko festgestellt werden. Steuerungen, bei denen eine Raumabhängigkeit enthalten war, haben bei ähnlichem Energieverbrauch geringfügig besser abgeschnitten.

Beim Einsatz einer Deckenheizung muss beachtet werden, dass es bei einem hohen Wärmebedarf, z.B. auf Grund schlechter Isolierung, ein erhöhtes Risiko für Strahlungsasymmetrien gibt.

Bei korrekter Dimensionierung der Fußbodenheizung hatte diese keine negative Auswirkung auf die lokale Behaglichkeit. Auch bei erhöhtem Wärmebedarf kann die Fußbodenheizung die Behaglichkeitsbedingungen erfüllen, das Risiko für Strahlungsasymmetrien ist vergleichsweise gering.

Lüftung - Reduzierte Lüftungsrate

Die Reduzierung der Lüftungsrate von Kategorie C (4 l/s-pers + 0.4 l/sm²) zu Kategorie „low“ (2 l/s-pers + 0.4 l/sm²) hatte unterschiedliche Folgen. In den Städten Kiruna und Göteborg, die ein allgemein kühleres Klima haben, blieben die Auswirkungen verhältnismäßig gering. Wie in Abbildung 4 zu sehen, wurde hingegen in Malmö und Stockholm Kategorie B in Bezug auf die thermische Behaglichkeit in mehr als 5% der Zeit verfehlt.

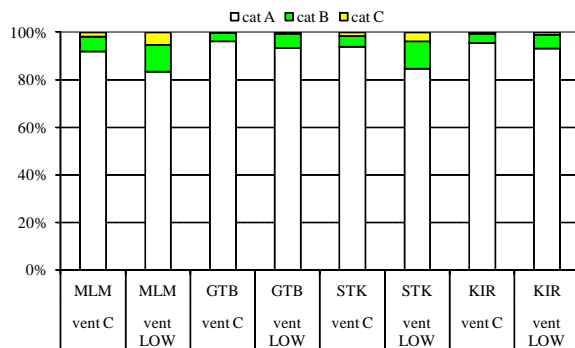


Abbildung 4 Thermische Behaglichkeit - Kategorien A bis C nach Standard EN ISO 15251

Der Einfluss auf die Taupunkttemperatur wird in Abbildung 5 deutlich. Durch die reduzierte Lüftungsrate steigt dieser um bis zu 2°C. Dies führt vor allem in Malmö und Stockholm zu Problemen, da die Taupunkttemperatur hier 24°C erreicht.

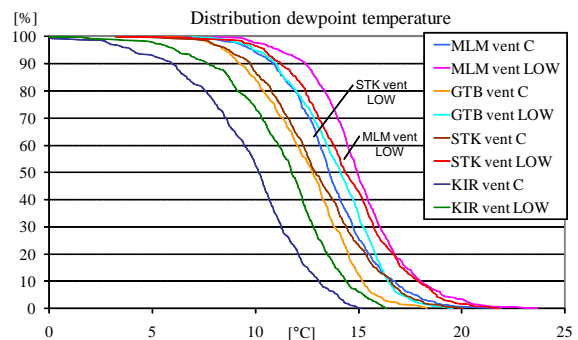


Abbildung 5 Akkumulierte Taupunkttemperatur in Abhängigkeit von Ort und Lüftungsrate

Wie aber in Abbildung 6 zu sehen ist, herrscht auch in Malmö und Stockholm zu jeder Zeit eine Temperaturdifferenz (ΔT) von wenigstens 2,5°C zwischen der Oberfläche des aktiven Bauteils (T_{surf}) und der Taupunkttemperatur (T_{dp}). Dies könnte in einigen Fällen zu Kondensation führen, unabhängig davon, ob die reduzierte oder aber die Lüftungsrate entsprechend Kategorie C gewählt wurde.

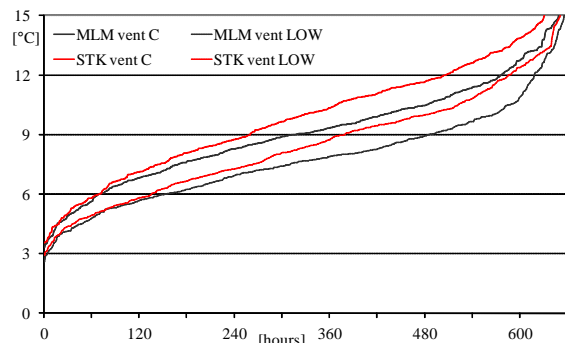


Abbildung 6 $\Delta T = T_{surf} - T_{dp}$ (Unterschied zwischen Oberflächen- und Taupunkttemperatur)

Taupunktmessung – Änderung der Messstelle

Um zu beurteilen, in wie weit eine ungeschickte Platzierung der Sensoren Einfluss auf die Güte des Raumklimas hat, wurde der Aufstellungsort variiert. Wie in Abbildung 7 zu sehen ist, wird bei der Platzierung der Sensoren in einem Büro eine höhere thermische Behaglichkeit in den Konferenzräumen erreicht. Dieses Verhalten war zu erwarten, da eine Begrenzung der Vorlauftemperatur nun nicht anhand der Zone mit den größten Lasten, sondern anhand eines eher unproblematischen Büros. Der Einfluss ist allerdings mit Änderungen kleiner 5% vergleichsweise gering. Beide Standorte sind daher Akzeptabel.

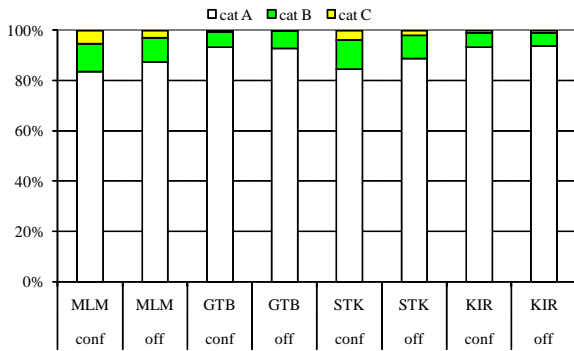


Abbildung 7 Auswirkungen der gewählten Messstelle auf die thermische Behaglichkeit

In Abbildung 8 werden die Auswirkungen der unterschiedlichen Plazierungen deutlich. Der Zeitraum, in dem die Vorlauftemperatur durch die Taupunkttemperatur begrenzt wird, unterscheidet sich in beiden Fällen deutlich. Es ist aber zu beachten, dass bei abnehmender Begrenzung durch die Taupunkttemperatur die Vorlauftemperatur stärker durch die minimale Vorlauftemperatur beschränkt wird.

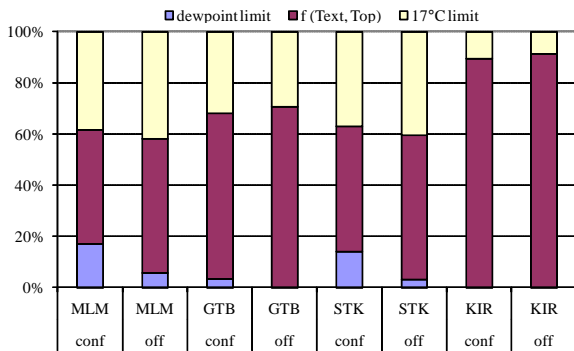


Abbildung 8 Vorlauftemperaturkontrolle in Abhängigkeit von der Sensorplatzierung

Der Temperaturunterschied zwischen Oberflächentemperatur und Taupunkttemperatur verändert sich, wie in Abbildung 9 gut zu sehen ist, nur bei kleineren Temperaturdifferenzen um 0,5 bis 1K. Dies führt zu einer erhöhten Wahrscheinlichkeit von Kondensation. Da die Oberflächentemperatur aber noch um 2K über der Taupunkttemperatur liegt besteht trotzdem nur ein Begrenztes Kondensationsrisiko.

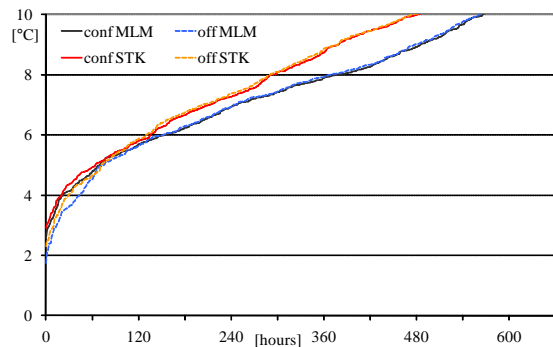


Abbildung 9 $\Delta T = T_{surf} - T_{dp}$ bei variation der Sensorstandorte

Kontrolle der Vorlauftemperatur

Beim Vergleich der beiden Strategien zur Kontrolle der Vorlauftemperatur konnten keine nennenswerten Unterschiede festgestellt werden. Wie in *Abbildung 10* zu sehen ist, ermöglichen beide Kontrollen das Erreichen von zumindest Kategorie B für deutlich über 90% der Zeit. Das Einbeziehen von T_{op} geht aber einher mit einer leichten Steigerung der thermischen Behaglichkeit. Dies wird durch die leicht erhöhten Anteile der Kategorie A deutlich.

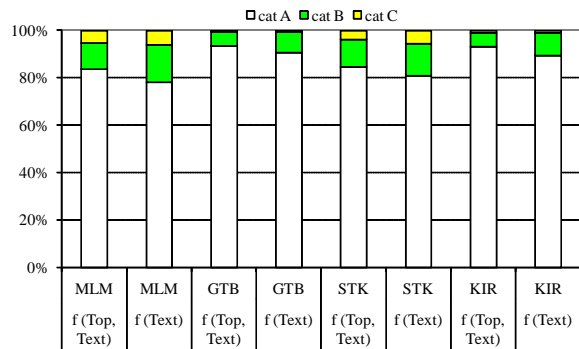


Abbildung 10 Auswirkungen der verwendeten Kontrollfunktion auf die thermische Behaglichkeit

Mit Hilfe von GenOpt wurden Gl. 1 und 2. optimiert. Dabei wurden für k bzw. h Werte entsprechend Tabelle 2 angenommen. Über die Berechnung des Index n , wie in Abbildung 11 exemplarisch dargestellt, können die Werte für k bzw. h in Abhängigkeit von den Anforderungen gewählt werden. Für die weitere Analyse wurden die in Tabelle 2 farblich markierten Werte gewählt.

Tabelle 2 Fälle für die GenOpt-Analyse

K WERTE FÜR GL. 1 $T_s = f(T_{ex}, T_{op})$		H WERTE FÜR GL. 2 $T_s = f(T_{ex})$	
$k_0=20$	$k_1=18$	$h_0=18$	$h_1=22$
$k_2=19$	$k_3=20$	$h_2=23$	$h_3=24$
$k_4=21$	$k_5=22$	$h_4=25$	$h_5=26$
$k_6=23$	$k_7=24$	[°C]	

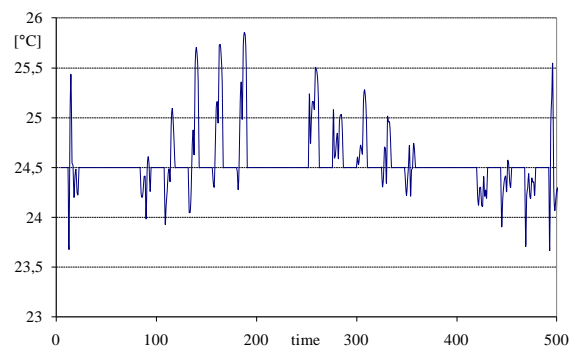


Abbildung 11 Exemplarische Berechnung des Index n bei einer neutralen Temperatur von 24,5°C

Abbildung 12 zeigt den Zusammenhang zwischen dem Komfort-Index n und dem Energieverbrauch auf.

Wird ein besserer, d. h. kleinerer Komfort-Index n angestrebt, steigt hier der Energieverbrauch grundsätzlich an.

Die in Abbildung 13 dargestellten Ergebnisse verdeutlichen, dass eine Feinjustierung der Kontrollfunktion zu einer erheblichen Verbesserung des Ergebnisses führen kann, ohne dabei den Energieverbrauch wesentlich zu verändern.

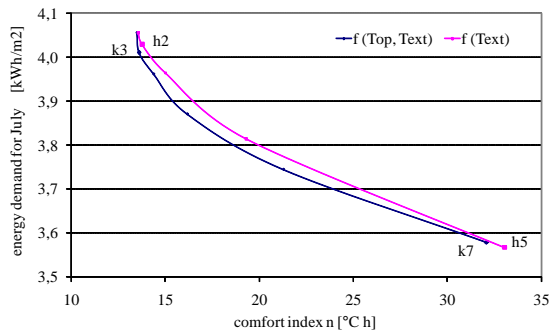


Abbildung 12 Abhängigkeit von Komfort-Index n und Energieverbrauch

Dies wird besonders beim Vergleich der in Abbildung 13 gegenüber gestellten Fälle k7 und h5 deutlich. In diesem Fall ist die Einbeziehung der operativen Temperatur in die Regelung der Anlage positiv zu bewerten. Vergleicht man hingegen die Fälle k3 und h2 miteinander, findet sich kein nennenswerter Unterschied zwischen den erreichten Kategorien.

Die Fälle k3 und h2 schneiden zwar gegenüber den Fällen k7 und h5 besser ab, erwartungsgemäß geht dies allerdings zu Lasten des Energieverbrauchs.

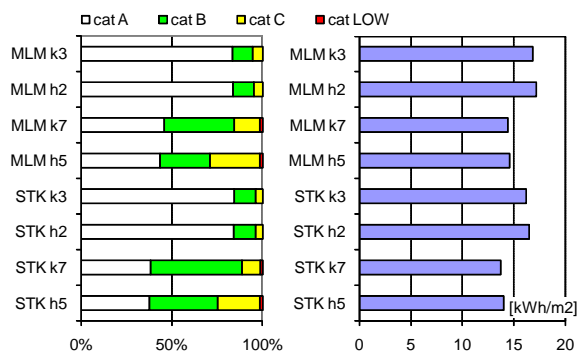


Abbildung 13 Unterschiede der Parameteruntersuchung der Kontrollfunktion für ausgesuchte Parameter

Aufhebung der minimalen Vorlauftemperatur

Verzichtet man auf eine absolute minimale Begrenzung der Vorlauftemperatur, erhöht sich sowohl die Zeit, in der die normale Kontrollfunktion zur Anwendung kommt, als auch der Zeitraum, in dem die Vorlauftemperatur durch die Taupunkttemperatur begrenzt wird. In Abbildung 14 wird deutlich, dass die Wahl des Standortes für die Temperatur- und Taupunktmessung erhebliche Auswirkungen haben kann. Bei ansonsten unveränderten Bedingungen wird die Vorlauftemperatur sowohl für den Fall Malmö als auch Stockholm 10% länger durch die

Taupunkttemperatur begrenzt, wenn die Sensoren im Konferenzraum platziert waren. In den Fällen, in denen sie in den Büros angeordnet waren, ist daher mit einem erhöhten Kondensationsrisiko in den Konferenzräumen zu rechnen.

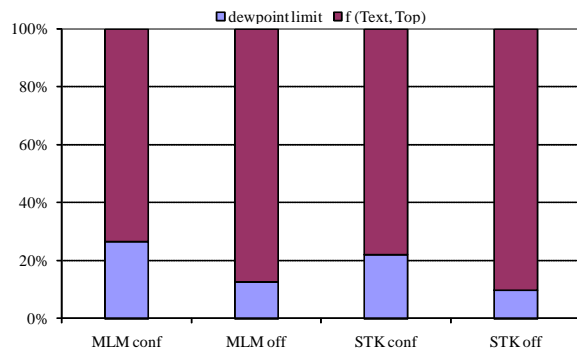


Abbildung 14 Vorlauftemperatur ohne minimale Begrenzung

Durch die veränderte Vorlauftemperatur ändert sich, wie in Abbildung 15 dargestellt, auch die Oberflächentemperatur über den gesamten Simulationszeitraum. In Malmö beschränken sich die größeren Abweichungen allerdings auf Temperaturen oberhalb von 22°C. Die Abweichungen bei niedrigeren Oberflächentemperaturen sind so geringfügig, dass nicht mit einer Beeinflussung des Kondensationsrisikos zu rechnen ist. Für Stockholm sind aber die Abweichungen größer als in Malmö und sie sind vor allem auch bei niedrigeren Temperaturen vorhanden. So sinkt die minimale Oberflächentemperatur um etwa 0,2°C, wenn die Sensorik im Büro steht. Zwar wird durch diese Änderung kein Einfluss auf den lokalen Komfort genommen, in ungünstigen Fällen kann diese Temperaturänderung aber zu einer vermehrten Kondensation am Boden führen.

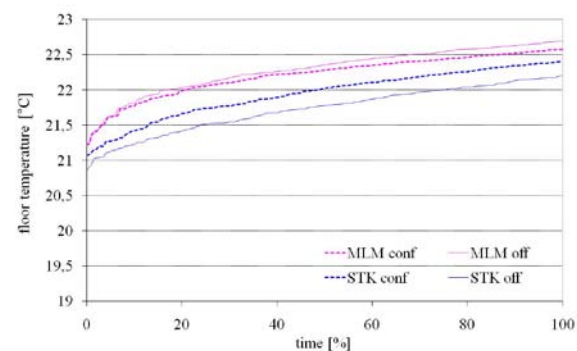


Abbildung 15 Verteilung der Oberflächentemperatur bei verändertem Aufstellungsort der Sensoren

SCHLUSSFOLGERUNGEN

Die durchgeführte Analyse hat sich hauptsächlich auf das Kondensationsrisiko bei Verwendung von Flächenstrahlungssystemen bezogen. Die Ergebnisse sind stark von den klimatischen Bedingungen abhängig. Der Sommer in Schweden zeichnet sich vor allem durch moderate Temperaturen und

vergleichsweise geringe Taupunkttemperaturen aus. Unter anderen Bedingungen ist zu erwarten, dass eine ähnliche Untersuchung zu anderen Ergebnissen kommt.

Das Kondensationsrisiko ist erwartungsgemäß mit einer Verringerung der Lüftungsrate bzw. bei Überbelegung des Raumes angestiegen. Gerade bei der Verwendung von Flächenstrahlungssystemen ist daher eine bedarfsorientierte Auslegung von besonderer Bedeutung.

Die Untersuchung hat ebenfalls erwartungsgemäß gezeigt, dass die Platzierung der Sensoren einen erheblichen Einfluss auf die Ergebnisse hat. Dies trifft im besonderen Maße zu, wenn es keine minimale Begrenzung der Vorlauftemperatur gibt. Zur Minimierung des Kondensationsrisikos sollten die Sensoren daher immer im Raum mit den höchsten Lasten platziert sein. Anders aber als in einer Simulation kann gerade diese Anforderung zu großen Problemen führen. Es ist zum Beispiel nicht anzunehmen, dass ein Konferenzraum im gleichen Umfang genutzt wird wie ein normales Büro. Empfehlenswert wäre daher eine individuelle Raumsteuerung. Um den Zusatzaufwand hierfür ins Verhältnis zum zusätzlichen Nutzen zu setzen, sind weitere Untersuchungen notwendig.

Die Güte der verwendeten Regelungssysteme hat direkten Einfluss auf die thermische Behaglichkeit und den Energieverbrauch. Die Wahl des Regelungssystems muss daher mit Blick auf den gewünschten thermischen Komfort und die benötigte Leistung getroffen werden. Es ist aufgefallen, dass in einzelnen Fällen eine Regelung, die ausschließlich auf der externen Temperatur beruht, mit einer Regelung, die zusätzlich die operative Temperatur berücksichtigt, konkurrieren kann. Bei ungünstigeren Bedingungen ist allerdings die Berücksichtigung der operativen Temperatur vorteilhaft. Bei annähernd gleichem Energieverbrauch kann dadurch ein besseres thermisches Raumklima geschaffen werden.

Der Verzicht auf eine untere Grenze der Vorlauftemperatur führt in den hier vorliegenden Fällen nicht zu einer Beeinträchtigung des thermalen Wohlbefindens. Die Oberflächentemperaturen erreichen auch ohne diese Begrenzung minimale Temperaturen geringfügig unterhalb von 21°C.

Abschließend ist festzustellen, dass Flächenkühlssysteme in Schweden anwendbar sind und dabei gute bis sehr gute Ergebnisse erwartet werden können, wenn die oben genannten Punkte bei der Planung und dem Betrieb der Anlage berücksichtigt werden.

LITERATUR

EN ISO 15251, Indoor environmental input parameters for design and assessment of energy

performance of buildings addressing indoor air quality, thermal environment, lighting and acoustics, CEN, 2006

GenOpt, Generic Optimization Program, LBNL, Berkeley, 2008

IDA Indoor Climate and Energy 3.0, EQUA Simulation Technology Group, Sweden

Olesen, B.W., Dossi, F.C., 2004. Operation and Control of Activated Slab Heating and Cooling system, CIB World Building Congress

The strong political market drive towards energy savings in the building sector calls for efficient solutions. Using so called low temperature heating and high temperature cooling systems such as for instance thermally activated building systems (TABS) has a significant impact on the required energy source. The present study introduces the reader to the Simple Simulation Tool for TABS as well as the Climate Classification for TABS. Both tools combined can provide good early design stage evaluations of the usability of TABS for a given building at a given location.

DTU Civil Engineering
Technical University of Denmark

Brovej, Bygning 118
2800 Kongens Lyngby

www.byg.dtu.dk

ISBN 9788778774545
ISSN 1601-2917